Journal of Statistical Physics, Vol. 123, No. 5, June 2006 (© 2006)
DOI: 10.1007/s10955-006-9089-8

Critical Dynamics in Thin Films

A. Gambassi[1,2] and S. Dietrich[1,2]

Received September 29, 2005; accepted March 13, 2006
Published Online: May 31, 2006

Critical dynamics in film geometry is analyzed within the field-theoretical approach. In particular we consider the case of purely relaxational dynamics (Model A) and Dirichlet boundary conditions, corresponding to the so-called ordinary surface universality class on both confining boundaries. The general scaling properties for the linear response and correlation functions and for dynamic Casimir forces are discussed. Within the Gaussian approximation we determine the analytic expressions for the associated universal scaling functions and study quantitatively in detail their qualitative features as well as their various limiting behaviors close to the *bulk* critical point. In addition we consider the effects of time-dependent fields on the fluctuation-induced dynamic Casimir force and determine analytically the corresponding universal scaling functions and their asymptotic behaviors for two specific instances of instantaneous perturbations. The universal aspects of nonlinear relaxation from an initially ordered state are also discussed emphasizing the different crossovers that occurring during this evolution. The model considered is relevant to the critical dynamics of actual uniaxial ferromagnetic films with symmetry-preserving conditions at the confining surfaces and for Monte Carlo simulations of spin system with Glauber dynamics and free boundary conditions.

KEY WORDS: Dynamic critical phenomena, confined geometry, finite-size scaling, magnetic properties of films, critical casimir force

1. INTRODUCTION

The microscopic understanding of collective dynamic phenomena in condensed matter poses one of the most difficult challenges for statistical physics. Accordingly the theory of these phenomena is in a significantly less mature state than for static properties in thermal equilibrium; also the corresponding experimental knowledge is very limited. At present theoretical insight into collective dynamics

[1] Max-Planck Institut für Metallforschung, Heisenbergstr. 3, D-70569 Stuttgart, Germany; [2]Institut für Theoretische una Angewandte Physik, Universität Stuttgart, Pfaffenwaldring 57, D-70569 Stuttgart, Germany; e-mail: gambassi@mf.mpg.de; dietrich@mf.mpg.de

can be gained either by simulations or by studying numerically or analytically rather simplified models of actual condensed matter systems. Whereas in the former case the limitations on system size and time scales are very severe, in the latter case one has to be careful in accounting within the model for all those aspects of the actual systems which are relevant for the collective behavior under study. Understanding the link between the microscopic physical parameters of the system and those defining the effective dynamic models is also a crucial issue. Due to these difficulties only in few cases one is able to provide theoretical predictions that can be *quantitatively* compared with experiments—provided that those can be carried out in the first place. Nevertheless there are instances in which a *universal* collective behavior emerges which is largely independent of the microscopic details of the system and, as a consequence, also of the specific model used to describe it. These highly valuable circumstances arise naturally upon approaching a critical point, where the system undergoes a continuous, i.e., second-order phase transition. For universal critical properties such as critical exponents, scaling functions, and amplitude ratios, one is usually able to provide theoretical predictions that can be tested *quantitatively* by comparison with experimental data. In view of the universality of the critical properties, which is justified by the framework of renormalization-group theory and supported by experimental evidence, it is possible to study the collective behavior in terms of suitable field-theoretical models, based on minimalistic fixed-point equations of motions following from Landau type fixed-point Hamiltonians. This approach has been carried out successfully during the last decades in order to study static and dynamic critical properties of systems both in the bulk and in the presence of surfaces. In many cases the agreement between such field-theoretical predictions and (mainly Monte Carlo) simulations or experimental data is striking.

The collective behavior of a system close to its critical point can be described in terms of the order parameter whose actual nature depends specifically on the system. Indeed, as long as one is interested in its behavior at length and time scales much larger than the microscopic ones, an effective Hamiltonian can be used which reflects the internal symmetries of the underlying microscopic system and which depends only on the order parameter and potentially a few other slow modes.

Within this framework one can determine the actually observed non-analytic behavior of thermodynamic quantities and structure factors upon approaching the critical point. Moreover some of the quantities characterizing such non-analyticities (e.g., critical exponents or amplitude ratios) turn out to be universal in the sense that they depend only on general features of the effective Hamiltonian such as the spatial dimension and internal symmetries but that they are independent of the details of the actual system. The numerical values of the universal properties and of the universal scaling functions characterize the so-called universality

classes.[1] On time scales much larger than the microscopic ones it is possible to describe the dynamics close to critical points in terms of stochastic evolution equations for the order parameter such that its resulting equilibrium distribution is given by the effective Hamiltonian of the universality class which the system belongs to.[2] This approach allows one to compute systematically the non-analytic behaviors observed in dynamical quantities, e.g., in the low-frequency limit of the dynamic structure factor. In turn the associated universal quantities define the dynamic universality class. One finds that each static universality class consists of several dynamic sub-universality classes which differ, e.g., by different conserved quantities, but nonetheless exhibit the same static universal properties. As an example, the static universality class of the phase transitions in uniaxial ferromagnets is the same as that of binary liquid mixtures although their universal dynamic behavior is captured by two different dynamic universality classes. Various analytical methods, in particular the renormalization-group theory, have been developed and applied to provide predictions for universal quantities. (See, e.g., Ref. 3 for a recent review of the results obtained for the most relevant static universality classes of critical phenomena in the bulk. A recent summary of bulk critical dynamics can be found in Ref. 4.)

Within this framework it is possible to account for the effects of surfaces on the critical behavior. Indeed real systems are always bounded by surfaces or interfaces between different phases which break translational invariance and thus are expected to influence the physical properties including universal features. In particular it turns out that compared to the bulk the critical behavior is locally altered within a distance from the surface of the order of the bulk correlation length. The resulting critical behavior depends only on general properties of the surface and in turn it can be classified in terms of different surface universality classes branching from the same bulk universality class and which are in general characterized by their own surface critical exponents different from the corresponding bulk ones (see Refs. 5–7 for comprehensive reviews). On the other hand it turns out that there are no independent dynamic critical surface exponents,[8] even if for a given *dynamic bulk* critical behavior and *static surface* critical behavior different *dynamic surface* universality classes exist.[9]

In addition to the local effects near surfaces, the properties of a system are influenced by its finite size when the correlation length ξ becomes comparable to the typical sample size L. Depending on the specific system and its geometry this can result even in a suppression of the phase transition or, generally, in a *shift of the critical point* and of coexistence curves which depends on L and vanishes in the bulk limit $L \to \infty$.[10] The scaling behavior that is observed upon approaching the critical point is expected to involve L/ξ and its theoretical understanding is based on the finite-size scaling theory.[10–12] As a consequence of confinement and boundary conditions fluctuation-induced effective forces on the confining

surfaces arise known as thermodynamic Casimir forces (see, e.g., Refs. 12–16 and references therein).

Thin films provide the simplest geometry for studying theoretically the effects of confinement on phase transitions; moreover they are particularly relevant experimental realizations of finite-size systems. Thin film are characterized by a finite width, which in the present context is taken to be much larger than the typical microscopic scale, and a macroscopicly large lateral extension, i.e., much larger than the correlation length. Thin films of magnetic materials, confined fluids, and wetting films represent specific systems with such a geometry which are indeed investigated experimentally. Their static critical properties have been theoretically and experimentally investigated in the past for different universality classes and boundary conditions (see Refs. 17,18 and references therein).

Dynamics in confined geometry is, instead, a less explored subject, both at the critical point and below. Novel phenomena have been observed in the dynamics of phase separation[19] occurring in the *two-phase region* of the phase diagram of confined binary liquid mixtures, after a quench from the homogeneous state. In particular the interplay between surface-directed spinodal decomposition (see, e.g., Ref. 20) and confinement has been studied numerically in Ref. 21 for a symmetric binary mixture with purely diffusive dynamics (Model B in the notion of Ref. 2), a simplified form of the actual dynamics of fluid mixtures (Model H[2]). At the *bulk critical point*, which is the focus of the present study, most of the theoretical results have been obtained for the case of a finite hypercubic geometry with periodic boundary conditions and purely dissipative dynamics [1,22–29] (Model A in the notion of Ref. 2) or dynamics coupled to a conserved density[30] (Model C in the notion of Ref. 2). The dynamic structure factor, the spin transport, and the thermal conductivity of the three-dimensional XY model[31] as well as some aspects of the non-equilibrium critical dynamics of the three-dimensional Ising model[32] have been studied by means of Monte Carlo simulations on a cubic lattice with periodic boundary conditions. In all the cases mentioned above, due to the translational invariance, there are no surface, i.e., spatially varying effects. Monte Carlo simulations have been performed to study the thermal conductivity of the planar magnet lattice model in a bar-like geometry ($H \times H \times L$ with $L \gg H$) with open boundary conditions,[33] striving for a comparison with experimental results for ^{4}He at the superfluid transition confined to an array of pores.[34] The same problem has been addressed within the field-theoretical approach, studying Model F dynamics[2,35] in a $L \times L \times \infty$ geometry with Dirichlet boundary conditions (DBC, i.e., vanishing surface fields) for the order parameter.[36] In both cases the agreement with experimental data is quite good. Critical dynamics in the film geometry has not yet been studied systematically, in spite of available experimental data for some specific systems. In particular, the thermal conductivity of ^{4}He close to the normal-superfluid transition and in confined geometry has been investigated experimentally in some detail. Field-theoretical methods have been employed to

analyze the so-called thermal boundary resistance (Kapitza resistance) between the superfluid ^{4}He and the wall confining the system. This can be carried out by considering Model F dynamics in a semi-infinite space with DBC.[18,37] In spite of these results, for a specific surface quantity, the theoretical prediction for the full finite-size behavior of the thermal resistance across a film is still lacking. Moreover, recent experimental findings[38] are in disagreement with the field-theoretical predictions of Ref. 37. It has been argued that this might be a consequence of the choice of DBC being inappropriate for describing helium confined to a film. Some other transport properties have also been investigated theoretically for the film geometry. In particular, in Ref. 39 the effects of confinement on the critical diffusivities have been studied within the decoupled-mode approximation[40] for the dynamic universality class of liquid-vapor phase transitions in a one-component fluid (Model H in the notion of Ref. 2) and for the superfluid transition (described by Model E[2]) with DBC at the confining plates. The diffusion constant considered is the one associated with the density current and the superfluid flow, respectively. For confined binary mixtures similar quantities were indeed studied previously[41] assuming for the order parameter non-wetting conditions (Neumann boundary conditions) at the confining plates and non-slip boundary conditions for the hydrodynamic shear modes. In Ref. 42 the finite-size behavior of the ultrasonic attenuation which is observed upon approaching the critical point of the superfluid transition in ^{4}He has been studied. The sound velocity can be related to the frequency-dependent specific heat (see Ref. 42 and references therein), allowing for a quite direct field-theoretical analysis within the Gaussian model. Instead of the full Model F dynamics, which is the appropriate one to describe the superfluid transition, it is possible to deal approximately with this problem by considering the simpler Model A dynamics of the superfluid order parameter. Then, by applying Dirichlet boundary conditions, the scaling functions for the ultrasonic attenuation have been computed, resulting in a good agreement with available experimental data.[42]

Recent efforts[43,44] address theoretically some aspects of non-equilibrium (critical) dynamics of a scalar fluctuating field ϕ (which can be, e.g., the order parameter of an Ising ferromagnet or the deformation of an elastic membrane) in film geometry with DBC. The dynamics of ϕ is assumed to be purely dissipative (as in Model A), the effective Hamiltonian is taken as a Gaussian, and the immobile confining walls to be actually "immersed" in the fluctuating medium. However, different from the usual Model A, the fluctuations of the field are taken either to be due to external forces[43] or as quasi-equilibrium thermal noise generated by a space- and time-dependent temperature profile[44] The main focus of these analyses is the computation of the Casimir-like non-equilibrium fluctuation-induced force that acts between the confining walls for different instances of driving forces and temperature profiles, whereas little attention is paid to the actual dynamics of the field ϕ in the space delimited by the walls.

In spite of these results a systematic investigation of the critical dynamics in film geometry is still lacking. In view of the rapidly developing experimental techniques able to resolve space- and time-dependent quantities on the proper mesoscopic scale it is important to provide theoretical predictions for experimentally accessible quantities such, e.g, time-dependent response and correlation functions, dynamics of fluctuation-induced forces, etc.

In the following we set up the field-theoretical description of the purely relaxational dynamics (Model A in the notion of Ref. 2) in film geometry with Dirichlet boundary conditions. We consider the static universality class of systems with a N-component order parameter and $O(N)$-symmetric interactions, such as the Ising model ($N = 1$) or the isotropic XY ($N = 2$) and Heisenberg ($N = 3$) models. Although it is possible to study the relaxational dynamics for general N by kinetic Monte Carlo simulations, for Model A $N = 1$ is the only physically relevant case, experimentally realized in anisotropic magnets. For systems with $N > 1$ the actual dynamics requires a description in terms of more complex models.[2,45] Moreover also the proper description of mixing-demixing transitions in binary liquid mixtures and liquid-vapor transitions in one-component fluids, whose static universal properties are given by the case $N = 1$, calls for different dynamical models and boundary conditions.[2,19] Accordingly, the model we consider here is relevant for the dynamics of actual uniaxial magnetic films (without energy conservation[2]) with symmetry-preserving boundary conditions and for Monte Carlo simulations with Glauber dynamics of $O(N)$ order parameter models with free boundary conditions. Keeping in mind these caveats the present analysis provides a theoretical framework which might nonetheless turn out to be useful also for the more complicated dynamical models. Explicit expressions for the universal scaling functions are obtained within mean-field theory (Gaussian model), whose actual behavior (independent of N) turns out to be already quite rich. We discuss in detail the surface behavior close to the confining walls and the temporal crossover between different regimes. The analysis carried out here lends itself for possible, future extensions within the field-theoretical approach to include the effect of fluctuations beyond mean-field theory.

In the following we shall be concerned with the critical properties of films close to the corresponding *bulk* critical temperature $T_{c,b}$. If the dimensionality d of the confined system (with geometry $\infty^{d-1} \times L$) is such that $d - 1 > d_{\rm lcd}$, where $d_{\rm lcd}$ is the lower critical dimensionality of the model ($d_{\rm lcd} = 1$ for $N = 1$, whereas $d_{\rm lcd} = 2$ for $N \geq 2$), then the effectively $d - 1$-dimensional system becomes critical at a *shifted* critical temperature $T_c(L) < T_{c,b}$.[46] The associated critical properties around $T_c(L)$ are those of the $d - 1$-dimensional bulk universality class. Interesting crossover phenomena take place in the film geometry if the temperature is lowered from $T_{c,b}$ – where the finite-size behavior of the system depends on the *bulk* d-dimensional critical behavior – to $T_c(L)$ where critical singularities with the exponents of the $d - 1$-dimensional universality class show up.

These crossovers have been studied by Monte Carlo simulation both for magnetic and non-magnetic systems (see, e.g., Refs. 5, 10, 47). The theoretical analysis is based on suitable generalizations of the standard renormalization-group theory (see Ref. 48 for a review) and turns out to be rather difficult already for static properties. It would be interesting and challenging to extend such an approach to dynamical properties.

After this introduction the paper is organized as follows. In Sec. 2 we recall some general scaling properties which will be useful in the following. In Sec. 3 the model is described and the universal scaling functions for the dynamic Gaussian linear response and correlation functions are derived and studied in detail in Sec. 4. In addition we discuss the effects of time-dependent fields on the fluctuation-induced Casimir force acting on the confining walls of the system, providing analytic expressions for the associated Gaussian scaling functions. In Sec. 5 the nonlinear relaxation of the order parameter is analyzed at the bulk critical point of the model and the crossover between bulk-like, surface-like, and eventual linear relaxation is emphasized. In Sec. 6 we provide a summary of the main results. Most of the details of the computations are reported in the Appendices B, C, and E–G. Instead, in Appendix A the computation of the bulk universal amplitude ratio associated with the divergence of the relaxation time is reported, whereas in Appendix D we determine and discuss the useful analytic expression for the static order parameter profile across the film in the low-temperature phase and for Dirichlet boundary conditions, which, to our knowledge, has never been reported in the literature.

> After submission the paper "Thickness dependence of second-order magnetic phase transitions in films," Phys. Lett. A **351**, 343 (2006) by J.-P. Adler and A. I. Buzdin, has been published, from which our expression for the order parameter profile can be recovered as a special case of their analysis.

2. GENERAL SCALING PROPERTIES

We consider a confined system in d dimensions with film geometry $\infty^{d-1} \times \mathrm{L}$, Dirichlet-Dirichlet boundary conditions (corresponding to the so-called ordinary-ordinary surface universality class[6]) and purely dissipative relaxational dynamics (Model A of Ref. 2).

For future reference we introduce here some of the notations used in the following. We define the reduced temperature

$$\tau = \frac{T - T_{c,b}}{T_{c,b}} \tag{1}$$

where T is the temperature and $T_{c,b}$ is the transition temperature in the bulk. With ξ and T_R we denote the true correlation length and the true relaxation time, respectively, as the characteristic length and time scales defined via the

exponential decay of two-point *bulk* correlation functions in thermal equilibrium. Upon approaching bulk the critical point ($\tau \to 0$) both ξ and T_R diverge with the following leading singularities:

$$\xi(\tau \to 0^{\pm}) = \xi_0^{\pm} |\tau|^{-\nu} \tag{2}$$

and

$$T_R(\tau \to 0^{\pm}) = T_0^{\pm} |\tau|^{-\nu z} = T_0^{\pm} (\xi/\xi_0^{\pm})^z \tag{3}$$

where ν and z are universal standard bulk critical exponents whereas $\xi_0^{\pm}$ and $T_0^{\pm}$ are non-universal amplitudes depending on the microscopic details of the system. Within mean-field theory (MFT) corresponding to $d > 4$ one has $\nu = 1/2$ and $z = 2$, whereas, for the Ising universality class ($N = 1$) in $d = 3$, $\nu = 0.6301(4)$[3] and $z \simeq 2.02$ (see Ref. 49 and references therein for a summary of the various estimates of z). The values of $\xi_0^{\pm}$ and $T_0^{\pm}$ are different for $\tau \to 0^+$ and $\tau \to 0^-$, forming universal amplitude ratios ξ_0^+/ξ_0^- and T_0^+/T_0^- with $\xi_0^+/\xi_0^- = \sqrt{2}$ within MFT, whereas $\xi_0^+/\xi_0^- = 1.896(10)$ [3] for the Ising universality class in $d = 3$. For the second-moment correlation length similar results can be found in the literature.[3,50] In Appendix 6 the ratio T_0^+/T_0^- is computed to first order in $\epsilon = 4 - d$ for the Ising universality class of Model A, leading to $T_0^+/T_0^- = 2$ within MFT and $T_0^+/T_0^- = 3.3(4)$ in $d = 3$ [4].

The bulk order parameter m vanishes for $\tau \to 0^-$ as

$$m = \mathfrak{m}_0 (-\tau)^{\beta}, \tag{4}$$

with the universal exponent β and the non-universal amplitude $\mathfrak{m}_0$; within MFT $\beta = 1/2$, whereas for the Ising universality class in $d = 3$, $\beta = 0.3265(3)$.[3]

In the following we will be concerned with quantities $\mathscr{O}$ defined in the film geometry. They generally depend on a set $\{\mathbf{x}, t\}$ of spatial coordinates and times, on the temperature (expressed in terms of τ), and on the film thickness L. Since upon approaching the critical point the dominant length and time scales are given by ξ and T_R, respectively, the following scaling behavior is expected in the critical region $|\tau| \ll 1$:

$$\begin{aligned} \mathscr{O}(\{\mathbf{x}, t\}; \tau \lessgtr 0, L) &= \mathfrak{o}_{\mathscr{O}}^{\pm} \left(\frac{\xi}{\xi_0^{\pm}} \right)^{-\Delta_{\mathscr{O}}} F_{\mathscr{O},\pm}^{(1)}(\{\mathbf{x}/\xi, t/T_R\}; L/\xi) \\ &= \mathfrak{o}_{\mathscr{O}}^{\pm} \left(\frac{L}{\xi_0^{\pm}} \right)^{-\Delta_{\mathscr{O}}} F_{\mathscr{O},\pm}^{(2)}(\{\mathbf{x}/L, (t/T_0^{\pm})(\xi_0^{\pm}/L)^z\}; L/\xi) \end{aligned} \tag{5}$$

[3] This quantity is denoted by $U_{\xi_{\text{gap}}}$ in Ref. 3. The numerical value quoted here, obtained by combining high-temperature expansions with a parametric representation of the equation of state, is taken from Tab. 11 therein.

[4] From Eq. (177) one has $T_0^+/T_0^- = 2(1 + 2\epsilon \ln 2/3) + O(\epsilon^2)$. In order to obtain a rough estimate of this ratio for $\epsilon = 1$ the [0, 1] and [1, 0] Padé approximants can be used, yielding the value 3.3(4).

where $\mathfrak{o}^{\pm}_{\mathcal{O}}$ are non-universal constants which have the same engineering dimension as the observable $\mathcal{O}$ and can be expressed in terms of ξ_0^+, $\mathfrak{m}0$, T_0^+, and universal amplitude ratios. $\Delta_{\mathcal{O}}$ is the scaling dimension of the quantity $\mathcal{O}$, and $F^{(i)}_{\mathcal{O},\pm}$, $i = 1, 2$, are universal scaling functions. The second line in Eq. (5) is the scaling form, equivalent to the first one, in which we shall present our results. For the two-point correlation function C (see Sec. 3) one has $\Delta_C = d - 2 + \eta$ (which agrees with the static two-point correlation function and defines the static bulk critical exponent η with $\eta = 0$ within MFT, whereas $\eta = 0.0364(5)^{(3)}$ for the three-dimensional Ising universality class) whereas for the response function R, $\Delta_R = \Delta_C + z = d - 2 + \eta + z$. For the magnetization one has $\Delta_m = \beta/(\nu z)$ ($\Delta_m = \Delta_C/(2z)$ if hyperscaling holds). Crossovers between surface and bulk singular behaviors characterized by surface and bulk critical exponents are related to the singular behavior of the scaling functions $F^{(i)}_{\mathcal{O},\pm}$ if $\mathbf{x}$ approaches the confining walls (see Sec. 5). In this respect one has to keep in mind that the scaling properties (Eq. (5)) only hold in the scaling limit, i.e., distances between two spatial points, distances from confining walls, and time differences must be sufficiently large compared to microscopic scales. The field-theoretical approach has been proven to be a powerful tool to compute both the exponents and the scaling functions appearing in Eq. (5) for various measurable quantities. In the following we present the mean-field form (i.e., Gaussian approximation in the field-theoretical language which is valid for $d = 4$ up to logarithmic corrections) of the scaling functions $F^{(2)}_{\mathcal{O}}$ for various observables. In many cases a reasonably good agreement between experimental or simulation data and field-theoretical computation is already obtained by using mean-field scaling functions combined with higher-order estimates for critical exponents entering into their scaling arguments.

3. THE MODEL

3.1. Definition

The time evolution of a N-component field $\varphi(\mathbf{x}, t) = (\varphi_i(\mathbf{x}, t), i = 1, \ldots, N)$ under purely dissipative relaxation dynamics (Model A of Ref. 2) is described by the stochastic Langevin equation

$$\partial_t \varphi(\mathbf{x}, t) = -\Omega \frac{\delta \mathcal{H}[\varphi]}{\delta \varphi(\mathbf{x}, t)} + \zeta(\mathbf{x}, t), \tag{6}$$

where Ω is a kinetic coefficient, $\zeta(\mathbf{x}, t)$ a zero-mean stochastic Gaussian noise with correlations

$$\langle \zeta_i(\mathbf{x}, t)\zeta_j(\mathbf{x}', t')\rangle = 2\Omega\, \delta(\mathbf{x} - \mathbf{x}')\delta(t - t')\delta_{ij}, \tag{7}$$

and $\mathcal{H}[\varphi]$ is the static Hamiltonian. The universal properties near the critical point of a second-order phase transition are captured by the Landau-Ginzburg

form[1,6,51,52]

$$\mathcal{H}[\varphi] = \int_V \mathrm{d}V \left[\frac{1}{2}(\nabla\varphi)^2 + \frac{1}{2}r_0\varphi^2 + \frac{1}{4!}g_0\varphi^4\right] + \int_{\partial V} \mathrm{d}^{d-1}\mathbf{x}_\parallel \, \frac{c}{2}\varphi^2, \qquad (8)$$

where $r_0 \propto T$ is a parameter that takes the value $r_{0,\mathrm{crit}}$ for $T = T_{c,b}$ ($r_{0,\mathrm{crit}} = 0$ within MFT) and $g_0 > 0$ is the coupling constant providing stability for $\tau < 0$. The surface term implies the boundary conditions $\varphi = c^{-1}\partial_{x_\perp}\varphi$ at $x_\perp = 0, L$ such that the fixed-point value $c = \infty$ leads to Dirichlet boundary conditions as considered in the following; we do not consider surface field contributions $h_s \int_{\partial V} \mathrm{d}^{d-1}\mathbf{x}_\parallel \, \varphi$. We use the notations $V = \mathbb{R}^{d-1} \times [0, L]$ and $\mathrm{d}V = \mathrm{d}^{d-1}\mathbf{x}_\parallel \mathrm{d}x_\perp$, where the position vector $\mathbf{x} = (\mathbf{x}_\parallel, x_\perp)$ is decomposed into the $d-1$-dimensional component $\mathbf{x}_\parallel$ parallel to the confining planar walls and the one-dimensional one $x_\perp$ perpendicular to them.

Instead of solving the Langevin equation for $\varphi[\zeta]$ and then averaging over the noise distribution $P[\zeta]$, the equilibrium correlation and response functions can be directly obtained by means of a suitable field-theoretical action $S[\varphi, \tilde{\varphi}]$[1,51,52] so that, for an observable $\mathcal{O}[\varphi]$,

$$\langle \mathcal{O} \rangle \equiv \int [\mathrm{d}\zeta] \, \mathcal{O}[\varphi[\zeta]] P[\zeta] = \int [\mathrm{d}\varphi \mathrm{d}\tilde{\varphi}] \, \mathcal{O} e^{-S[\varphi,\tilde{\varphi}]}. \qquad (9)$$

(Note that within the conventions we adopt, $\int [\mathrm{d}\varphi \mathrm{d}\tilde{\varphi}] \, e^{-S[\varphi,\tilde{\varphi}]} = 1$[52]). For the Langevin equation (6) with the Gaussian noise (Eq. (7)) the field-theoretical action is given by[1,51,52]

$$S[\varphi, \tilde{\varphi}] = \int \mathrm{d}t \int_V \mathrm{d}V \left[\tilde{\varphi}\partial_t\varphi + \Omega\tilde{\varphi}\frac{\delta\mathcal{H}[\varphi]}{\delta\varphi} - \tilde{\varphi}\Omega\tilde{\varphi}\right], \qquad (10)$$

where $\tilde{\varphi}(\mathbf{x}, t)$ is an auxiliary field, conjugate to an external bulk field h which linearly couples to the order parameter φ so that $\mathcal{H}[\varphi, h] = \mathcal{H}[\varphi] - \int \mathrm{d}V h\varphi$. As a consequence, for an observable $\mathcal{O}$ the following relation for the linear response to the field h holds:

$$\left.\frac{\delta\langle\mathcal{O}\rangle_h}{\delta h(\mathbf{x}, t)}\right|_{h=0} = \Omega\langle\tilde{\varphi}(\mathbf{x}, t)\mathcal{O}\rangle_{h=0} \, , \qquad (11)$$

where $\langle\cdot\rangle_h$ is the average taken with respect to the action $S[\varphi, \tilde{\varphi}; h]$ associated with $\mathcal{H}[\varphi, h]$. In view of Eq. (11), $\tilde{\varphi}(\mathbf{x}, t)$ is called response field. In the following we will be mainly concerned with the response of the order parameter field to the external perturbation h, given by

$$R(\mathbf{x}_1, t_1; \mathbf{x}_2, t_2) = \left.\frac{\delta\langle\varphi(\mathbf{x}_2, t_2)\rangle_h}{\delta h(\mathbf{x}_1, t_1)}\right|_{h=0} = \Omega\langle\tilde{\varphi}(\mathbf{x}_1, t_1)\varphi(\mathbf{x}_2, t_2)\rangle_{h=0}. \qquad (12)$$

Causality implies that $\langle\varphi(\mathbf{x}_2, t_2)\rangle_h$ does not depend on $h(\mathbf{x}_1, t_1)$ whenever $t_1 > t_2$, i.e., the order parameter at a given time does not depend on possible perturbations at later times. Accordingly $R(\mathbf{x}_1, t_1; \mathbf{x}_2, t_2)$ vanishes for $t_2 < t_1$.

The effect of confining walls in the case we are interested in amounts to the Dirichlet boundary condition for the field φ (i.e., infinite surface enhancement c; see above and Ref. 6),

$$\varphi(\mathbf{x}_{\mathcal{B}}, t) = 0\,, \qquad \forall t, \tag{13}$$

where we denote by $\mathbf{x}_{\mathcal{B}}$ the position vector on the boundary ∂V. The Gaussian (i.e., $g_0 = 0$) equation of motion for the field $\tilde{\varphi}$ given by $-\partial_t\tilde{\varphi} + \Omega(-\Delta\tilde{\varphi} + r_0\tilde{\varphi}) = 0$ and Eq. (13) yield the boundary condition.[5]

$$\tilde{\varphi}\partial_{x_\perp}\varphi|_{x_\perp=0}^{L} = 0\,, \tag{14}$$

which is fulfilled by imposing

$$\tilde{\varphi}(\mathbf{x}_{\mathcal{B}}, t) = 0\,, \qquad \forall t. \tag{15}$$

In order to diagonalize the Gaussian part of Eq. (10) it is useful to decompose both fields φ and $\tilde{\varphi}$ in terms of eigenfunctions of the Laplacian Δ fulfilling the boundary conditions (13) and (15)[8,13] according to

$$\phi(\mathbf{x}, t) = \sum_{n=1}^{\infty}\int_{\mathbf{p},\omega} e^{i(\mathbf{p}\cdot\mathbf{x}_\parallel - \omega t)}\hat{\phi}_n(\mathbf{p}, \omega)\Phi_n(x_\perp; L), \tag{16}$$

where $\phi = \varphi, \tilde{\varphi}$, and

$$\int_{\mathbf{p},\omega} \equiv \int_{\mathbb{R}^{d-1}} \frac{\mathrm{d}^{d-1}\mathbf{p}}{(2\pi)^{d-1}}\int_{\mathbb{R}}\frac{\mathrm{d}\omega}{2\pi} \tag{17}$$

with $\mathbf{p}$ as the $d-1$-dimensional momentum parallel to the confining walls. The transverse momentum takes, instead, discrete values $k_n = \pi n/L$ with $n = 1, 2, \ldots$. The eigenfunctions $\Phi_n(x_\perp; L)$ are given by

$$\Phi_n(x_\perp; L) = \sqrt{2/L}\,\sin(k_n x_\perp), \tag{18}$$

so that $\Phi_n(x_\perp = 0; L) = \Phi_n(x_\perp = L; L) = 0$. Note that for the total momentum $\mathbf{q}_n \equiv (\mathbf{p}, k_n)$ one has $|\mathbf{q}_n| \geq \pi/L$ and thus the homogeneous fluctuation mode is suppressed by the boundary conditions. In terms of the functions introduced above, the Gaussian part S_0 of Eq. (10) can be written as

$$S_0[\hat{\varphi}, \hat{\tilde{\varphi}}] = \frac{1}{2}\sum_{n=1}^{\infty}\int_{\mathbf{p},\omega}(\hat{\varphi}_n(-\mathbf{p}, -\omega), \hat{\tilde{\varphi}}_n(-\mathbf{p}, -\omega))\mathbb{M}\begin{pmatrix}\hat{\varphi}_n(\mathbf{p}, \omega)\\ \hat{\tilde{\varphi}}_n(\mathbf{p}, \omega)\end{pmatrix}, \tag{19}$$

where the inverse propagator $\mathbb{M}$ is given by the matrix

$$\mathbb{M} \equiv \begin{pmatrix} 0 & -i\omega + \Omega\left(\mathbf{q}_n^2 + r_0\right)\\ i\omega + \Omega\left(\mathbf{q}_n^2 + r_0\right) & -2\Omega\end{pmatrix}. \tag{20}$$

[5] Indeed $\int_0^L \mathrm{d}x_\perp\tilde{\varphi}\partial_{x_\perp}^2\varphi = \int_0^L \mathrm{d}x_\perp\varphi\partial_{x_\perp}^2\tilde{\varphi} + (\tilde{\varphi}\partial_{x_\perp}\varphi - \varphi\partial_{x_\perp}\tilde{\varphi})|_{x_\perp=0}^{L}$, where $f|_{x_\perp=0}^{L} \equiv f(x_\perp = L) - f(x_\perp = 0)$.

Within MFT, the two-point response and correlation function $R^{(0)}$ and $C^{(0)}$, respectively, are determined by $\mathbb{M}^{-1}$:

$$R^{(0)}_{i_1 i_2 n_1 n_2}(\mathbf{p}_1, \omega_1; \mathbf{p}_2, \omega_2) \equiv \Omega \langle \hat{\tilde{\varphi}}_{i_1 n_1}(\mathbf{p}_1, \omega_1) \hat{\varphi}_{i_2 n_2}(\mathbf{p}_2, \omega_2) \rangle_{g_0 = 0}$$
$$= (2\pi)^d \delta^{(d-1)}(\mathbf{p}_1 + \mathbf{p}_2) \delta(\omega_1 + \omega_2) \delta_{i_1 i_2} \delta_{n_1 n_2} R^{(0)}(\mathbf{q}_{n_2}, \omega_2) \tag{21}$$

where i_k and n_k indicate the field component and the Fourier mode according to Eq. (16), respectively. For the correlation function one finds

$$C^{(0)}_{i_1 i_2 n_1 n_2}(\mathbf{p}_1, \omega_1; \mathbf{p}_2, \omega_2) \equiv \langle \hat{\varphi}_{i_1 n_1}(\mathbf{p}_1, \omega_1) \hat{\varphi}_{i_2 n_2}(\mathbf{p}_2, \omega_2) \rangle_{g_0 = 0}$$
$$= (2\pi)^d \delta^{(d-1)}(\mathbf{p}_1 + \mathbf{p}_2) \delta(\omega_1 + \omega_2) \delta_{i_1 i_2} \delta_{n_1 n_2} C^{(0)}(\mathbf{q}_{n_2}, \omega_2) \tag{22}$$

while $\langle \hat{\tilde{\varphi}}_{i_1 n_1}(\mathbf{p}_1, \omega_1) \hat{\tilde{\varphi}}_{i_2 n_2}(\mathbf{p}_2, \omega_2) \rangle_{g_0 = 0} = 0$ due to causality. From Eq. (20) one obtains

$$R^{(0)}(\mathbf{q}, \omega) = \frac{\Omega}{-i\omega + \Omega(\mathbf{q}^2 + r_0)} \tag{23}$$

and

$$C^{(0)}(\mathbf{q}, \omega) = \frac{2\Omega}{\omega^2 + [\Omega(\mathbf{q}^2 + r_0)]^2}. \tag{24}$$

Note that $R^{(0)}$ and $C^{(0)}$ are the mean-field response and correlation function, respectively, of the system in the bulk. Within MFT the presence of the boundaries is accounted for by the spatial dependence of the eigenfunctions $\Phi_n(x_\perp; L)$ (see Eq. (18)) and by the quantization of the allowed momenta.

For later purposes it will be useful to provide for these functions their representation in terms of time and transversal coordinates $x_{i\perp}$. Following Eq. (16) we define

$$\phi(\mathbf{p}, x_\perp, t) = \sum_{n=1}^{\infty} \int \frac{\mathrm{d}\omega}{2\pi} e^{-i\omega t} \hat{\phi}_n(\mathbf{p}, \omega) \Phi_n(x_\perp; L), \tag{25}$$

and

$$\phi(\mathbf{p}, x_\perp, \omega) = \sum_{n=1}^{\infty} \hat{\phi}_n(\mathbf{p}, \omega) \Phi_n(x_\perp; L), \tag{26}$$

so that, according to Eq. (22),

$$C^{(0)}_{i_1 i_2}(\mathbf{p}_1, x_{1\perp}, t_1; \mathbf{p}_2, x_{2\perp}, t_2) \equiv \langle \varphi_{i_1}(\mathbf{p}_1, x_{1\perp}, t_1) \varphi_{i_2}(\mathbf{p}_2, x_{2\perp}, t_2) \rangle_{g_0 = 0}$$
$$= (2\pi)^{d-1} \delta^{(d-1)}(\mathbf{p}_1 + \mathbf{p}_2) \delta_{i_1 i_2} C^{(0)}(\mathbf{p}_2, x_{1\perp}, x_{2\perp}, t_2 - t_1) \tag{27}$$

and

$$C^{(0)}_{i_1 i_2}(\mathbf{p}_1, x_{1\perp}, \omega_1; \mathbf{p}_2, x_{2\perp}, \omega_2) \equiv \langle \varphi_{i_1}(\mathbf{p}_1, x_{1\perp}, \omega_1) \varphi_{i_2}(\mathbf{p}_2, x_{2\perp}, \omega_2) \rangle_{g_0 = 0}$$
$$= (2\pi)^d \delta^{(d-1)}(\mathbf{p}_1 + \mathbf{p}_2) \delta(\omega_1 + \omega_2) \delta_{i_1 i_2} C^{(0)}(\mathbf{p}_2, x_{1\perp}, x_{2\perp}, \omega_2) \tag{28}$$

with an analogous expression for the response function. Using the above formulae we obtain (recalling that $\mathbf{q}_n \equiv (\mathbf{p}, \pi n/L)$)

$$C^{(0)}(\mathbf{p}, x_{1\perp}, x_{2\perp}, t) = \sum_{n=1}^{\infty} \Phi_n(x_{1\perp}; L)\Phi_n(x_{2\perp}; L) \int \frac{\mathrm{d}\omega}{2\pi} e^{-i\omega t} C^{(0)}(\mathbf{q}_n, \omega) \quad (29)$$

and

$$C^{(0)}(\mathbf{p}, x_{1\perp}, x_{2\perp}, \omega) = \sum_{n=1}^{\infty} \Phi_n(x_{1\perp}; L)\Phi_n(x_{2\perp}; L) C^{(0)}(\mathbf{q}_n, \omega), \quad (30)$$

with $C^{(0)}(\mathbf{q}, \omega)$ given in Eq. (24). In Appendix 6 we show how one recovers the known results for the equal-time correlation function in the film geometry discussed in Refs. 17 and 53 for various boundary conditions and in Ref. 6, Sec. IVA, in the case of a film with equal boundary conditions. Analogous relations hold for the response function.

3.2. The Fluctuation-Dissipation Theorem

For small fluctuations within equilibrium dynamics the two-point response and correlation functions are not independent quantities. The relation between them is provided by the fluctuation-dissipation theorem (FDT):

$$\frac{\mathrm{d}C(t)}{\mathrm{d}t} = -R(t), \qquad \text{for} \qquad t > 0, \quad (31)$$

where with $C(t)$ and $R(t)$ we indicate summarily the time-dependent two-point correlation function and the response function, respectively. As equilibrium quantities their dependence on two time variables reduces to a dependence on the time difference only. Indeed the theorem is a consequence of the time-translation invariance and time-reversal symmetry of equilibrium dynamics. Keeping in mind that correlations vanish in the long-time limit, one thus has

$$C(t) = \int_t^{\infty} \mathrm{d}s \; R(s) \,, \qquad \text{for} \qquad t > 0. \quad (32)$$

Time-reversal symmetry in the equilibrium state implies $C(t) = C(-t)$, which, combined with Eq. (32), allows one to determine completely the correlation function from the response function. Let us recall that the causality of the response function (linear or not) implies $R(t) \propto \theta(t)$ where $\theta(t) = 1$ for $t > 0$ and 0 otherwise. For later purposes it is useful to express the FDT also in other forms. Defining the Fourier transform of $C(t)$ as

$$C(\omega) = \int_{-\infty}^{+\infty} \mathrm{d}t \; e^{i\omega t} C(t) \quad (33)$$

and with an analogous definition for $R(\omega)$ the FDT (Eq. (31)) can be written also as

$$C(\omega) = \frac{2}{\omega} \mathrm{Im} R(\omega) \tag{34}$$

where Im indicates the imaginary part of the expression. Equation (32) and causality yield another useful form of the theorem:

$$C(t = 0) = R(\omega = 0). \tag{35}$$

It is straightforward to verify that $R^{(0)}$ and $C^{(0)}$ given in Eqs. (23) and (24) as well as Eqs. (29) and (30) satisfies the FDT (34). Moreover it can be shown that, as expected on general grounds, this is true also if the effect of fluctuations are taken into account, i.e., beyond MFT.

3.3. Some Mean-Field Results

According to the general scaling properties discussed in Sec. 2, within the Gaussian approximation one can identify the correlation length ξ and the relaxation time T_R from Eqs. (23) and (24):

$$\xi(\tau > 0) = r_0^{-1/2} \tag{36}$$

and

$$T_R(\tau > 0) = (\Omega r_0)^{-1}, \tag{37}$$

respectively. Thus within MFT $\nu = 1/2$ and $z = 2$ as expected, and the kinetic coefficient Ω in Eq. (6) can be expressed in terms of the experimentally accessible (non-universal) amplitudes ξ_0 and T_0 (see Eqs. (2) and (3)) as

$$\Omega = \frac{\xi_0^{+2}}{T_0^+} \tag{38}$$

and

$$r_0 = \frac{\tau}{(\xi_0^+)^2}. \tag{39}$$

Moreover, for $T < T_{c,b}$ the mean-field equation of state for the bulk order parameter m leads to

$$m = (-6 r_0 / g_0)^{1/2}, \tag{40}$$

i.e., $\beta = 1/2$, and

$$g_0 = 6(\mathfrak{m}_0 \xi_0^+)^{-2}. \tag{41}$$

The relations in Eqs. (36)–(41) hold for the present continuum model (Eqs. (6)–(8)).

4. LINEAR BEHAVIOR

In this section we study in some detail the behavior of the response and correlation function for the model introduced in Sec. 3. By virtue of the FDT linear response and correlation functions are not independent but the correlation function can be obtained from the response function and vice versa. We shall first focus on the response function in Subsec. 4.2 and then in Subsec. 4.4 we shall determine correlation functions by applying the FDT.

4.1. Scaling Forms for the Response and Correlation Functions

For future reference we provide here the general scaling forms for some of the quantities we shall discuss in the following. As already stated in Sec. 2 (see Eq. (5)), scaling occurs upon approaching the critical point. In the specific case of the two-point response function in the $(\mathbf{p}, x_\perp, \omega)$-representation one has

$$R(\mathbf{p}, x_{1\perp}, x_{2\perp}, \omega) = \hat{\mathfrak{o}}_R^{\pm} \left(\frac{L}{\xi_0^{\pm}}\right)^{1-\eta} \mathscr{R}_{\pm}(\mathbf{p}L, x_{1\perp}/L, x_{2\perp}/L, \omega T_0^{\pm}(L/\xi_0^{\pm})^z, L/\xi), \tag{42}$$

where $\hat{\mathfrak{o}}_R^{\pm}$ are non-universal amplitudes which we fix to be equal to the corresponding bulk ones. The functions $\mathscr{R}_{\pm}$ are universal scaling functions. In the $(\mathbf{p}, x_\perp, t)$-representation, this reads

$$R(\mathbf{p}, x_{1\perp}, x_{2\perp}, t) = \frac{\hat{\mathfrak{o}}_R^{\pm}}{T_0^{\pm}} \left(\frac{L}{\xi_0^{\pm}}\right)^{1-\eta-z} \bar{\mathscr{R}}_{\pm}(\mathbf{p}L, x_{1\perp}/L, x_{2\perp}/L, (t/T_0^{\pm})(\xi_0^{\pm}/L)^z, L/\xi), \tag{43}$$

where the universal functions $\bar{\mathscr{R}}_{\pm}$ are the Fourier transforms of $\mathscr{R}_{\pm}$ with respect to their fourth argument.

Analogously, for the correlation function in the $(\mathbf{p}, x_\perp, \omega)$-representation one has

$$C(\mathbf{p}, x_{1\perp}, x_{2\perp}, \omega) = \hat{\mathfrak{o}}_C^{\pm} \left(\frac{L}{\xi_0^{\pm}}\right)^{1-\eta+z} \mathscr{C}_{\pm}(\mathbf{p}L, x_{1\perp}/L, x_{2\perp}/L, \omega T_0^{\pm}(L/\xi_0^{\pm})^z, L/\xi), \tag{44}$$

where $\hat{\mathfrak{o}}_C^{\pm}$ are non-universal amplitudes, which again we fix to be equal to the corresponding bulk ones, and the functions $\mathscr{C}_{\pm}$ are universal scaling functions. In the $(\mathbf{p}, x_\perp, t)$-representation, this reads

$$C(\mathbf{p}, x_{1\perp}, x_{2\perp}, t) = \hat{\mathfrak{o}}_C^{\pm} \frac{1}{T_0^{\pm}} \left(\frac{L}{\xi_0^{\pm}}\right)^{1-\eta} \bar{\mathscr{C}}_{\pm}(\mathbf{p}L, x_{1\perp}/L, x_{2\perp}/L, (t/T_0^{\pm})(\xi_0^{\pm}/L)^z, L/\xi), \tag{45}$$

where the universal functions $\bar{\mathscr{C}}_\pm$ are the Fourier transforms of $\mathscr{C}_\pm$ with respect to their fourth argument. In view of the previous scaling forms it is convenient to introduce the following suitable set of dimensionless scaling variables, defined as $\bar{\mathbf{p}} = \mathbf{p}L$, $\bar{x}_{i\perp} = x_{i\perp}/L$, $\bar{t}^{\pm} = (t/T_0^{\pm})(\xi_0^{\pm}/L)^z$, $\bar{\omega}^{\pm} = \omega T_0^{\pm}(L/\xi_0^{\pm})^z$, and $\bar{L} = L/\xi$.

As stated above, concerning the non-universal amplitudes $\hat{\mathfrak{o}}_R^{\pm}$ and $\hat{\mathfrak{o}}_C^{\pm}$ we consider the corresponding correlation functions (Eqs. (42) and (45)) in the bulk. The critical structure factor in the bulk is given by

$$C_{\text{crit}}^{\text{bulk}}(\mathbf{q}, t = 0) = \frac{D_\infty}{q^{2-\eta}}, \tag{46}$$

which defines the non-universal amplitude D_∞ (see, e.g., Ref. 50). Here and in the following using the subscript "crit" means that the function corresponds to $\tau = 0$, i.e., to bulk criticality. Beyond MFT (in this case two-scale universality holds[50]) D_∞ can be expressed in terms of the universal amplitude ratios Q_3, R_c, and R_ξ^+ (see Ref. 50 for their definitions and numerical values) and the non-universal bulk amplitudes $\mathfrak{m}_0$ and ξ_0^+ (see also Ref. 17), as

$$D_\infty = \frac{Q_3 R_c}{(R_\xi^+)^d} \mathfrak{m}_0^2 (\xi_0^+)^{d-2+\eta}. \tag{47}$$

From Eq. (46), via a Fourier transform in one of the d dimensions, one finds

$$C_{\text{crit}}^{\text{bulk}}(\mathbf{p}, x_{1\perp}, x_{2\perp} = x_{1\perp}, t = 0) = \mathcal{G}_V p^{-1+\eta} \tag{48}$$

where $\mathcal{G}_V$ has been introduced in Appendix A of Ref. 17 and is given by

$$\mathcal{G}_V = \frac{D_\infty}{2\sqrt{\pi}} \frac{\Gamma(1/2 - \eta/2)}{\Gamma(1 - \eta/2)}. \tag{49}$$

In view of Eqs. (48) and (45) this leads to

$$\hat{\mathfrak{o}}_C^{\pm} = \mathcal{G}_V T_0^{\pm} (\xi_0^{\pm})^{1-\eta} = \frac{1}{2\sqrt{\pi}} \frac{\Gamma(1/2 - \eta/2)}{\Gamma(1 - \eta/2)} \frac{Q_3 R_c}{(R_\xi^+)^d} \mathfrak{m}_0^2 T_0^{\pm} (\xi_0^{\pm})^{d-1}. \tag{50}$$

The FDT (see Eq. (32)) establishes the following relation between the correlation and response function:

$$C(\mathbf{p}, x_{1\perp}, x_{2\perp}, t = 0) = R(\mathbf{p}, x_{1\perp}, x_{2\perp}, \omega = 0) \tag{51}$$

so that in the bulk one has

$$R_{\text{crit}}^{\text{bulk}}(\mathbf{p}, x_{1\perp}, x_{2\perp} = x_{1\perp}, \omega = 0) = \mathcal{G}_V p^{-1+\eta}. \tag{52}$$

Comparing this equation with Eq. (42) leads to

$$\hat{\mathfrak{o}}_R^{\pm} = \mathcal{G}_V (\xi_0^{\pm})^{1-\eta} = \frac{1}{2\sqrt{\pi}} \frac{\Gamma(1/2 - \eta/2)}{\Gamma(1 - \eta/2)} \frac{Q_3 R_c}{(R_\xi^+)^d} \mathfrak{m}_0^2 (\xi_0^{\pm})^{d-1}. \tag{53}$$

Thus the non-universal amplitudes of R and C are determined by the experimentally accessible non-universal bulk amplitudes $\mathfrak{m}_0$, ξ_0^+, and T_0^+. This fixes the normalization of the scaling functions $\bar{\mathscr{R}}_\pm$ and $\bar{\mathscr{C}}_\pm$. For the present model and within mean-field theory these non-universal amplitudes are

$$D_\infty^{(0)} = 1 \tag{54}$$

and

$$\mathcal{G}_V^{(0)} = \frac{1}{2} \tag{55}$$

so that

$$\hat{\mathfrak{o}}_C^{\pm(0)} = \frac{T_0^\pm \xi_0^\pm}{2} \tag{56}$$

and

$$\hat{\mathfrak{o}}_R^{\pm(0)} = \frac{\xi_0^\pm}{2}. \tag{57}$$

Here and in the following with the superscript (0) we indicate the mean-field value of the quantities which the superscript refers to. The FDT (see Eq. (32)) provides, together with Eqs. (50) and (53), the following relation between the scaling functions $\bar{\mathscr{R}}_\pm$ and $\bar{\mathscr{C}}_\pm$ (and thus between $\mathscr{R}$ and $\mathscr{C}$):

$$\bar{\mathscr{C}}_\pm(\tilde{\mathbf{p}}, \bar{x}_{1\perp}, \bar{x}_{2\perp}, \bar{t}, \bar{L}) = \int_{|\bar{t}|}^\infty \mathrm{d}\bar{s}\, \bar{\mathscr{R}}_\pm(\tilde{\mathbf{p}}, \bar{x}_{1\perp}, \bar{x}_{2\perp}, \bar{s}, \bar{L}). \tag{58}$$

In the following we shall be mainly concerned with the case $\tau > 0$. In order to avoid a clumsy notation we thus shall omit in the following the specification $\pm$ from scaling forms and amplitudes.

In Subsec. 4.2 we shall discuss the behavior of the response function in the semi-infinite geometry close to a confining wall (see, c.f., Eq. (90)). It can be obtained from the scaling function Eq. (43) in the limit $L \to \infty$ with $x_{i\perp}$, ξ, and t fixed. Thus one expects a well-defined limit for the response function, i.e.,

$$\begin{aligned} &\bar{\mathscr{R}}(\mathbf{p}L, x_{1\perp}/L, x_{2\perp}/L, (t/T_0)(\xi_0/L)^z, L/\xi) \\ &\xrightarrow[L\to\infty]{} \left(\frac{L}{\xi}\right)^{-(1-\eta-z)} \bar{\mathscr{R}}^{\infty/2}(\mathbf{p}\xi, x_{1\perp}/\xi, x_{2\perp}/\xi, (t/T_0)(\xi_0/\xi)^z) \end{aligned} \tag{59}$$

where $\bar{\mathscr{R}}^{\infty/2}$ is the scaling function for the semi-infinite geometry. By using the short-distance expansion (6) one easily concludes that for $x_{i\perp} \to 0$ (i.e., $x_{i\perp} \ll$

$\xi, |\mathbf{p}|^{-1}, \xi_0(t/T_0)^{1/z})$ and[6] $t \neq 0$

$$\bar{\mathscr{R}}^{\infty/2}(\mathbf{p}\xi, x_{1\perp}/\xi, x_{2\perp}/\xi, (t/T_0)(\xi_0/\xi)^z)$$
$$\xrightarrow{x_{i\perp}\to 0} \left(\frac{x_{1\perp}}{\xi}\frac{x_{2\perp}}{\xi}\right)^{(\beta_1-\beta)/\nu} \bar{\mathscr{R}}_W^{\infty/2}(\mathbf{p}\xi, (t/T_0)(\xi_0/\xi)^z) \tag{60}$$

where β_1 is the critical exponent for the surface magnetization (6) ($\beta_1 = 1$ at the ordinary transition within mean-field approximation, whereas $\beta_1 \simeq 0.77(2)$[(6)] for the three-dimensional Ising universality class). Considering the case $\mathbf{p} = \mathbf{0}$ and $T \to T_{c,b}$ (i.e., $\xi \to \infty$) one expects

$$\lim_{y\to 0} \bar{\mathscr{R}}_W^{\infty/2}(\mathbf{0}, y) = \mathcal{D} y^{-2(\beta_1-\beta)/(\nu z)+(1-\eta-z)/z}, \tag{61}$$

where $\mathcal{D}$ is a universal constant. Thus, for $T = T_{c,b}$ and $x_{i\perp} \ll \xi_0(t/T_0)^{1/z}$

$$R_{\infty/2}(\mathbf{p} = \mathbf{0}, x_{1\perp}, x_{2\perp}, t \to \infty)$$
$$= \mathcal{D}\frac{\hat{\mathfrak{o}}_R}{T_0}\left(\frac{T_0}{t}\right)^{2(\beta_1-\beta)/(\nu z)-(1-\eta-z)/z} \left(\frac{x_{1\perp}}{\xi_0}\frac{x_{2\perp}}{\xi_0}\right)^{(\beta_1-\beta)/\nu} \tag{62}$$

where $R_{\infty/2}$ is the response function in the semi-infinite geometry.

In Sec. 4.4 we shall discuss in detail the mean-field behavior of the correlation function $C(\mathbf{p}, x_\perp, x_\perp, \omega)$ in planes parallel to the confining walls. For this function we present in the following some scaling properties valid beyond the mean-field approximation.

From a short-distance expansion one concludes that the scaling function $\mathscr{C}$ (see Eq. (44)) of the correlation function C behaves as

$$\mathscr{C}(\mathbf{p}L, x_{1\perp}/L, x_{2\perp}/L, \omega T_0(L/\xi_0)^z, L/\xi)$$
$$\xrightarrow{x_{i\perp}\to 0} \left(\frac{x_{1\perp}}{L}\frac{x_{2\perp}}{L}\right)^{(\beta_1-\beta)/\nu} \mathscr{C}_W(\mathbf{p}L, \omega T_0(L/\xi_0)^z, L/\xi) \tag{63}$$

for $x_{i\perp} \ll L, \xi_0(\omega T_0)^{-1/z}, \xi, |\mathbf{p}|^{-1}$, where $\mathscr{C}_W$ is the universal scaling function associated with the behavior close to the walls (in this case the one located at

[6] Note that in general on the r.h.s. of Eq. (59) the following term appears in addition:

$$\mathcal{S}_R^{\infty/2}\,\delta_+((t/T_0)(\xi_0/\xi)^z)\left(\frac{x_\perp^<}{\xi}\right)^{(\beta_1-\beta)/\nu}\left(\frac{x_\perp^<}{\xi}\right)^{1-\eta_\perp}$$

where $\mathcal{S}_R^{\infty/2}$ is a universal constant, $\delta_+(\bar{t})$ the delta function restricted the positive real axis (such that $\int_0^\infty \mathrm{d}\bar{t}\,\delta_+(\bar{t})f(\bar{t}) = f(0)$ with f test function), $x_\perp^< = \min\{x_{1\perp}, x_{2\perp}\}$, and $\eta_\perp = (\beta_1-\beta)/\nu + \eta$ ($\eta_\perp = 1$ within MFT). This term shows up as a constant in the short-distance expansion of $\bar{\mathscr{R}}^{\infty/2}$ as function of frequency and, via the FDT, in the short-distance expansion of the *static* correlation function (see p. 197 in Ref. 6 and Ref. 54). From Eq. (96) one finds $\mathcal{S}_R^{\infty/2,(0)} = 2$.

$x_\perp = 0$). The behavior of $\mathscr{C}_W$ allows one to define the universal constant

$$\mathcal{A}^W \equiv \mathscr{C}_W(\mathbf{0}, 0, 0), \tag{64}$$

that appears in the scaling behavior

$$C_{\text{crit}}(\mathbf{p} = \mathbf{0}, x_\perp, x_\perp, \omega = 0) = \hat{\mathfrak{o}}_C \, \mathcal{A}^W \left(\frac{L}{\xi_0}\right)^{1-\eta+z} \left(\frac{x_\perp}{L}\right)^{2(\beta_1-\beta)/\nu} \tag{65}$$

of the critical (i.e., $\tau = 0$) correlation function for $x_\perp \ll L$. Analogously we can define the following universal constants:

$$\lim_{w\to\infty} \mathscr{C}_W(\mathbf{0}, 0, w) = \mathcal{A}^W_\infty w^{2(\beta_1-\beta)/\nu-(1-\eta+z)}, \tag{66}$$

$$\lim_{v\to\infty} \mathscr{C}_W(\mathbf{0}, v, 0) = \mathcal{B}^W_\infty v^{2(\beta_1-\beta)/(\nu z)-(1-\eta+z)/z}, \tag{67}$$

and

$$\lim_{\mathbf{u}\to\infty} \mathscr{C}_W(\mathbf{u}, 0, 0) = \mathcal{C}^W_\infty |\mathbf{u}|^{2(\beta_1-\beta)/\nu-(1-\eta+z)} \tag{68}$$

entering into the scaling functions

$$C(\mathbf{p} = \mathbf{0}, x_\perp, x_\perp, \omega = 0) = \hat{\mathfrak{o}}_C \mathcal{A}^W_\infty \left(\frac{\xi}{\xi_0}\right)^{1-\eta+z} \left(\frac{x_\perp}{\xi}\right)^{2(\beta_1-\beta)/\nu} \tag{69}$$

for $x_\perp \ll \xi \ll L$,

$$C_{\text{crit}}(\mathbf{p} = \mathbf{0}, x_\perp, x_\perp, \omega) = \hat{\mathfrak{o}}_C \mathcal{B}^W_\infty (\omega T_0)^{-(1-\eta+z)/z+2(\beta_1-\beta)/(\nu z)} \left(\frac{x_\perp}{\xi_0}\right)^{2(\beta_1-\beta)/\nu} \tag{70}$$

for $(\xi_0/L)^z \ll \omega T_0 \ll (\xi_0/x_\perp)^z$, and

$$C_{\text{crit}}(\mathbf{p}, x_\perp, x_\perp, \omega = 0) = \hat{\mathfrak{o}}_C \mathcal{C}^W_\infty (|\mathbf{p}|\xi_0)^{-(1-\eta+z)+2(\beta_1-\beta)/\nu} \left(\frac{x_\perp}{\xi_0}\right)^{2(\beta_1-\beta)/\nu} \tag{71}$$

for $1/L \ll |\mathbf{p}| \ll 1/x_\perp$, respectively.

From the previous equations we recover the values of well-known surface critical exponents for the semi-infinite geometry, i.e., $\sigma^{(s)}_\tau$, $\sigma^{(s)}_\omega$, and $\sigma^{(s)}_p$.[8,55] They describe the divergence of the two-point correlation function parallel to the surface, so that for $\mathbf{p} = \mathbf{0}$ and $\omega = 0$ it diverges $\sim \tau^{-\sigma^{(s)}_\tau}$, for $\tau = 0$ and $\omega = 0$ it diverges $\sim |\mathbf{p}|^{-\sigma^{(s)}_p}$, whereas for $\mathbf{p} = \mathbf{0}$ and $\tau = 0$ it diverges for $\omega \to 0$ as $\omega^{-\sigma^{(s)}_\omega}$.[55]

As far as the behavior of the correlation function in the middle of the film, i.e., $C(\mathbf{p}, L/2, L/2, \omega)$ is concerned we define (see Eq. (44))

$$\mathscr{C}(\mathbf{p}L, 1/2, 1/2, \omega T_0 (L/\xi_0)^z, L/\xi) = \mathscr{C}_I(\mathbf{p}L, \omega T_0 (L/\xi_0)^z, L/\xi) \tag{72}$$

where $\mathscr{G}_I$ is a universal scaling function. As already discussed for $\mathscr{G}_W$ we can define also from $\mathscr{G}_I$ the following universal constants:

$$\mathscr{G}_I(\mathbf{0}, 0, 0) = \mathcal{A}^I, \tag{73}$$

$$\lim_{w\to\infty} \mathscr{G}_I(\mathbf{0}, 0, w) = \mathcal{A}^I_\infty w^{-(1-\eta+z)}, \tag{74}$$

$$\lim_{v\to\infty} \mathscr{G}_I(\mathbf{0}, v, 0) = \mathcal{B}^I_\infty v^{-(1-\eta+z)/z}, \tag{75}$$

and

$$\lim_{\mathbf{u}\to\infty} \mathscr{G}_I(\mathbf{u}, 0, 0) = \mathcal{C}^I_\infty |\mathbf{u}|^{-(1-\eta+z)}. \tag{76}$$

These constants enter into the following scaling functions:

$$C_{\rm crit}(\mathbf{p} = \mathbf{0}, L/2, L/2, \omega = 0) = \mathcal{A}^I \hat{\mathfrak{o}}_C \left(\frac{L}{\xi_0}\right)^{1-\eta+z}, \tag{77}$$

$$C(\mathbf{p} = \mathbf{0}, L/2, L/2, \omega = 0) = \hat{\mathfrak{o}}_C \mathcal{A}^I_\infty \left(\frac{\xi}{\xi_0}\right)^{1-\eta+z} \quad \text{for} \quad \xi \ll L, \tag{78}$$

$$C_{\rm crit}(\mathbf{p} = \mathbf{0}, L/2, L/2, \omega) = \hat{\mathfrak{o}}_C \mathcal{B}^I_\infty (\omega T_0)^{-(1-\eta+z)/z} \quad \text{for} \quad \omega T_0 \ll \left(\frac{\xi_0}{L}\right)^z, \tag{79}$$

and

$$C_{\rm crit}(\mathbf{p}, L/2, L/2, \omega = 0) = \hat{\mathfrak{o}}_C \mathcal{C}^I_\infty (|\mathbf{p}|\xi_0)^{-(1-\eta+z)} \quad \text{for} \quad |\mathbf{p}| \gg \frac{1}{L}, \tag{80}$$

respectively. In Sec. 4.4 we shall confirm these scaling forms within mean-field approximation and determine also the mean-field values of the universal constants involved.

4.2. Response Function

Our aim here is to discuss, in different representations, the response function introduced in Sec. 3. Combining the analogue of Eq. (29) for the response function and taking into account the explicit expression in Eq. (23) we have

$$\int_{-\infty}^{+\infty} \frac{d\omega}{2\pi} e^{-i\omega t} R^{(0)}(\mathbf{q}_n, \omega) = \theta(t)\, \Omega\, e^{-\Omega(\mathbf{q}_n^2 + r_0)t} \tag{81}$$

and thus

$$R^{(0)}(\mathbf{p}, x_{1\perp}, x_{2\perp}, t) = \theta(t)\, \Omega\, e^{-\Omega(\mathbf{p}^2 + r_0)t} \sum_{n=1}^{\infty} \Phi_n(x_{1\perp}; L)\Phi_n(x_{2\perp}; L) e^{-\Omega(\pi n/L)^2 t}. \tag{82}$$

Using the results of Appendix C we can write

$$R^{(0)}(\mathbf{p}, x_{1\perp}, x_{2\perp}, t)$$
$$= \theta(t)\frac{\xi_0^z}{T_0}\frac{1}{L}e^{-[(\mathbf{p}L)^2+(L/\xi)^2](t/T_0)(\xi_0/L)^z}\Psi(x_{1\perp}/L, x_{2\perp}/L, (t/T_0)(\xi_0/L)^z) \quad (83)$$

with the mean-field expression of the scaling function Ψ given in Eq. (186), which, within MFT, does not depend on $\mathbf{p}$ or ξ. Within the same approximation the scaling variable $(t/T_0)(\xi_0/L)^z$ is given by

$$\bar{t} \equiv (t/T_0)(\xi_0/L)^z = \Omega t/L^2. \quad (84)$$

In favor of a compact notation in the following we use this abbreviation keeping in mind that it can be replaced by the r.h.s. of Eq. (84). The scaling properties of the response function clearly emerge from this expression. Comparing with the general scaling form Eq. (43) it is easy to see that ($\tilde{\mathbf{p}} = \mathbf{p}L$, $\bar{x}_{i\perp} = x_{i\perp}/L$, $\bar{L} = L/\xi$)

$$\bar{\mathscr{R}}^{(0)}(\tilde{\mathbf{p}}, \bar{x}_{1\perp}, \bar{x}_{2\perp}, \bar{t}, \bar{L}) = 2e^{-(\tilde{\mathbf{p}}^2+\bar{L}^2)\bar{t}}\Psi(\bar{x}_{1\perp}, \bar{x}_{2\perp}, \bar{t}) \quad (85)$$

where we used Eq. (57). Moreover, one can easily recover the result for the semi-infinite geometry. Indeed, using Eq. (188) we find that for $\bar{x}_{i\perp} \ll 1$ (i.e., close to the near wall at $x_\perp = 0$) and $\bar{t} \ll 1$ (so that the influence from the wall at $x_\perp = L$ can be neglected near $x_\perp = 0$)

$$R^{(0)}(\mathbf{p}, x_{1\perp} \ll L, x_{2\perp} \ll L, t)$$
$$= \theta(t)\frac{\xi_0^2}{T_0}\frac{1}{L}\frac{e^{-(\tilde{\mathbf{p}}^2+\bar{L}^2)\bar{t}}}{\sqrt{4\pi\bar{t}}}\left[e^{-(\bar{x}_{1\perp}-\bar{x}_{2\perp})^2/(4\bar{t})} - e^{-(\bar{x}_{1\perp}+\bar{x}_{2\perp})^2/(4\bar{t})}\right] \quad (86)$$

in agreement with Eqs. (II.18) and (II.19) in Ref. (8). Note that the previous expression is indeed independent of L, as expected for the limit we are considering. Equation (188) provides also a representation of the response function in terms of the bulk response to a set of image excitations. Let us recall that the response function in the bulk is given by

$$R^{(0)}_{\text{bulk}}(\mathbf{p}, x_{1\perp}, x_{2\perp}, t)$$
$$= \theta(t)\frac{\xi_0}{T_0}e^{-(\mathbf{p}^2\xi_0^2+\xi_0^2/\xi^2)t/T_0}\frac{1}{\sqrt{4\pi t/T_0}}e^{-(x_{1\perp}-x_{2\perp})^2/(4\xi_0^2 t/T_0)}. \quad (87)$$

According to Eqs. (83) and (188) one has

$$R^{(0)}(\mathbf{p}, x_{1\perp}, x_{2\perp}, t) = \sum_{n=-\infty}^{+\infty}\left[R^{(0)}_{\text{bulk}}(\mathbf{p}, x^+_{n\perp}, x_{2\perp}, t) - R^{(0)}_{\text{bulk}}(\mathbf{p}, x^-_{n\perp}, x_{2\perp}, t)\right] \quad (88)$$

where $x^+_{n\perp} \equiv x_{1\perp} + 2nL$ and $x^-_{n\perp} \equiv -x_{1\perp} + 2nL$. The set $\{x^+_{n\perp}\}_{n\neq 0}$ represents the positions at which the "positive" images are located, whereas $\{x^-_{n\perp}\}_n$ gives the

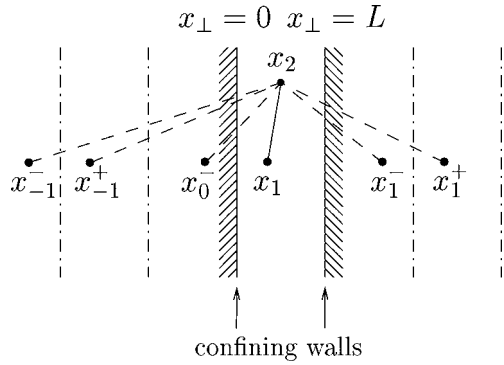

Fig. 1. Set of images corresponding to a perturbation actually applied at x_1. x_2 is the point at which the effects of the perturbation are observed. Image sources are obtained by successive reflections of the real and image sources with respect to the confining walls. At each reflection the sign of the contribution to the total response changes, starting from a positive sign for the actual source.

positions of the "negative" ones. This construction is illustrated in Fig. 1. By virtue of the FDT Eq. (88) is also valid for the correlation function, with R replaced by C in the expression. Moreover it is an extention to the dynamics of the analogous formula known for the static correlation function (see, e.g., Subsec. IVA of Ref. 6 and Ref. 43).

Let us consider the long-time limit of the response function in Eq. (82). For $\bar{t} \gg 1$, i.e., when the effect of confinement is no longer negligible, the sum in Eq. (82) is dominated by the lowest mode of the system, i.e., by $n = 1$. Thus one has

$$R^{(0)}(\mathbf{p}, x_{1\perp}, x_{2\perp}, t \to \infty) = \theta(t)\frac{\xi_0^2}{T_0} e^{-(\bar{\mathbf{p}}^2+\bar{L}^2)\bar{t}}[\Phi_1(x_{1\perp}; L)\Phi_1(x_{2\perp}; L)e^{-\pi^2\bar{t}} + O(e^{-4\pi^2\bar{t}})], \quad (89)$$

i.e., the linear response to an external perturbation decays in time *exponentially* with a factor $\exp[-(\bar{\mathbf{q}}_1^2 + \bar{L}^2)\bar{t}]$ where, according to our notation, $\mathbf{q}_n = (\mathbf{p}, \pi n/L)$. This exponential decay also holds for the two-point correlation functions. Even at $T_{c,b}$ and for excitations which do not break the translational invariance in lateral direction $\mathbf{x}_\parallel$, i.e., for $\mathbf{p} = 0$, there is an exponential decay due to $|\mathbf{q}_1| \geq \pi/L$. This is the result of the combined effect of confinement *and* Dirichlet boundary conditions which suppress homogeneous modes (with vanishing total momentum $\mathbf{q}_0 = \mathbf{0}$) in the system. In the case of periodic and Neumann–Neumann boundary conditions for this confined system we expect an *algebraic* decay as function of time for the critical response to an external perturbation with $\mathbf{p} = \mathbf{0}$, given that the mode with $\mathbf{q}_0 = \mathbf{0}$ does occur in the corresponding spectra. On the other hand an algebraic decay can be recovered also in the case we are considering.

Indeed for $T < T_{c,b}$ the dimensionless variable $\bar{L}^2 = (L/\xi)^2$ appearing in the previous equations has to be replaced by $-1/2(L/\xi)^2$ within MFT leading to the decay $\sim \exp[-(\bar{\mathbf{q}}_1^2 - \bar{L}^2/2)\bar{t}\,]$. Accordingly, upon decreasing the temperature T a critical value $T_c(L) < T_{c,b}$ exist for which this exponent vanishes. For $T = T_c(L)$ the bulk correlation length ξ attains the value $\xi_c = L/\sqrt{2}\pi$. This corresponds to the critical-point shift in film geometry, that can also be determined from the onset of a non-trivial order-parameter profile (see Appendix D). From this point of view the fact that at $T = T_{c,b}$ the response and correlation functions decay exponentially reflects that $T_{c,b}$ is above the critical temperature of the system in the film, i.e., located within the disordered phase of the film. In the case of a semi-infinite system the asymptotic decay of the response function is indeed algebraic even for Dirichlet boundary conditions, as one can see directly from Eq. (86) for $\mathbf{p} = \mathbf{0}$, $T = T_{c,b}$, and $t/T_0 \gg x_{i\perp}^2/\xi_0^2$:

$$R_{\infty/2}^{(0)}(\mathbf{p} = \mathbf{0}, x_{1\perp}, x_{2\perp}, t \to \infty)$$
$$= \frac{1}{\sqrt{4\pi}} \frac{\xi_0}{T_0} \left(\frac{t}{T_0}\right)^{-3/2} \frac{x_{1\perp}}{\xi_0} \frac{x_{2\perp}}{\xi_0} [1 + O((x_{i\perp}/\xi_0)^2 (T_0/t))]. \tag{90}$$

This expression is in agreement with the general scaling form in Eq. (62) with the mean-field values of the exponents and amplitudes (see Eqs. (38) and (57)), and the universal constant $\mathcal{D}$ (see Eq. (61)) takes the value

$$\mathcal{D}^{(0)} = \frac{1}{\sqrt{\pi}}. \tag{91}$$

This can also be interpreted as reflecting the fact that in the semi-infinite geometry there is no critical point shift. The same conclusion can be reached in the case of the film geometry with periodic or Neumann-Neumann boundary conditions which, as mentioned previously, within mean-field theory do not lead to a critical point shift in films.

From Eq. (89) we can see that for asymptotically large times, the spatial dependence of the response function in the film geometry is given by $\sin(\pi x_{1\perp}/L)\sin(\pi x_{2\perp}/L)$.

According to Eq. (11) the linear response function R represent the order-parameter profile due to a δ-like perturbation applied at an early time. Of course, being derived in linear approximation, this function is useful only as long as the subsequent values assumed by the order parameter are small enough compared to nonlinear terms. The case of nonlinear relaxation will be discussed in Sec. 5.

In Fig. 2. the function $\Psi(\bar{x}_{1\perp}, \bar{x}_{2\perp}, \bar{t}\,)$, i.e., $R^{(0)}(\mathbf{p}, x_{1\perp}, x_{2\perp}, t)$ up to a spatially constant prefactor (see Eqs. (43), (83), and (85)), is shown for two values of $\bar{x}_{1\perp}$, i.e., the point at which the perturbation has been applied at time $t = 0$. In accordance with our previous observation, the response function for $\bar{t} \gg 1$ turns into a sine function with period $\bar{x}_{2\perp} = 2$. We observe clearly that there is

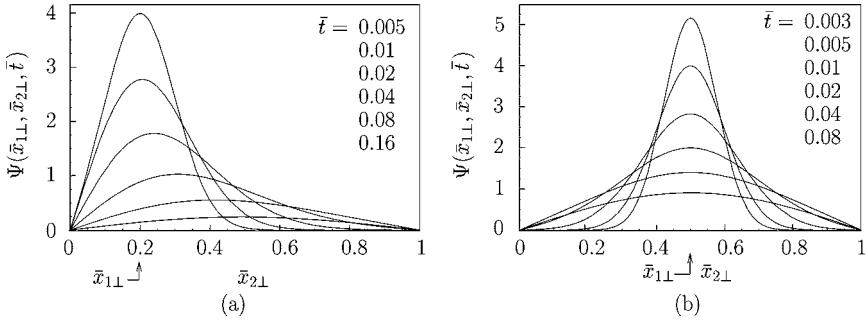

Fig. 2. Time evolution of the scaling function $\Psi(\bar{x}_{1\perp}, \bar{x}_{2\perp}, \bar{t})$ which enters into the expression of the response function in Eq. (83) (see also Eqs. (43) and (85)) with $\bar{x}_{i\perp} = x_{i\perp}/L$ and $\bar{t} = (t/T_0)(\xi_0/L)^z$. In (a) the relaxation follows an excitation at the point $\bar{x}_{1\perp} = 0.2$ and in (b) at the point $\bar{x}_{1\perp} = 0.5$. Reduced times $\bar{t}$ listed in (a) and (b) refer to the various curves shown from top to bottom.

a qualitative change in the shape of the responding order-parameter profile as time increases. In particular the inflection points, which are present just after the perturbation has been applied,[7] disappear in the long-time limit, after having reached the closest surfaces.

In Fig. 3. we report the time $\bar{t}_I(\bar{x}_{1\perp})$ at which the inflection point (of Ψ as a function of $\bar{x}_{2\perp}$) close to the wall at $\bar{x}_\perp = 0$ disappears. Given the symmetry of the problem the analogous time for the inflection close to the wall at $\bar{x}_\perp = 1$ is simply given by $\bar{t}_I(1 - \bar{x}_{1\perp})$. The behavior of $\bar{t}_I(\bar{x}_{1\perp} \to 0)$ can be easily predicted by taking into account that in the semi-infinite geometry, for a given $x_{1\perp}$, we expect a finite non-zero value t_I. According to this argument, in the limit $L \to \infty$ with fixed $x_{1\perp}$, the relation

$$\bar{t}_I = F_{t_I}(\bar{x}_{1\perp}) \tag{92}$$

should become independent of L, i.e., (see Eq. (84))

$$F_{t_I}(y \to 0) \sim y^2 \tag{93}$$

and thus (see Fig. 3)

$$\bar{t}_I(\bar{x}_{1\perp} \to 0) \sim \bar{x}_{1\perp}^2. \tag{94}$$

As discussed in Appendix E it is possible to determine analytically, within MFT, the proportionality factor in Eq. (94), which turns out to be $1/6$. Moreover $F_{t_I}(y = 1)$ can also be determined.

[7] According to Eq. (188), for $\bar{t} \ll 1$, $\Psi(\bar{x}_{1\perp}, \bar{x}_{2\perp}, \bar{t})$ has a Gaussian form as function of $\bar{x}_{2\perp}$ for fixed $\bar{x}_{1\perp}$ and vice versa.

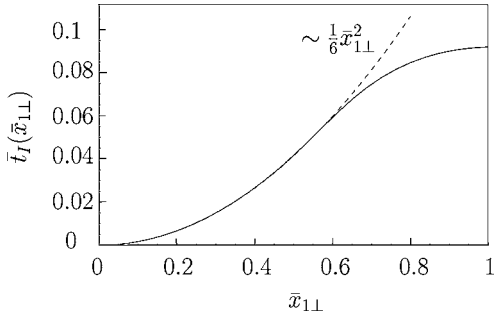

Fig. 3. Time $t_I(\bar{x}_{1\perp})$ at which the inflection in the response function disappears as a function of the position $\bar{x}_{1\perp}$ at which the perturbation is applied. The dashed curve $\bar{t}(\bar{x}_{1\perp}) = \bar{x}_{1\perp}^2/6$ is the quadratic behavior expected for small $\bar{x}_{1\perp}$ which actually describes the curve even for a wide range of values of $\bar{x}_{1\perp}$.

Interestingly, within mean-field theory it is possible to prove (c.f., Subsec. 4.3) that $t_I(\bar{x}_{1\perp})$ has also the meaning of being the time at which the fluctuation-induced force acting on the confining walls is maximal.

Figures 2(a) and 2(b) clearly show that for $\bar{t}$ small enough the order parameter profile is well localized around the point at which the perturbation has been applied, in accordance with the expectation that the effects of the perturbation reach the different points of the system only with a certain delay. On the other hand, irrespective of how small $\bar{t}$ is, the order parameter is non-zero in the *whole* range $0 < \bar{x}_{2\perp} < 1$ (even *everywhere* in the case of unbounded geometries), as one realizes from Eqs. (85) and (186). This absence of a *finite* front propagation speed is a consequence of the coarse-grained description underlying the field-theoretical approach, in which the *microscopic* time and length scales are assumed to be negligible compared to the *mesoscopic* ones, to the effect that the microscopic dynamics, which of course exhibits a speed limit for the front propagation, appears to be actually arbitrarily fast. (This is analogous to the case of random-walk models of free diffusion and their corresponding continuum descriptions.)

For studies of the dynamical properties in the film geometry by means of elastic scattering experiments one is interested in the two-point correlation function in the $(\mathbf{p}, x_\perp, \omega)$-representation. (The corresponding static properties of thin films near continuous phase transitions have been studied theoretically in Ref. 17.) By applying the FDT we can compute the corresponding function once the expression for the response function is known in the same representation. In doing so we can take advantage of the analytical results known for the static correlation function (see Ref. 53 and Appendix B) given that, apart from a factor Ω^{-1}, the expression for $R^{(0)}$ in Eq. (23) is related to that for the static correlation function (i.e., $\int \mathrm{d}\omega/(2\pi) C^{(0)}(\mathbf{q}, \omega) = 1/(\mathbf{q}^2 + \xi^{-2})$) by means of a formal shift $\xi^{-2} \mapsto \xi^{-2} -$

$i\omega/\Omega$. Using Eq. (182) we find[8]

$$R^{(0)}(\mathbf{p}, x_{1\perp}, x_{2\perp}, \omega) = L\frac{\sinh(ax_\perp^<)\sinh[a(L-x_\perp^>)]}{aL\sinh(aL)},$$
$$a^2 \equiv \mathbf{p}^2 + \xi^{-2} - i\omega/\Omega, \tag{95}$$

where $x_\perp^> = \max\{x_{1\perp}, x_{2\perp}\} = (x_{1\perp} + x_{2\perp} + |x_{1\perp} - x_{2\perp}|)/2$, and $x_\perp^< = \min\{x_{1\perp}, x_{2\perp}\} = (x_{1\perp} + x_{2\perp} - |x_{1\perp} - x_{2\perp}|)/2$. Equation (95) agrees with what was found in Ref. 39, Eq. (7), and Ref. 44, Eq. (13). Using Eq. (57) one can write this expression in the scaling form given in Eq. (42):

$$\mathscr{R}^{(0)}(\bar{\mathbf{p}}, \bar{x}_{1\perp}, \bar{x}_{2\perp}, \bar{\omega}, \bar{L}) = 2\frac{\sinh(\bar{a}\bar{x}_\perp^<)\sinh[\bar{a}(1-\bar{x}_\perp^>)]}{\bar{a}\sinh\bar{a}}, \tag{96}$$

where $\bar{x}_\perp^{<,>} = x_\perp^{<,>}/L$,

$$\bar{a}^2 \equiv \bar{\mathbf{p}}^2 + \bar{L}^2 - i\bar{\omega}, \quad \bar{\mathbf{p}} = \mathbf{p}L, \quad \bar{L} = L/\xi, \quad \text{and} \quad \bar{\omega} = (\omega T_0)(L/\xi_0)^z. \tag{97}$$

4.3. Casimir Force

In a confined system the spectrum of the allowed critical fluctuations of the order parameter is modified compared to the bulk case, depending on the specific boundary conditions (i.e., surface universality classes) and on the film thickness L. This leads to a finite-size contribution to the free energy. Accordingly, by varying L one observes that the confining walls are subject to an L-dependent effective force F per cross-section area of the film and per $k_B T_{c,b}$ (where k_B is the Boltzmann constant) which is the statistical analogue[12,15] of the Casimir force of quantum electrodynamics. In the case of the film geometry with the confining plates belonging to (a, b)-surface universality classes [the case we are currently interested in is the ordinary-ordinary (O, O) one] and in the *st*atic case F has been shown to scale as function of the thermodynamic parameters (up to contributions from additive renormalizations) as[14]

$$F(\tau, h, L) = \frac{1}{L^d}\,\mathscr{F}^{(\mathrm{st})}_{a,b}((h/\mathfrak{h}_0)(L/\xi_0)^{\beta\delta/\nu}, L/\xi) \tag{98}$$

where the universal exponent δ and the nonuniversal amplitude $\mathfrak{h}_0$ are defined through the critical equation of state

$$h = \mathfrak{h}_0\frac{m}{\mathfrak{m}_0}\left|\frac{m}{\mathfrak{m}_0}\right|^{\delta-1}, \tag{99}$$

[8] Note that fixing the branch of the square root defining $a = \sqrt{\mathbf{p}^2 + \xi^{-2} - i\,\omega/\Omega}$ is irrelevant, because Eq. (181) is symmetric in a.

which expresses the dependence of the bulk order parameter m on the external field h along the bulk critical isotherm $T = T_{c,b}$. Within MFT one has $\delta = 3$. Because of the two scale-factor universality (see, e.g, Ref. 50) the nonuniversal amplitude $\mathfrak{h}_0$ is related to the nonuniversal amplitudes $\mathfrak{m}_0$ and ξ_0 introduced in Sec. 2 via

$$\mathfrak{h}_0 = \frac{R_\chi (R_\xi^+)^d}{R_c} (\xi_0^+)^{-d} \mathfrak{m}_0^{-1}, \tag{100}$$

where R_c, R_ξ^+ [see also Eq. (47)], and R_χ are universal amplitude ratios whose actual definitions and values can be found in Ref. 50. In Eq. (98) the function $\mathscr{F}_{a,b}^{(\mathrm{st})}$ is a universal scaling function with $\mathscr{F}_{a,b}^{(\mathrm{st})}(0,0) = (d-1)\Delta_{a,b}$. The amplitude $\Delta_{a,b}$ is the so-called universal Casimir amplitude corresponding to (a, b) surface universality classes. The effective force F between the confining walls is attractive when $F < 0$ and repulsive otherwise. In this sense F can be viewed as a special case of the more general case of fluctuation-induced effective interaction between different objects immersed in a critical medium. In the following we consider only the case (O, O) of ordinary-ordinary boundary conditions and therefore we shall omit the specification (a, b) from the scaling functions and amplitudes. Within the Gaussian approximation Δ is given by[13]

$$\Delta = -\frac{1}{(4\pi)^{d/2}} N\, \Gamma(d/2)\zeta(d) \tag{101}$$

where $\Gamma(z)$ and $\zeta(z)$ denote the Gamma function and Riemann's zeta function, respectively. The universal amplitude Δ and the universal scaling function $\mathscr{F}^{(\mathrm{st})}$ can be determined by computing the singular part of the free energy of the system in confined geometry, based on the Hamiltonian (8). An alternative approach, more suited for extensions to dynamics, is based on the connection between the Casimir force and the expectation value of the stress-tensor $T_{\mu\nu}$. (We refer the reader to the literature[15] for details.) In particular one finds that the force density per $k_\mathrm{B} T_{c,b}$ on one of the confining walls ∂V is given by

$$F = \langle T_{\perp\perp} \rangle|_{\partial V} \tag{102}$$

where $T_{\perp\perp}$ is suitably defined in terms of the order parameter field φ. For the case we are interested in one has, in the absence of surface fields (see, e.g., Ref. 15),

$$F_{l(r)}(\mathbf{x}_\parallel) = \langle T_{\perp\perp} \rangle|_{\partial V} = \frac{1}{2} \left\langle \left(\frac{\partial \varphi(\mathbf{x})}{\partial x_\perp} \right)^2 \right\rangle \Bigg|_{\mathbf{x} \in \partial V}. \tag{103}$$

Note that in the *static* case, for which $\partial \langle T_{\mu\nu} \rangle / \partial x_\mu = 0$, where $\mu, \nu = \perp, \parallel$, $\langle T_{\perp\perp} \rangle$ is actually independent of the point of evaluation, including the surfaces. In the *dynamic* case, in general the force density on the left wall (l) is different from the

one on the right wall (r) and it may vary spatially along the walls. The mean force per area on the wall $l(r)$ is given by

$$F_{l(r)} = \frac{1}{A} \int_A \mathrm{d}^{d-1}\mathbf{x}_\parallel \; F_{l(r)}(\mathbf{x}_\parallel). \tag{104}$$

The relation between the thermodynamic Casimir force (defined from the finite-size behavior of the free energy, see, e.g., Ref. 15) and the expectation value of the stress tensor is based on the fact that the *equilibrium* distribution function of the order parameter field φ is proportional to $\exp\{-\mathcal{H}[\varphi]\}$. In the case we are interested in, $\mathcal{H}[\varphi]$ is the Landau–Ginzburg Hamiltonian in Eq. (8). (In turn, the specific expression of the stress-tensor in terms of φ (Eq. (103)) is determined by $\mathcal{H}$.) When studying critical dynamics and the effects of time-dependent external fields, such a connection is no longer evident because equal-time correlation functions are generated through the distribution $\propto \exp\{-\mathcal{H}[\varphi]\}$ only asymptotically for large times, i.e., long after any perturbation has been switched off. In principle it is not even obvious how to define a *thermodynamic* Casimir force when studying dynamics, because strictly speaking in this case the *equilibrium* free energy loses its significance. Therefore we *assume* as the definition of the dynamic Casimir force the time-dependent expectation value of the equilibrium stress-tensor, which renders the static Casimir force in thermal equilibrium (see also Refs. 43, 44). Heuristically, this amounts to assume that at each time, analogous to thermal equilibrium, there is an "energy cost" $A\delta L \langle T_{\perp\perp} \rangle$ associated with the displacement δL of one of the confining walls, i.e., $\langle T_{\perp\perp} \rangle$ provides the *local pressure*.[43,44] It is desirable to establish a clearer connection between this definition of the dynamic Casimir force and the force that can be measured directly in actual experiments and molecular dynamics simulations. The previous definition is particularly suited for field-theoretical analysis. On the other hand it does not lend itself straightforwardly for the study of the dynamic force via Monte Carlo simulations. First, the explicit expression of the stress tensor in terms of the order parameter field can be determined in general only perturbatively in terms of the coupling constant g_0. Second, one has to construct the lattice version of the stress tensor in terms of the microscopic degrees of freedom (e.g., spin variables); this construction is in general not free from ambiguities. An alternative approach to this problem has been taken in Ref. 56 to study the statistical fluctuations of the Casimir force[57] via Monte Carlo simulations. However, so far this approach could be implemented only for periodic boundary conditions.

We now consider the case in which the film, thermodynamically close to $T_{c,b}$, is perturbed by a time-dependent external field $h(\mathbf{x}, t)$. For the ensuing *dy*namic force density per $k_\mathrm{B} T_{c,b}$ exerted on one of the confining walls one expects a scaling

behavior, as in Eq. (98),

$$F_{l(r)}(\mathbf{x}_\parallel, \tau, L, t, \{h(\mathbf{x}, t)\}) = \frac{1}{L^d} \mathscr{F}^{(\mathrm{dy})}_{a,b}(\mathbf{x}_\parallel/L, L/\xi, (t/T_0)(\xi_0/L)^z, \{(h(\mathbf{x}/L, (t/T_0)(\xi_0/L)^z)/\mathfrak{h}_0)(L/\xi_0)^{\beta\delta/\nu}\}) \tag{105}$$

in terms of the scaling field $\bar{h}$ defined via

$$h(\mathbf{x}, t) = \mathfrak{h}_0(L/\xi_0)^{-\beta\delta/\nu}\bar{h}(\mathbf{x}/L, (t/T_0)(\xi_0/L)^z). \tag{106}$$

In Eq. (105) we have assumed that L does not vary as function of time. For a time-independent, spatially homogeneous external field h, $\mathscr{F}^{(\mathrm{dy})}_{a,b}$ reduces to $\mathscr{F}^{(\mathrm{st})}_{a,b}$ introduced in Eq. (98). As explained in Appendix F, within the Gaussian approximation it is possible to compute the force F exactly for a general external applied field $h(\mathbf{x}, t)$. In order to elucidate some qualitative features of the dynamics of the Casimir force after the perturbation, we consider the particular case in which the field is instantaneously applied at a given time t_1 and then immediately switched off again, i.e., $h(\mathbf{x}, t) = h(\mathbf{x})\delta(t - t_1)$ with $h(\mathbf{x})$ localized in the interior of the film. After the perturbation the response starts to propagate in the film. At the very early stage the response has practically not yet reached the confining walls, so that the force acting on them is basically the equilibrium one corresponding to a vanishing magnetic field. In course of time the perturbation induced by the field hits the confining walls and correspondingly the force exerted on them changes. Finally, because of the relaxational character of the dynamics, in the limit of long times the perturbation induced by h disappears and accordingly the effective force reaches again its equilibrium value.

4.3.1. Planar Perturbation

In order to illustrate such a behavior we consider the case in which the perturbation does not break the translational symmetry along the confining walls and is localized in the plane $x_\perp = x_{1\perp}$, i.e., $h(\mathbf{x}, t) = h_W\delta(x_\perp - x_{1\perp})\delta(t - t_1)$. From Eqs. (231) and (232) one finds for the left wall (the upper index $^{(0)}$ indicates the Gaussian approximation)

$$\mathscr{F}^{(\mathrm{dy})(0)}_{l}(\bar{L}, \bar{t}, \hat{h}_W) = \mathscr{F}^{(\mathrm{st})(0)}(0, \bar{L}) + \frac{1}{8}\hat{h}^2_W \left[\partial_{\bar{x}_{2\perp}}\bar{\mathscr{R}}^{(0)}_l(\bar{\mathbf{p}} = \mathbf{0}, \bar{x}_{1\perp}, \bar{x}_{2\perp}, \bar{t} - \bar{t}_1, \bar{L})|_{\bar{x}_{2\perp}=0}\right]^2, \tag{107}$$

where the scaling function $\bar{\mathscr{R}}^{(0)}$ of the response function is given by Eq. (85) and

$$\hat{h}_W = \xi_0^{(d+2)/2} \left(\frac{L}{\xi_0}\right)^{\beta\delta/\nu - z - 1} \frac{1}{\xi_0 T_0} h_W \tag{108}$$

is the scaling variable associated with h_W. In the present case the functional dependence of the force density on $h(\mathbf{x}, t)$ reduces to the dependences on h_W, $x_{1\perp}$, and t_1 and there is no spatial dependence of the force on the lateral coordinates. According to Eq. (107), the response of the Casimir force to an external field is related to the square of the spatial derivative of the response function evaluated at one of the confining walls. As expected, the Casimir force depends only on the time $\delta\bar{t} = \bar{t} - \bar{t}_1$ elapsed since the application of the external perturbation.

In the following we discuss in more detail the relaxation of the Casimir force at the bulk critical point $T = T_{c,b}$, i.e., for $\bar{L} = 0$. In this case $\bar{\mathscr{R}}^{(0)}(\bar{\mathbf{p}} = \mathbf{0}, \bar{x}_{1\perp}, \bar{x}_{2\perp}, \delta\bar{t}, \bar{L} = 0) = 2\Psi(\bar{x}_{1\perp}, \bar{x}_{2\perp}, \delta\bar{t})$ [see Eq. (85)] and plots of the function Ψ are provided in Fig. 2 for various values of its scaling arguments. In the present context the square of the derivative of these graphs at $\bar{x}_{2\perp} = 0$ matters; $\bar{x}_{1\perp}$ is the position of the applied perturbation. Moreover, the static contribution in Eq. (107) is simply given by the Casimir amplitude Δ [see Eq. (101)], i.e., $\mathscr{T}^{(\mathrm{st})(0)}(0, \bar{L} = 0) = (d-1)\Delta$. Note that $\Delta < 0$ for the case we are interested in,[13] whereas the contribution stemming from the field perturbation is always positive. Therefore the overall sign of the effective force on the left wall depends on the strength $\hat{h}_W$ of the applied field and on the actual position where it has been applied; in particular it may become positive, i.e., repulsive within a time window during the relaxation process. Given the expression of Ψ in Appendix 6 [see Eq. (186)] it is possible to compute analytically the critical scaling function in Eq. (107). According to the qualitative behavior described above and according to Fig. 4.2, $|\partial_{\bar{x}_{2\perp}} \bar{\mathscr{R}}^{(0)}(\bar{\mathbf{p}} = \mathbf{0}, \bar{x}_{1\perp}, \bar{x}_{2\perp}, \bar{t}, \bar{L} = 0)|_{\bar{x}_{2\perp}=0}| = 2|\partial_{\bar{x}_{2\perp}} \Psi(\bar{x}_{1\perp}, \bar{x}_{2\perp}, \bar{t})|_{\bar{x}_{2\perp}=0}|$ displays, as function of time, a maximum for $\bar{t} = \bar{t}_M(\bar{x}_{1\perp})$ which is implicitly defined by the condition

$$\partial_{\bar{t}} \partial_{\bar{x}_{2\perp}} \Psi(\bar{x}_{1\perp}, \bar{x}_{2\perp}, \bar{t})|_{\bar{x}_{2\perp}=0, \bar{t}=\bar{t}_M(\bar{x}_{1\perp})} = 0\,. \tag{109}$$

On the other hand, from the definition of Ψ in Eq. (183), together with Eq. (18) it is easy to realize that $\partial_{\bar{t}} \Psi(\bar{x}_{1\perp}, \bar{x}_{2\perp}, \bar{t}) = \partial^2_{\bar{x}_{1\perp}} \Psi(\bar{x}_{1\perp}, \bar{x}_{2\perp}, \bar{t}) = \partial^2_{\bar{x}_{2\perp}} \Psi(\bar{x}_{1\perp}, \bar{x}_{2\perp}, \bar{t})$. Accordingly $\partial_{\bar{t}} \partial_{\bar{x}_{2\perp}} \Psi(\bar{x}_{1\perp}, \bar{x}_{2\perp}, \bar{t}) = \partial^3_{\bar{x}_{2\perp}} \Psi(\bar{x}_{1\perp}, \bar{x}_{2\perp}, \bar{t})$ and the necessary condition (109) can be written as

$$\partial^3_{\bar{x}_{2\perp}} \Psi(\bar{x}_{1\perp}, \bar{x}_{2\perp}, \bar{t})|_{\bar{x}_{2\perp}=0, \bar{t}=\bar{t}_M(\bar{x}_{1\perp})} = \Psi^{(0,3)}(\bar{x}_{1\perp}, 0, t_M(\bar{x}_{1\perp})) = 0\,. \tag{110}$$

where we use the notation introduced after Eq. (215) in Appendix E. Comparing Eq. (110) with Eq. (221) one sees that $\bar{t}_M(\bar{x}_{1\perp})$ and $\bar{t}_I(\bar{x}_{1\perp})$ (Eq. (92)) satisfy the same equation. On the basis of the qualitative behavior of Ψ one expects the solution to be unique and thus $\bar{t}_M(\bar{x}_{1\perp}) = t_I(\bar{x}_{1\perp})$, i.e., the time at which

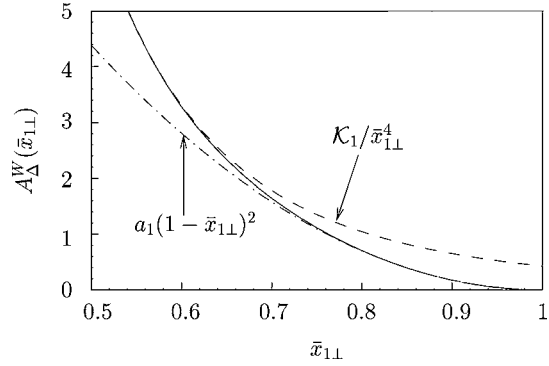

Fig. 4. Dependence of the amplitude $A_\Delta^W(\bar{x}_{1\perp})$, which determines the critical Casimir force maximum $(d-1)\Delta + \hat{h}_W^2 A_\Delta^W(\bar{x}_{1\perp})$ on the left wall [Eq. (111)], on the normal distance $\bar{x}_{1\perp}$ where the planar perturbation is applied. The asymptotic behaviors for $\bar{x}_{1\perp} \to 0$ and $\bar{x}_{1\perp} \to 1$ are indicated as dashed and dashed-dotted lines, with $\mathcal{K}_1 = 27e^{-3}/\pi \simeq 0.427889$ and $a_1 \simeq 17.541$, respectively. Note that already for $\bar{x}_{1\perp} \lesssim 0.6$ the asymptotic behavior $\mathcal{K}_1/\bar{x}_{1\perp}^4$ for $\bar{x}_{1\perp} \to 0$ provides a rather good estimate of the actual value $A_\Delta^W(\bar{x}_{1\perp})$.

$|\partial_{\bar{x}_{2\perp}} \Psi(\bar{x}_{1\perp}, \bar{x}_{2\perp}, \bar{t})|_{\bar{x}_{2\perp}=0}|$ displays a maximum for a fixed value of $\bar{x}_{1\perp}$ equals the time $\bar{t}_I(\bar{x}_{1\perp})$ at which the inflection point of $\Psi(\bar{x}_{1\perp}, \bar{x}_{2\perp}, \bar{t})$ as a function of $\bar{x}_{2\perp}$ reaches the surface at $\bar{x}_{2\perp} = 0$ (see Fig. 3).

Motivated by Eq. (107) we define

$$A_\Delta^W(\bar{x}_{1\perp}) = \frac{\mathscr{T}_l^{(\mathrm{dy})(0)}(0, \bar{t}_I(\bar{x}_{1\perp}), \hat{h}_W) - \mathscr{T}^{(\mathrm{st})(0)}(0,0)}{\hat{h}_W^2}$$

$$= \frac{1}{2}\left[\partial_{\bar{x}_{2\perp}} \Psi(\bar{x}_{1\perp}, \bar{x}_{2\perp}, \bar{t}_I(\bar{x}_{1\perp}))|_{\bar{x}_{2\perp}=0}\right]^2 \tag{111}$$

so that $(d-1)\Delta + \hat{h}_W^2 A_\Delta^W(\bar{x}_{1\perp})$ is the maximum value of the force to which the left wall at $\bar{x}_\perp = 0$ is subject if the field is applied at the normal distance $\bar{x}_{1\perp}$. Figure 4 shows the dependence of the maximum of the field-induced force on the position $x_{1\perp}$ of the perturbation whereas in Fig. 5 we show the time dependence of the normalized dynamic part of the force

$$\mathscr{T}_\Delta^W(\bar{x}_{1\perp}, \bar{t}) = \frac{\mathscr{T}_l^{(\mathrm{dy})(0)}(0, \bar{t}, \hat{h}_W) - \mathscr{T}^{(\mathrm{st})(0)}(0,0)}{\hat{h}_W^2 A_\Delta^W(\bar{x}_{1\perp})} \tag{112}$$

for various values of $\bar{x}_{1\perp}$. The asymptotic behaviors of $A_\Delta^W(\bar{x}_{1\perp})$ for $\bar{x}_{1\perp} \to 0$ and $\bar{x}_{1\perp} \to 1$ are given by $A_\Delta^W(\bar{x}_{1\perp} \to 0) = \mathcal{K}_1/\bar{x}_{1\perp}^4$ with $\mathcal{K}_1 = 27e^{-3}/\pi \simeq 0.427889$ and $A_\Delta^W(\bar{x}_{1\perp} \to 1) = a_1(1-\bar{x}_{1\perp})^2$ with $a_1 \simeq 17.541$, respectively (see Appendix F.2). As Fig. 4 clearly shows, they provide very good approximations to the actual function A_Δ^W already for $\bar{x}_{1\perp} \lesssim 0.6$ and $\bar{x}_{1\perp} \gtrsim 0.75$, respectively. As

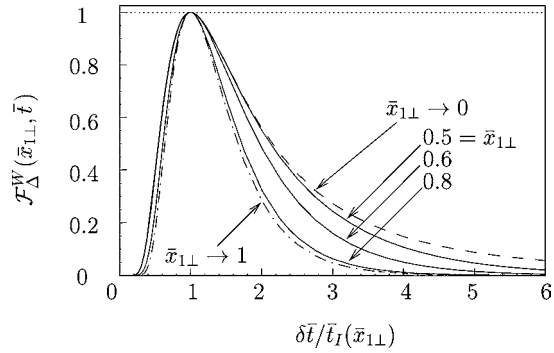

Fig. 5. Time dependence of the normalized dynamic part of the critical Casimir force $\mathscr{T}^W_\Delta(\bar{x}_{1\perp}, \bar{t}\,) = [\mathscr{T}^{(\mathrm{dy})(0)}_l(0, \bar{t}, \hat{h}_W) - \mathscr{T}^{(\mathrm{st})(0)}(0, 0)]/[\hat{h}^2_W A^W_\Delta(\bar{x}_{1\perp})]$ for various values of the position $\bar{x}_{1\perp}$ where the perturbation is applied. For $\bar{t} = \bar{t}_I(\bar{x}_{1\perp})$ the Casimir force reaches its maximum (compare Fig. 3). The dashed and dash-dotted lines indicate the limiting shapes of the curves for $\bar{x}_{1\perp} \to 0$ and $\bar{x}_{1\perp} \to 1$, respectively. For $\bar{t} \gg 1/(3\pi^2)$ the actual curves decay as $\sim e^{-2\pi^2\bar{t}}$.

expected, when the plane in which the external field is applied approaches the distant wall (i.e., $\bar{x}_{1\perp} \to 1$), the actual response of the system is reduced due to the Dirichlet boundary condition there and, due to the relaxational character of the dynamics, the ensuing perturbation affects only slightly the wall at $\bar{x}_\perp = 0$. This qualitative behavior clearly emerges from Fig. 4. On the other hand, if the external field is applied close to that wall where the response is monitored, the spatial variation of the response function as a function of $\bar{x}_{2\perp}$ is sufficiently pronounced to induce a strong force on the close wall. However, this force quickly decays with time, and indeed $\bar{t}_I(\bar{x}_{1\perp} \to 0) \to 0$ (see Fig. 3). The time dependence of the normalized dynamic part of the force $\mathscr{T}^W_\Delta(\bar{x}_{1\perp}, \bar{t}\,)$, reported in Fig. 5, depends only weakly on $\bar{x}_{1\perp}$ when plotted as a function of the scaled time $\bar{t}/\bar{t}_I(\bar{x}_{1\perp})$. In Eqs. (245) and (246) we provide the asymptotic expressions for $\mathscr{T}^W_\Delta(\bar{x}_{1\perp} \to 1, \bar{t}\,)$ and $\mathscr{T}^W_\Delta(\bar{x}_{1\perp} \to 0, \bar{t}\,)$, respectively, shown in Fig. 5. For $\bar{x}_{1\perp}$ fixed and within mean-field theory $\mathscr{T}^W_\Delta$ decays asymptotically as $\mathscr{T}^W_\Delta(\bar{x}_{1\perp}, \bar{t} \to \infty) \sim e^{-2\pi^2\bar{t}}$ (see Eq. (247)).

4.3.2. Localized Perturbation

Here we discuss the case in which the external field is localized at a single point $(\mathbf{x}_{1\parallel}, x_{1\perp})$ within the film, i.e., $h(\mathbf{x}, t) = h_P\delta(\mathbf{x}_\parallel - \mathbf{x}_{1\parallel})\delta(x_\perp - x_{1\perp})\delta(t - t_1)$. From Eqs. (231) and (232) one finds for the left wall at $\bar{x}_\perp = 0$

$$\mathscr{T}^{(\mathrm{dy})(0)}_l(\bar{L}, \bar{t}, \hat{h}_P) = \mathscr{T}^{(\mathrm{st})(0)}(0, \bar{L}) + \frac{1}{2}\hat{h}^2_P \frac{e^{-(\delta\bar{\mathbf{x}}_\parallel)^2/(2\delta\bar{t}) - 2\bar{L}^2\delta\bar{t}}}{(4\pi\delta\bar{t}\,)^{d-1}} \left[\partial_{\bar{x}_{2\perp}} \Psi(\bar{x}_{1\perp}, \bar{x}_{2\perp}, \delta\bar{t}\,)|_{\bar{x}_{2\perp}=0}\right]^2, \quad (113)$$

where $\delta\bar{t} = \bar{t} - \bar{t}_1$ and $\delta\bar{\mathbf{x}}_\parallel = \bar{\mathbf{x}}_\parallel - \bar{\mathbf{x}}_{1\parallel}$. The function Ψ is given by Eq. (186) and

$$\hat{h}_P = \xi_0^{(d+2)/2} \left(\frac{L}{\xi_0}\right)^{\beta\delta/\nu - z - d} \frac{1}{\xi_0^d T_0} h_P. \tag{114}$$

In the following we discuss in more detail the relaxation of the Casimir force at bulk criticality $T = T_{c,b}$, i.e., $\bar{L} = 0$. Different from the case of a planar perturbation, here at a given time the force varies laterally. It depends on the normal distance of the epicenter from the wall under consideration and on the radial distance $|\delta\bar{\mathbf{x}}_\parallel|$ from the epicenter projected on this wall. The force decreases monotonically for increasing radial distances $|\delta\bar{\mathbf{x}}_\parallel|$. The qualitative time dependence of the force, generated by a point-like perturbation, is expected to be independent of the actual lateral position where it acts: As in the case of planar perturbations, the force equals the equilibrium one for very short and very long times with a maximum in between at $\bar{t} = \bar{t}_M(\delta\bar{\mathbf{x}}_\parallel, \bar{x}_{1\perp})$ measured from $\bar{t}_1$. Upon increasing the lateral distance $|\delta\bar{\mathbf{x}}_\parallel|$ from the source of the perturbation $\bar{t}_M$ is expected to increase, because the perturbation has to cover a larger distance until it hits the wall at the specified point. The asymptotic behavior of $\bar{t}_M$ for large $|\delta\bar{\mathbf{x}}_\parallel|$ can be inferred from Eq. (113) by taking into account that

$$\Psi^{(0,1)}(\bar{x}_{1\perp}, 0, \bar{t}\,) \equiv \partial_{\bar{x}_{2\perp}} \Psi(\bar{x}_{1\perp}, \bar{x}_{2\perp}, \bar{t}\,)|_{\bar{x}_{2\perp}=0} = 2\pi \sum_{n=1}^{\infty} n e^{-\pi^2 n^2 \bar{t}} \sin(\pi n \bar{x}_{1\perp}) \,. \tag{115}$$

For $\pi^2\bar{t} \gg 1$ the sum is dominated by its first term. This allows one to determine its extremum as function of $\bar{t}$. At leading order the result is independent of $\bar{x}_{1\perp}$:

$$\bar{t}_M(|\delta\bar{\mathbf{x}}_\parallel| \gg 1, \bar{x}_{1\perp}) = \frac{\sqrt{4\pi^2(\delta\bar{\mathbf{x}}_\parallel)^2 + (d-1)^2} - (d-1)}{4\pi^2}. \tag{116}$$

It is remarkable that in spite of the diffusive propagation of the perturbation (Eq. (113)), the maximum of the laterally varying force moves asymptotically with constant velocity: $\bar{t}_M(|\delta\bar{\mathbf{x}}_\parallel| \to \infty) = |\delta\bar{\mathbf{x}}_\parallel|/(2\pi)$ so that with Eq. (84) this asymptotic speed v is given by

$$v = 2\pi(\xi_0/T_0)(\xi_0/L)^{z-1}. \tag{117}$$

Thus this speed decreases with increasing film thickness. It is possible to provide an estimate of the typical value of v by considering the values of ξ_0 and T_0 that have been experimentally determined. In Ref. 58 the critical dynamics of a ultrathin film (bilayer) of iron grown on a tungsten substrate has been investigated via the magnetic ac susceptibility. This system should provide a realization of the two-dimensional Ising universality class with Model A dynamics ($z \simeq 2.1$ [49,58]). In particular $T^+_{0,\mathrm{exp}}$ for the exponential relaxation time (see Appendix 6) has been obtained from the fit of experimental data, yielding $T^+_{0,\mathrm{exp}} = 2.6 \pm 0.6 \times 10^{-10}$ s.

For ξ_0 we take $\xi_0 \simeq 3\text{Å}$ corresponding to the lattice constant, as it is usually the case in magnetic materials.[45] Accordingly, for a thin film with $L = 50\,\xi_0$, one finds $v \simeq 0.1$ m/s.

By using the behavior of $\Psi^{(0,1)}$ for $\pi^2\bar{t} \ll 1$ reported in Eqs. (236) and (237) for $\bar{x}_{1\perp} \to 1$ and $\bar{x}_{1\perp} \to 0$, respectively, one can determine the corresponding behaviors of $\bar{t}_M$ under the assumption $\pi^2\bar{t}_M \ll 1$ for which they are given by

$$\bar{t}_M = \frac{d + 5 + (\delta\bar{\mathbf{x}}_\parallel)^2 - \sqrt{[d + 5 + (\delta\bar{\mathbf{x}}_\parallel)^2]^2 - 4(d+2)[(\delta\bar{\mathbf{x}}_\parallel)^2 + 1]}}{4(d+2)} \tag{118}$$

for $\bar{x}_{1\perp} \to 1$ and

$$\bar{t}_M = \frac{(\delta\bar{\mathbf{x}}_\parallel)^2 + \bar{x}_{1\perp}^2}{2(d+2)} \quad \text{for} \quad \bar{x}_{1\perp} \to 0. \tag{119}$$

Comparing with the numerical determination of $\bar{t}_M(\delta\bar{\mathbf{x}}_\parallel, \bar{x}_{1\perp})$ it turns out that Eq. (119) provides a good approximation for $\bar{t}_M$ up to few percent in the region $|\delta\bar{\mathbf{x}}_\parallel|, \bar{x}_{1\perp} \lesssim 0.5$, which corresponds to $\bar{t}_M \lesssim 0.1$. (Note that for $d = 1$ and $\delta\bar{\mathbf{x}}_\parallel = 0$ we formally recover the result for the planar perturbation, as can be seen by comparing Eqs. (107) and (113).) In particular, from Eq. (118) one finds $\bar{t}_M(\delta\bar{\mathbf{x}}_\parallel = 0, \bar{x}_{1\perp} \to 1) = (4 - \sqrt{11})/10 \simeq 0.0683375$ for $d = 3$ and $\bar{t}_M(\delta\bar{\mathbf{x}}_\parallel = 0, \bar{x}_{1\perp} \to 1) = (9 - \sqrt{57})/20 \simeq 0.0604236$ for $d = 4$ for which the Gaussian approximation becomes exact apart from logarithmic corrections. In the case $\bar{x}_{1\perp} \to 0$ one finds from Eq. (119), $\bar{t}_M(\delta\bar{\mathbf{x}}_\parallel = 0, \bar{x}_{1\perp} \to 0) = \bar{x}_{1\perp}^2/[2(d+2)]$.

Figure 6(a) shows $\bar{t}_M(\delta\bar{\mathbf{x}}_\parallel, \bar{x}_{1\perp})$ in $d = 3$ as a function of $|\delta\bar{\mathbf{x}}_\parallel|$ for certain values of $\bar{x}_{1\perp}$. The asymptotic behaviors for $\bar{x}_{1\perp} \to 1$ (Eq. (118)) and for $\bar{x}_{1\perp} \to 0$ (Eq. (119)) as functions of $|\delta\bar{\mathbf{x}}_\parallel|$ are also shown as dashed lines up to a corresponding value of $\bar{t}_M \simeq 0.1$ (fulfilling the condition $\pi^2\bar{t}_M \lesssim 1$ under which Eqs. (118) and (119) have been derived). The dash-dotted line in Fig. 6(a) indicates the leading linear behavior of $\bar{t}_M$ for large $|\delta\bar{\mathbf{x}}_\parallel|$ [see Eq. (116)], which provides a rather good approximation of the actual dependence already for $|\delta\bar{\mathbf{x}}_\parallel| \geq 1.0$. Figure 6(b) shows the comparison between $\bar{t}_M(\delta\bar{\mathbf{x}}_\parallel = 0, \bar{x}_{1\perp})$ in $d = 3, 4$ and $\bar{t}_I(\bar{x}_{1\perp})$ (see also Fig. 3) [formally corresponding to the case $d = 1$]. The dashed curves indicate the approximate expression Eq. (119) valid for small $\bar{x}_{1\perp}$, actually providing a rather good approximation already for $\bar{x}_{1\perp} \leq 0.6 - 0.8$. Figure 6(b) clearly indicates that t_M decreases upon increasing d. Indeed, for fixed $\bar{x}_{1\perp}$, the factor $\bar{t}^{d-1}$ in the denominator of Eq. (113) increases the force at short times compared to the case of the planar perturbation (Eq. (107)) where it is absent. This causes the maximum of the resulting force to occur at earlier times $\bar{t}$, as indicated by Fig. 6(b).

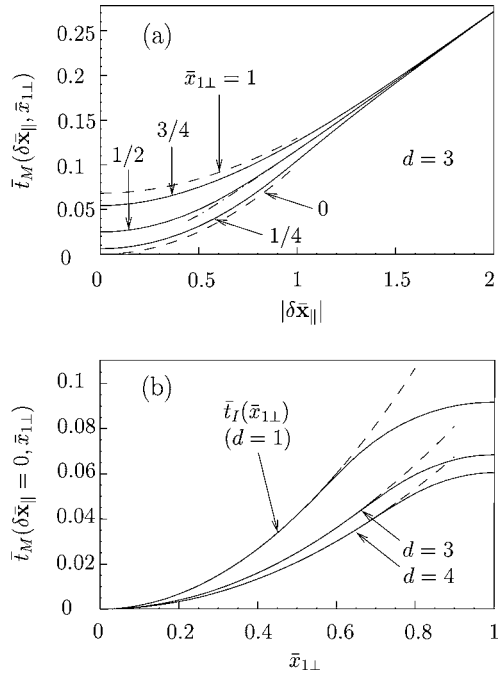

Fig. 6. Time $\bar{t}_M(\delta\bar{\mathbf{x}}_\parallel, \bar{x}_{1\perp})$, at which the critical Casimir force at the point on the left wall at $\bar{\mathbf{x}}_{1\parallel} + \delta\bar{\mathbf{x}}_\parallel$ reaches its maximum, as a function of $|\delta\bar{\mathbf{x}}_\parallel|$ in $d = 3$ (a). The external field has been applied at $(\mathbf{x}_{1\parallel}, x_{1\perp})$. The solid lines, from top to bottom, refer to the cases $\bar{x}_{1\perp} = 3/4$, $1/2$, and $1/4$, whereas the dashed lines show the asymptotic behaviors for $\bar{x}_{1\perp} \to 0$ (Eq. (119)) and $\to 1$ (Eq. (118)) for $\pi^2\bar{t}_M \ll 1$. The dash-dotted line indicates the approximation of $\bar{t}_M$ for large $|\delta\mathbf{x}_\parallel|$ given by Eq. (116), which is already rather good for $|\delta\mathbf{x}_\parallel| \gtrsim 1.0$. For large $|\delta\bar{\mathbf{x}}_\parallel|$ the time $\bar{t}_M$ becomes independent of $\bar{x}_{1\perp}$; it increases linearly with the slope giving the inverse of the speed for the propagation of the force maximum on the left wall (see Eq. (117)). In (b) we compare the time $\bar{t}_M(\delta\bar{\mathbf{x}}_\parallel = 0, \bar{x}_{1\perp})$ for $d = 3, 4$ with $\bar{t}_I(\bar{x}_{1\perp})$ (see Fig. 3), formally corresponding to the case $d = 1$. The dashed curves indicate the quadratic behaviors expected for small $\bar{x}_{1\perp}$ and arbitrary d (see Eq. (119)) which actually describe the curves rather well even for a wide range of values of $\bar{x}_{1\perp}$.

In analogy to Eq. (111), we define as a measure of the maximum force

$$A_\Delta^P(\delta\bar{\mathbf{x}}_\parallel, \bar{x}_{1\perp}) = \frac{\mathscr{T}_l^{(\mathrm{dy})(0)}(0, \bar{t}_M(\delta\bar{\mathbf{x}}_\parallel, \bar{x}_{1\perp}), \hat{h}_P) - \mathscr{T}^{(\mathrm{st})(0)}(0,0)}{\hat{h}_P^2}$$

$$= \frac{1}{2}\frac{e^{-(\delta\bar{\mathbf{x}}_\parallel)^2/[2\bar{t}_M(\delta\bar{\mathbf{x}}_\parallel, \bar{x}_{1\perp})]}}{[4\pi\,\bar{t}_M(\delta\bar{\mathbf{x}}_\parallel, \bar{x}_{1\perp})]^{d-1}}\left[\partial_{\bar{x}_{2\perp}}\Psi(\bar{x}_{1\perp}, \bar{x}_{2\perp}, \bar{t}_M(\delta\bar{\mathbf{x}}_\parallel, \bar{x}_{1\perp}))|_{\bar{x}_{2\perp}=0}\right]^2 . \tag{120}$$

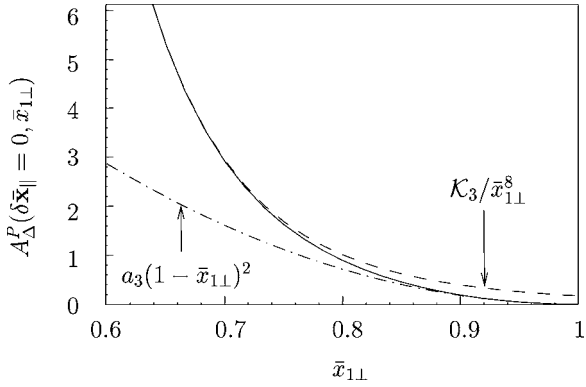

Fig. 7. Dependence of the amplitude $A^P_\Delta(\delta\bar{\mathbf{x}}_\parallel = 0, \bar{x}_{1\perp})$, which determines the critical Casimir force maximum $(d-1)\Delta + \hat{h}^2_P A^P_\Delta(\delta\bar{\mathbf{x}}_\parallel = 0, \bar{x}_{1\perp})$ at the point of the left wall closest to the point within the film where the external field was applied, on the normal distance of the perturbation from the left wall. The curves refer to the three-dimensional case, although the qualitative behavior is the same in $d = 4$. The asymptotic behaviors for $\bar{x}_{1\perp} \to 0$ and $\bar{x}_{1\perp} \to 1$ (see Appendix F2) are indicated as dashed and dashed-dotted lines, respectively, with $\mathcal{K}_3 = 5^5/(4\pi^2 e^5) \simeq 0.169773$ and $a_3 \simeq 17.927$. Note that, as in the case in Fig. 4.3.1, the asymptotic behavior $\mathcal{K}_3/\bar{x}^8_{1\perp}$ for $\bar{x}_{1\perp} \to 0$ provides a rather good estimate of the actual values already for $\bar{x}_{1\perp} \lesssim 0.65$.

We first discuss $A^P_\Delta(\delta\bar{\mathbf{x}}_\parallel = 0, \bar{x}_{1\perp})$, i.e., the maximum of the field-induced force at the point of the wall closest to the source of the perturbation. Figure 7 shows the function $A_\Delta(\delta\bar{\mathbf{x}}_\parallel = 0, \bar{x}_{1\perp})$ for $d = 3$, together with its asymptotic behaviors determined in Appendix F.2. According to Eqs. (250) and (251) they are given by $A^P_\Delta(\delta\bar{\mathbf{x}}_\parallel = 0, \bar{x}_{1\perp} \to 0) = \mathcal{K}_d/\bar{x}^{2(d+1)}_{1\perp}$, with $\mathcal{K}_d$ defined in Eq. (243), and $A^P_\Delta(\delta\bar{\mathbf{x}}_\parallel = 0, \bar{x}_{1\perp} \to 1) = a_d(1-\bar{x}_{1\perp})^2$, with a_d defined by Eq. (252). The qualitative dependence of $A^P_\Delta(\delta\bar{\mathbf{x}}_\parallel = 0, \bar{x}_{1\perp})$ on $\bar{x}_{1\perp}$ is the same as that of $A^W_\Delta(\bar{x}_{1\perp})$.

According to Eq. (113), at a given time $\delta\bar{t}$ elapsed after the perturbation, the field-induced part of the Casimir force is a decreasing function of $|\delta\bar{\mathbf{x}}_\parallel|$. Therefore the maximum amplitude $A^P_\Delta(\delta\bar{\mathbf{x}}_\parallel, \bar{x}_{1\perp})$ decreases with increasing lateral distance $|\delta\bar{\mathbf{x}}_\parallel|$ from the point where the field has been applied. Figure 8 shows the dependence of the maximum force amplitude $A^P_\Delta(\delta\bar{\mathbf{x}}_\parallel, \bar{x}_{1\perp})$ in $d = 3$ on $\delta\bar{\mathbf{x}}_\parallel$ for fixed values of $\bar{x}_{1\perp}$, normalized to its value at $\delta\bar{\mathbf{x}}_\parallel = 0$ (compare Fig. 7). The solid lines correspond, from top to bottom, to $\bar{x}_{1\perp} = 1, 3/4, 1/2$, and $1/4$. For $\bar{x}_{1\perp}$, $|\delta\bar{\mathbf{x}}_\parallel| \lesssim 0.5$ the approximate expression of $A^P_\Delta(\delta\bar{\mathbf{x}}_\parallel, \bar{x}_{1\perp})/A^P_\Delta(\delta\bar{\mathbf{x}}_\parallel = 0, \bar{x}_{1\perp}) \simeq [1 + (\delta\bar{\mathbf{x}}_\parallel)^2/\bar{x}^2_{1\perp}]^{-(d+2)}$ (Eq. (254)) provides a very good approximation of the actual curves. For $|\delta\bar{\mathbf{x}}_\parallel| \to \infty$ this ratio decays $\sim \exp(-2\pi|\delta\bar{\mathbf{x}}_\parallel|)$ (Eq. (253)). In Fig. 8 the dashed line refers to this asymptotic behavior for $\bar{x}_{1\perp} \to 1$. It is interesting to note that for all $\bar{x}_{1\perp}$ the maximum of the field-induced force decays rapidly with $|\delta\bar{\mathbf{x}}_\parallel|$ and is practically negligible compared with its value at $\delta\bar{\mathbf{x}}_\parallel = 0$ already for $|\delta\bar{\mathbf{x}}_\parallel| \simeq 1$.

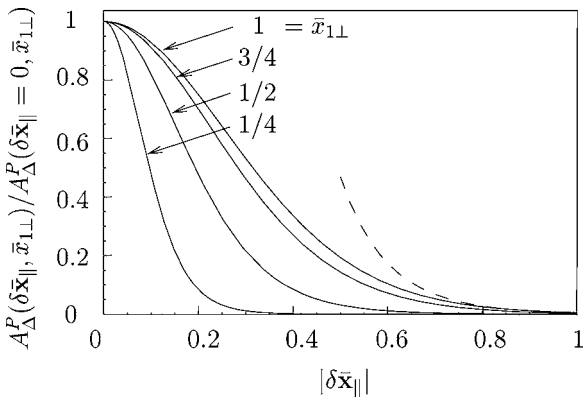

Fig. 8. Dependence of the normalized amplitude $A^P_\Delta(\delta\bar{\mathbf{x}}_\parallel, \bar{x}_{1\perp})$ of the critical Casimir force maximum with $d = 3$ on $|\delta\bar{\mathbf{x}}_\parallel|$ for various fixed $\bar{x}_{1\perp}$. The dashed line is the asymptotic behavior for $|\delta\bar{\mathbf{x}}_\parallel| \gg 1$ and $\bar{x}_{1\perp} \to 1$, as obtained from Eq. (253). For $|\delta\bar{\mathbf{x}}_\parallel| \to \infty$ the curves vanish as $\sim \exp(-2\pi|\delta\bar{\mathbf{x}}_\parallel|)$ (Eq. (253)).

Figure 9 shows the time dependence of the normalized dynamic part of the Casimir force

$$\mathscr{F}^P_\Delta(\delta\bar{\mathbf{x}}_\parallel, \bar{x}_{1\perp}, \bar{t}\,) = \frac{\mathscr{F}^{(\mathrm{dy})(0)}_l(0, \bar{t}, \hat{h}_P) - \mathscr{F}^{(\mathrm{st})(0)}(0, 0)}{\hat{h}^2_P A^P_\Delta(\delta\bar{\mathbf{x}}_\parallel, \bar{x}_{1\perp})} \tag{121}$$

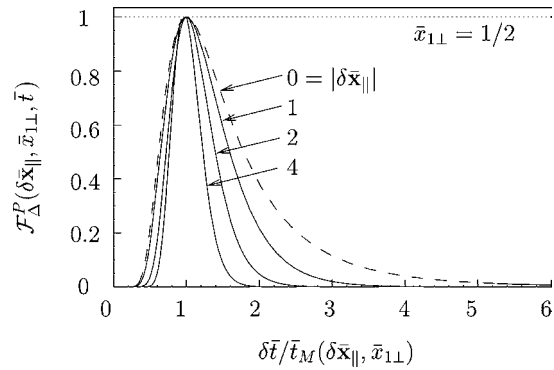

Fig. 9. Time dependence of the normalized dynamic part of the critical Casimir force $\mathscr{F}^P_\Delta(\bar{x}_{1\perp}, \bar{t}\,) = [\mathscr{F}^{(\mathrm{dy})(0)}_l(0, \bar{t}, \hat{h}_P) - \mathscr{F}^{(\mathrm{st})(0)}(0, 0)]/[\hat{h}^2_P A^P_\Delta(\delta\bar{\mathbf{x}}_\parallel, \bar{x}_{1\perp})]$ for various lateral distances $|\delta\bar{\mathbf{x}}_\parallel|$ from the location of the perturbation at $\bar{x}_{1\perp} = 1/2$, with $d = 3$. For $\bar{t} = \bar{t}_M(\delta\bar{\mathbf{x}}_\parallel, \bar{x}_{1\perp})$ the Casimir force reaches its maximum (compare Fig. 6). The different curves refer to $|\delta\bar{\mathbf{x}}_\parallel| = 0$, 1, 2 and 4, from top to bottom. The qualitative behavior of the curves is the same for other values of $\bar{x}_{1\perp}$. For $\delta\bar{t} \to \infty$ the curve vanish as $(\delta\bar{t})^{-(d-1)} e^{-2\pi^2\delta\bar{t}}$.

for $d = 3$, fixed $\bar{x}_{1\perp} = 1/2$, and various values of $|\delta\bar{\mathbf{x}}_\parallel| = 0, 1, 2$, and 4, from top to bottom. When the $\mathscr{T}^P_\Delta$ is plotted as a function of $\bar{t}/\bar{t}_M$ its shape does neither depend sensitively on the specific value of $\bar{x}_{1\perp}$ nor on the value of $|\delta\bar{\mathbf{x}}_\parallel|$. For fixed $\delta\bar{\mathbf{x}}_\parallel$ and $\bar{x}_{1\perp}$, $\mathscr{T}^P_\Delta$ decays asymptotically as $\mathscr{T}^P_\Delta(\delta\bar{\mathbf{x}}_\parallel, \bar{x}_{1\perp}, \bar{t} \to \infty) \sim (\delta\bar{t})^{-(d-1)} e^{-2\pi^2\,\delta\bar{t}}$ (see Eqs. (113) and (115)).

4.4. Correlation Function

4.4.1. General Expressions

As discussed in Subsec. 3.2, the FDT relates the correlation function and the response function via Eq. (31). Thus, taking into account Eq. (83), one finds that the correlation function can be cast into the scaling form given in Eq. (45) with

$$\bar{\mathscr{C}}^{(0)}(\bar{\mathbf{p}}, \bar{x}_{1\perp}, \bar{x}_{2\perp}, \bar{t}, \bar{L}) = 2\int_{|\bar{t}|}^{\infty} \mathrm{d}\bar{s}\, e^{-\bar{s}/\bar{t}_0(\bar{\mathbf{p}},\bar{L})} \Psi(\bar{x}_{1\perp}, \bar{x}_{2\perp}, \bar{s}) \tag{122}$$

where the value of the non-universal amplitude $\hat{\mathrm{o}}_C$ is given by Eq. (56) and where we have introduced

$$\bar{t}_0 = \frac{1}{\bar{\mathbf{p}}^2 + \bar{L}^2}. \tag{123}$$

The dependence of the scaling function $\bar{\mathscr{C}}^{(0)}$ on $\bar{t}$ for selected values of $\bar{x}_{1\perp}$ is shown in Fig. 10 at criticality and for $\mathbf{p} = \mathbf{0}$, i.e., $\bar{t}_0 = \infty$, and for $\bar{t}_0 < \infty$ in Fig. 11. As expected, $\bar{\mathscr{C}}^{(0)}$ vanishes in the limit $\bar{t} \to \infty$. According to Eqs. (182) and (45) the scaling function $\bar{\mathscr{C}}^{(0)}_{\mathrm{st}}(\bar{\mathbf{p}}, \bar{x}_{1\perp}, \bar{x}_{2\perp}, \bar{L}) = \bar{\mathscr{C}}^{(0)}(\bar{\mathbf{p}}, \bar{x}_{1\perp}, \bar{x}_{2\perp}, \bar{t} = 0, \bar{L})$

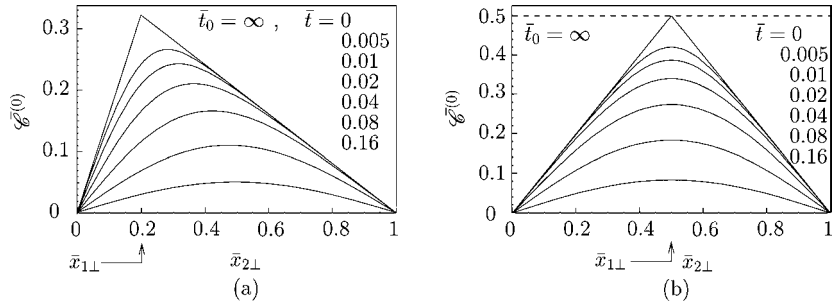

Fig. 10. Time evolution of the mean-field scaling function $\bar{\mathscr{C}}^{(0)}(\bar{\mathbf{p}}, \bar{x}_{1\perp}, \bar{x}_{2\perp}, \bar{t}, \bar{L})$ which enters into the expression of the correlation function in Eq. (44) with $\bar{x}_{i\perp} = x_{i\perp}/L$, $\bar{t} = (t/T_0)(\xi_0/L)^z$, $\bar{L} = L/\xi$, and $\bar{t}_0 = 1/(\bar{\mathbf{p}}^2 + \bar{L}^2)$ for $\mathbf{p} = \mathbf{0}$ and $T = T_{c,b}$, i.e., $\bar{t}_0 = \infty$. We show correlations between points $\bar{x}_{2\perp}$ and $\bar{x}_{1\perp} = 0.2$ (a) and $\bar{x}_{1\perp} = 0.5$ (b). Reduced times $\bar{t}$ listed in (a) and (b) refer to the various curves shown from top to bottom. At $\bar{t} = 0$, the static correlation function $\bar{\mathscr{C}}^{(0)}$ exhibits a cusp at $\bar{x}_{1\perp} = \bar{x}_{2\perp}$.

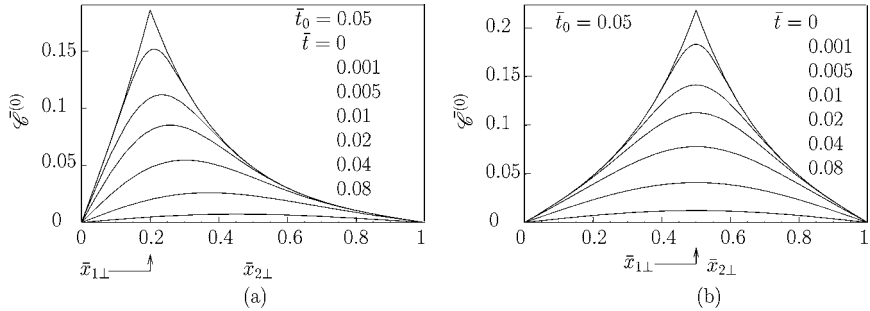

Fig. 11. Same as in Fig. 10 but for $\bar{t}_0 = 0.05$ which leads to reduced correlations compared to $\bar{t}_0 = \infty$. The cusps at $\bar{x}_{1\perp} = \bar{x}_{2\perp}$ remain also for $\bar{t}_0 < \infty$.

of the static correlation function is given by

$$\bar{\mathscr{C}}^{(0)}_{\rm st}(\bar{\mathbf{p}}, \bar{x}_{1\perp}, \bar{x}_{2\perp}, \bar{L}) = 2\frac{\sinh\left(\bar{t}_0^{-1/2}\bar{x}_\perp^<\right)\sinh\left[\bar{t}_0^{-1/2}(1-\bar{x}_\perp^>)\right]}{\bar{t}_0^{-1/2}\sinh\left(\bar{t}_0^{-1/2}\right)}, \tag{124}$$

which, independently of the value of $\bar{t}_0$, is characterized by a cusp-like singularity for $\bar{x}_{1\perp} = \bar{x}_{2\perp}$, clearly displayed in Figs. 10 and 11. In particular at bulk criticality, i.e., $\bar{L} = 0$ and for $\bar{\mathbf{p}} = \mathbf{0}$ (i.e., $\bar{t}_0 = \infty$), one finds (compare Eq. (95))

$$\bar{\mathscr{C}}^{(0)}_{\rm st}(\bar{\mathbf{p}} = \mathbf{0}, \bar{x}_{1\perp}, \bar{x}_{2\perp}, \bar{L} = 0) = 2\,\bar{x}_\perp^<(1-\bar{x}_\perp^>), \tag{125}$$

which corresponds to a triangularly shaped correlation function vanishing at the boundaries [see Fig. 10 and Eq. (182)]. The two-point correlation function in thin films can be probed by scattering X-rays or neutrons under grazing incidence.[17,59] The dependence of the corresponding scattering cross section on the lateral momentum transfer is dominated by the singular behavior of the two-point correlation function in planes parallel to the surfaces of the film. With future technologies it might be possible to extend such kind of scattering experiment into the time domain. Therefore we discuss the particular case $x_{1\perp} = x_{2\perp}$, i.e., $C(\mathbf{p}, x_\perp, x_\perp, \omega)$. The analysis of this particular case may also serve to enhance the general physical insight into correlations in films.

In order to understand the behavior of this quantity we shall consider two relevant limits: (a) the behavior close to the confining walls, i.e., $x_\perp \ll L$ (surface behavior; see Appendix G), and (b) the behavior in the interior, i.e., $x_\perp = L/2$. Crossover effects are expected to occur in between.

4.4.2. Behavior Near the Wall

To this end we rewrite Eq. (95), use the FDT (see Eq. (34)), cast it into the scaling form given in Eq. (44), and use Eq. (56) for the nonuniversal amplitude:

$$\mathscr{C}^{(0)}(\tilde{\mathbf{p}}, \bar{x}_{1\perp}, \bar{x}_{2\perp}, \bar{\omega}, \bar{L}) = \frac{2}{\bar{\omega}} \mathrm{Im} \frac{\cosh[\bar{a}(1 - |\bar{x}_{1\perp} - \bar{x}_{2\perp}|)] - \cosh[\bar{a}(1 - \bar{x}_{1\perp} - \bar{x}_{2\perp})]}{\bar{a} \sinh \bar{a}} \tag{126}$$

where $\bar{a}$ has been defined in Eq. (97). By using the previous equation we obtain

$$\mathscr{C}^{(0)}(\tilde{\mathbf{p}}, \bar{x}_{\perp}, \bar{x}_{\perp}, \bar{\omega}, \bar{L}) = \frac{2}{\bar{\omega}} \mathrm{Im} \frac{\cosh \bar{a} - \cosh[\bar{a}(1 - 2\bar{x}_{\perp})]}{\bar{a} \sinh \bar{a}} \tag{127}$$

so that for $|\bar{a}|\bar{x}_{\perp} = |a|x_{\perp} \ll 1$ (i.e., sufficiently close to one of the walls)

$$\mathscr{C}^{(0)}(\tilde{\mathbf{p}}, \bar{x}_{\perp}, \bar{x}_{\perp}, \bar{\omega}) = -4 \frac{\bar{x}_{\perp}^2}{\bar{\omega}} \mathrm{Im} \left\{ \bar{a} \coth \bar{a} (1 + O(|\bar{a}|\bar{x}_{\perp})) \right\}, \tag{128}$$

in agreement with the general behavior of $\mathscr{C}$close to one wall, given in Eq. (63) with

$$\mathscr{C}^{(0)}_{W}(\tilde{\mathbf{p}}, \bar{\omega}, \bar{L}) = -\frac{4}{\bar{\omega}} \mathrm{Im} \left\{ \bar{a} \coth \bar{a} (1 + O(|\bar{a}|\bar{x}_{\perp})) \right\}. \tag{129}$$

We can distinguish two regimes, i.e., $|\bar{a}| = |a|L \gg 1$ (relevant for discussing the connection with the results for the semi-infinite geometry) and $|\bar{a}| = |a|L \ll 1$.

- $|\bar{a}| = |a|L \gg 1$: In this case $\bar{a} \coth \bar{a} = \bar{a}(1 + O(e^{-2\bar{a}}))$ (we choose the branch with positive real part in the square root defining $\bar{a}$, see footnote 8) and thus

$$\mathscr{C}^{(0)}_{W}(\tilde{\mathbf{p}}, \bar{x}_{\perp}, \bar{x}_{\perp}, \bar{\omega}) = -\frac{4}{\bar{\omega}} \mathrm{Im} \left\{ \bar{a}(1 + O(|\bar{a}|\bar{x}_{\perp}, e^{-2\bar{a}})) \right\}. \tag{130}$$

Using the definition of $\bar{a}$, one obtains

$$\mathscr{C}^{(0)}_{W}(\tilde{\mathbf{p}}, \bar{x}_{\perp}, \bar{x}_{\perp}, \bar{\omega}) = 2\sqrt{2} \frac{1}{\sqrt{\tilde{\mathbf{p}}^2 + \bar{L}^2 + \sqrt{(\tilde{\mathbf{p}}^2 + \bar{L}^2)^2 + \bar{\omega}^2}}},$$

$$\sqrt[4]{(\tilde{\mathbf{p}}^2 + \bar{L}^2)^2 + \bar{\omega}^2} \gg 1 \quad \text{and} \quad \bar{x}_{\perp} \sqrt[4]{(\tilde{\mathbf{p}}^2 + \bar{L}^2)^2 + \bar{\omega}^2} \ll 1. \tag{131}$$

Equation (131) renders the limiting behaviors listed in Eqs. (69), (70), and (71) with the mean-field universal amplitudes

$$\mathcal{A}_{\infty}^{W(0)} = 2, \tag{132}$$

$$\mathcal{B}_{\infty}^{W(0)} = 2\sqrt{2}, \tag{133}$$

$$\mathcal{C}_{\infty}^{W(0)} = 2, \tag{134}$$

and the mean-field values of the critical exponents. Corrections to the formulae (69), (70), and (71) are exponentially small.

- $|\bar{a}| = |a|L \ll 1$: In this case one has (see Appendix G, Eq. (261)),

$$\mathscr{C}^{(0)}(\bar{\mathbf{p}}, \bar{x}_\perp, \bar{x}_\perp, \bar{\omega}) = \frac{4}{3}\bar{x}_\perp^2(1-\bar{x}_\perp)^2$$
$$\times\left\{1 - \frac{2}{15}(1 + 2\bar{x}_\perp - 2\bar{x}_\perp^2)(\bar{\mathbf{p}}^2 + \bar{L}^2)\right.$$
$$\left. + \frac{2}{105}\left(1 + 2\bar{x}_\perp - \frac{\bar{x}_\perp^2}{2} - 3\bar{x}_\perp^3 + \frac{3}{2}\bar{x}_\perp^4\right)\left[(\bar{\mathbf{p}}^2 + \bar{L}^2)^2 - \frac{1}{3}\bar{\omega}^2\right] + \ldots\right\},$$
$$\sqrt[4]{(\bar{\mathbf{p}}^2 + \bar{L}^2)^2 + \bar{\omega}^2} \ll 1, \quad \bar{x}_\perp \le 1. \tag{135}$$

Near one wall, i.e., for $\bar{x}_\perp \ll 1$ this expression leads to

$$\mathscr{C}_W^{(0)}(\bar{\mathbf{p}}, \bar{x}_\perp, \bar{x}_\perp, \bar{\omega}) = \frac{4}{3}\left[1 - \frac{2}{15}(\bar{\mathbf{p}}^2 + \bar{L}^2) + \frac{2}{105}(\bar{\mathbf{p}}^2 + \bar{L}^2)^2 - \frac{2}{315}\bar{\omega}^2 + \ldots\right]. \tag{136}$$

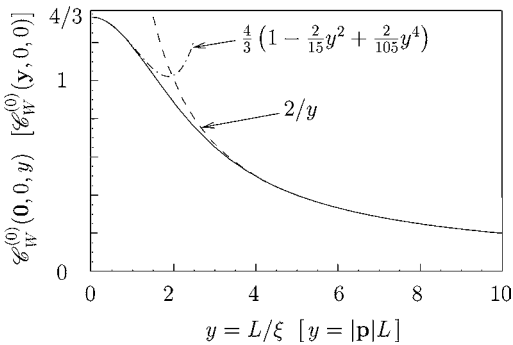

Fig. 12. Mean-field scaling function $\mathscr{C}_W^{(0)}(\mathbf{0}, 0, y)$ $[\mathscr{C}_W^{(0)}(\mathbf{y}, 0, 0)]$ which enters into the expression of the correlation function $C(\mathbf{p} = \mathbf{0}, x_\perp, x_\perp, \omega = 0) = \hat{\mathbf{o}}_C(L/\xi_0)^{1-\eta-z}(x_\perp/L)^{2(\beta_1-\beta)/\nu}\,\mathscr{C}_W(\mathbf{0}, 0, y = L/\xi)$ $[C_{\mathrm{crit}}(\mathbf{p}, x_\perp, x_\perp, \omega = 0) = \hat{\mathbf{o}}_C(L/\xi_0)^{1-\eta-z}(x_\perp/L)^{2(\beta_1-\beta)/\nu}\,\mathscr{C}_W(\mathbf{y} = \mathbf{p}L, 0, 0)]$ for $L/x_\perp \gg 1$, L/ξ $[L/x_\perp \gg 1, |\mathbf{p}|L]$, so that $\mathscr{C}_W^{(0)}(\mathbf{0}, 0, y \to 0)$ $[\mathscr{C}_W^{(0)}(\mathbf{y} \to \mathbf{0}, 0, 0)] = (4/3)[1 - (2/15)y^2 + (2/105)y^4 + O(y^6)]$ and $\mathscr{C}_W^{(0)}(\mathbf{0}, 0, y \to \infty)[\mathscr{C}_W^{(0)}(\mathbf{y} \to \infty, 0, 0)] = 2/y + O(1/y^2)$. Beyond mean-field theory the asymptotic behavior of $\mathscr{C}_W(\mathbf{0}, 0, y = L/\xi)$ and $\mathscr{C}_W(\mathbf{y} = \mathbf{p}L, 0, 0)$ for large y is given by Eqs. (66) and (68), respectively. The index W of the scaling function here and in Fig. 13 indicates the behavior near the wall.

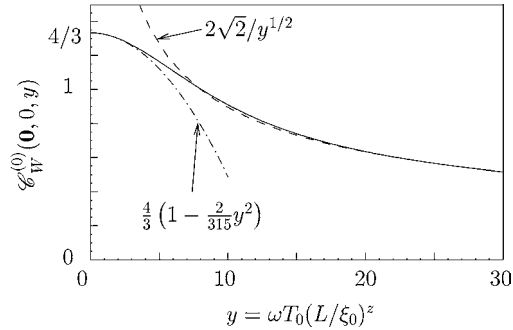

Fig. 13. Mean-field scaling function $\mathscr{C}_W^{(0)}(\mathbf{0}, y, 0)$ which enters into the expression of the correlation function $C_{\rm crit}(\mathbf{p}=\mathbf{0}, x_\perp, x_\perp, \omega) = \hat{\mathbf{o}}_C (L/\xi_0)^{1-\eta-z}(x_\perp/L)^{2(\beta_1-\beta)/\nu}\,\mathscr{C}_W(\mathbf{0}, y=\omega T_0(L/\xi_0)^z, 0)$ for $T = T_{c,b}$ and $L/x_\perp \gg 1, \omega T_0 (L/\xi_0)^z$, so that $\mathscr{C}_W^{(0)}(\mathbf{0}, y\to 0, 0) = (4/3)[1-(2/315)y^2 + O(y^4)]$ and $\mathscr{C}_W^{(0)}(\mathbf{0}, y\to\infty, 0) = 2\sqrt{2}/y^{1/2} + O(1/y)$. Beyond mean-field theory the asymptotic behavior of $\mathscr{C}_W(\mathbf{0}, y=\omega T_0(L/\xi_0)^z, 0)$ for large y is given by Eq. (67).

From this expression we can identify the mean-field value of the universal constant introduced in Eq. (64):

$$\mathcal{A}^{W(0)} = 4/3\,. \tag{137}$$

Figures 12 and 13 display the functions $\mathscr{C}_W^{(0)}(\bar{\mathbf{p}}=\mathbf{0}, \bar\omega=0, \bar L)$, $\mathscr{C}_W^{(0)}(\bar{\mathbf{p}}, \bar\omega = 0, \bar L = 0)$, and $\mathscr{C}_W^{(0)}(\bar{\mathbf{p}}=\mathbf{0}, \bar\omega, \bar L = 0)$, respectively, together with their asymptotic behaviors given in Eqs. (69)–(71) and (136).

Thus, in contrast to the case of a semi-infinite geometry (in which the validity of the behaviors in Eqs. (69), (70), and (71) extends down to $1/\xi = 0$, $\omega = 0$, or $\mathbf{p} = \mathbf{0}$, respectively), the critical correlation function in the film does not diverge upon approaching the origin of the $(\xi^{-1}, \mathbf{p}, \omega)$-space. This is a consequence of the critical point shift in the film geometry. Of course this divergence is correctly recovered in the limit $L\to\infty$ (i.e., in the semi-infinite limit), where this shift is absent.

4.4.3. Film Behavior

Now we consider the behavior of $C^{(0)}(\mathbf{p}, x_\perp, x_\perp, \omega)$ in the middle of the film, i.e., $C^{(0)}(\mathbf{p}, L/2, L/2, \omega)$. According to Eqs. (44) and (77) this amounts to studying $\mathscr{C}_I^{(0)}(\bar{\mathbf{p}}, \bar\omega, \bar L)$. In that case we find (see Eq. (127))

$$\mathscr{C}_I^{(0)}(\bar{\mathbf{p}}, \bar\omega, \bar L) = \mathscr{C}^{(0)}(\bar{\mathbf{p}}, 1/2, 1/2, \bar\omega, \bar L) = \frac{2}{\bar\omega}\,\mathrm{Im}\frac{\tanh(\bar a/2)}{\bar a}. \tag{138}$$

Again, we consider the two possible regimes $|\bar{a}| = |a|L \gg 1$ and $|\bar{a}| = |a|L \ll 1$.

- $|\bar{a}| = |a|L \gg 1$: In this regime one has

$$\mathscr{C}_I^{(0)}(\tilde{\mathbf{p}}, \bar{\omega}, \bar{L}) = \frac{2}{\bar{\omega}} \mathrm{Im} \left\{ \frac{1}{\bar{a}} \left(1 + O\left(e^{-2|\bar{a}|} \right) \right) \right\} \tag{139}$$

so that

$$\mathscr{C}_I^{(0)}(\tilde{\mathbf{p}}, \bar{\omega}, \bar{L}) = \sqrt{2} \frac{1}{\sqrt{\left(\tilde{\mathbf{p}}^2 + \bar{L}^2 \right)^2 + \bar{\omega}^2} \sqrt{\tilde{\mathbf{p}}^2 + \bar{L}^2 + \sqrt{(\tilde{\mathbf{p}}^2 + \bar{L}^2)^2 + \bar{\omega}^2}}},$$

$$\sqrt[4]{(\tilde{\mathbf{p}}^2 + \bar{L}^2)^2 + \bar{\omega}^2} \gg 1. \tag{140}$$

From this equation one easily recovers the limiting behaviors given in Eqs. (74), (75), and (76), with the mean-field universal amplitudes

$$\mathcal{A}_\infty^{I(0)} = 1 \tag{141}$$

$$\mathcal{B}_\infty^{I(0)} = \sqrt{2}, \tag{142}$$

$$\mathcal{C}_\infty^{I(0)} = 1, \tag{143}$$

and with the corresponding mean-field values of the critical exponents.

- $|\bar{a}| = |a|L \ll 1$: On the other hand, in the limit $|\bar{a}| = |a|L \ll 1$ one can make use of Eq. (135) (valid in the case $|a|L, |a|x_\perp \ll 1$ and arbitrary $x_\perp < L$), with $\bar{x}_\perp = 1/2$, leading to

$$\mathscr{C}_I^{(0)}(\tilde{\mathbf{p}}, \bar{\omega}, \bar{L}) = \frac{1}{12} \left[1 - \frac{1}{5}(\tilde{\mathbf{p}}^2 + \bar{L}^2) + \frac{17}{560}(\tilde{\mathbf{p}}^2 + \bar{L}^2)^2 - \frac{17}{1680}\bar{\omega}^2 + \ldots \right],$$

$$\sqrt[4]{(\tilde{\mathbf{p}}^2 + \bar{L}^2)^2 + \bar{\omega}^2} \ll 1. \tag{144}$$

From Eq. (144) one infers the universal amplitude

$$\mathcal{A}^{I(0)} = \frac{1}{12} \tag{145}$$

introduced in Eq. (73). As it is the case near a wall (see the remark at the end of Subsec. 4.4.2), also in the middle of the film the correlation function does not diverge at the origin of the $(\mathbf{p}, \xi^{-1}, \omega)$-space; divergences appear only in the limit $L \to \infty$, for which the critical-point shift disappears and $T_{c,b}$ coincides with the critical temperature of the system. In particular, from Eq. (135) one finds

$$\mathscr{C}_{\mathrm{crit}}^{(0)}(\tilde{\mathbf{p}} = \mathbf{0}, \bar{x}_\perp, \bar{x}_\perp, \bar{\omega} = 0) = \frac{4}{3}\bar{x}_\perp^2(1 - \bar{x}_\perp)^2. \tag{146}$$

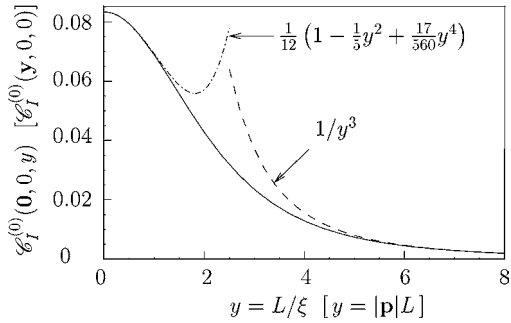

Fig. 14. Mean-field scaling function $\mathscr{C}_I^{(0)}(\mathbf{0}, 0, y)$ $[\mathscr{C}_I^{(0)}(\mathbf{y}, 0, 0)]$ which enters into the expression of the correlation function $C(\mathbf{p} = \mathbf{0}, x_\perp = L/2, x_\perp = L/2, \omega = 0) = \hat{\mathbf{o}}_C(L/\xi_0)^{1-\eta-z}\,\mathscr{C}_I(\mathbf{0}, 0, y = L/\xi)$ $[C_{\text{crit}}(\mathbf{p}, x_\perp = L/2, x_\perp = L/2, \omega = 0) = \hat{\mathbf{o}}_C(L/\xi_0)^{1-\eta-z}\,\mathscr{C}_I(\mathbf{y} = \mathbf{p}L, 0, 0)]$, so that $\mathscr{C}_I^{(0)}(\mathbf{0}, 0, y \to 0)$ $[\mathscr{C}_I^{(0)}(\mathbf{y} \to \mathbf{0}, 0, 0)] = (1/12)[1 - (1/5)y^2 + (17/560)y^4 + O(y^6)]$ and $\mathscr{C}_I^{(0)}(\mathbf{0}, 0, y \to \infty)$ $[\mathscr{C}_I^{(0)}(\mathbf{y} \to \infty, 0, 0)] = 1/y^3 + O(1/y^4)$. Beyond mean-field theory the asymptotic behavior of $\mathscr{C}_I(\mathbf{0}, 0, y = L/\xi)$ and $\mathscr{C}_I(\mathbf{y} = \mathbf{p}L, 0, 0)$ for large y is given by Eqs. (74) and (76), respectively. The index I of the scaling functions here and in Fig. 15 indicates the behavior within the interior (i.e., middle) of the film.

In Fig. 14 we show the functions $\mathscr{C}_I^{(0)}(\bar{\mathbf{p}} = \mathbf{0}, \bar{\omega} = 0, \bar{L})$ and $\mathscr{C}_I^{(0)}(\bar{\mathbf{p}}, \omega = 0, \bar{L} = 0)$ which have (within MFT) the same scaling function if the scaling variables are appropriately chosen. (In Fig. 14 the quantities in square brackets refer to $\mathscr{C}_I^{(0)}(\bar{\mathbf{p}}, \omega = 0, \bar{L} = 0)$.) The limiting behaviors of this function as given by Eqs. (74), (76) and (73) are indicated as dashed and dash-dotted lines. In Fig. 15, we plot $\mathscr{C}_I^{(0)}(\bar{\mathbf{p}} = \mathbf{0}, \bar{\omega}, \bar{L} = 0)$ and its limiting behaviors given by Eqs. (73) and (75).

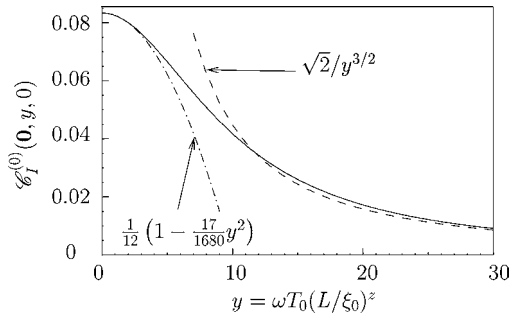

Fig. 15. Mean-field scaling function $\mathscr{C}_I^{(0)}(\mathbf{0}, y, 0)$ which enters into the expression of the correlation function $C_{\text{crit}}(\mathbf{p} = \mathbf{0}, x_\perp = L/2, x_\perp = L/2, \omega) = \hat{\mathbf{o}}_C(L/\xi_0)^{1-\eta-z}\,\mathscr{C}_I(\mathbf{0}, y = \omega T_0(L/\xi_0)^z, 0)$ for $T = T_{c,b}$, so that $\mathscr{C}_I^{(0)}(\mathbf{0}, y \to 0, 0) = (1/12)[1 - (17/1680)y^2 + O(y^4)]$ and $\mathscr{C}_I^{(0)}(\mathbf{0}, y \to \infty, 0) = \sqrt{2}/y^{3/2} + O(1/y^2)$. Beyond mean-field theory the asymptotic behavior of $\mathscr{C}_I(\mathbf{0}, y = \omega T_0(L/\xi_0)^z, 0)$ for large y is given by Eq. (75).

The comparison between the scaling functions near the wall (Figs. 12 and 13) and in the interior of the film (Figs. 14 and 15) shows that they exhibit the same qualitative behaviors. However, the scaling functions in the interior decay more rapidly for large scaling variables than their counterparts near the wall. Moreover, their absolute values scale very differently as functions of L.

5. NONLINEAR BEHAVIOR

In the previous sections we investigated the linear response and correlation functions within the Gaussian approximation for the dynamical functional (Eq. (10)). The response function captures the behavior of *small* perturbations around the equilibrium state of the system. The response function analyzed in Subsec. 4.2 is useful to describe the relaxation process from an initial state with a small value of the order parameter such that nonlinear terms can be neglected. On the other hand both in experiments and numerical simulations this is often not the case given that it is much easier to investigate the response of the system to *finite* changes of the control parameters (such as temperature and external fields). While typically the former relaxation process is characterized by exponential decays in time, the latter leads to power-law behaviors. As a concrete example one can think of an experimental protocol in which the system is initially prepared in an equilibrium state with a non-zero value of the order parameter. This can be realized, for example in magnetic systems, by preparing the sample in its low-temperature phase or by applying an external field. Then the external parameters are changed in a way that the order parameter in the corresponding equilibrium state vanishes, as it is the case above or at the critical temperature, in the absence of external fields. In order to describe the ensuing relaxation it is crucial to account for the effects of nonlinear terms, as will be discussed below.

Let us now consider in more detail the case in which an external field $h(\mathbf{x}, t)$, coupling linearly to the order parameter in the Hamiltonian $\mathcal{H}$, is present during the relaxation. The evolution equation for the quantity $m(\mathbf{x}, t) = \langle \varphi(\mathbf{x}, t) \rangle$ can be derived in a standard way[60,61] and, at the lowest level in the loop expansion (tree-level), it reads

$$h(\mathbf{x}, t) = \partial_t m(\mathbf{x}, t) + \Omega[-\Delta + \xi^{-2} + \frac{g_0}{3!} m^2(\mathbf{x}, t)] m(\mathbf{x}, t). \tag{147}$$

In the case of confined geometries this equation, which is valid in the bulk, has to be supplemented with the proper boundary conditions. For bulk systems with homogeneous external fields the linear regime is identified as that one in which the nonlinear term in Eq. (147) is negligible compared to ξ^{-2}, i.e., $\frac{g_0}{3!} m^2(\mathbf{x}, t) \ll \xi^{-2}$. In view of Eq. (41) this means $m(\mathbf{x}, t)/\mathfrak{m}_0 \ll \xi_0/\xi$. (At the ordinary transition, the equilibrium magnetization close to the surface vanishes as $\sim (T_{c,b} - T)^{\beta_1}$ for $T \to T_{c,b}^-$, with $\beta_1 = 1$ within MFT. Therefore, sufficiently close to $T_{c,b}$, the

previous inequality is always fulfilled. Nevertheless the spatial inhomogeneity caused by the boundary condition at the surface yields a contribution – due to the term $-\Delta m$ in Eq. (147)– which effectively reduces the one due to the linear term previously considered. Eventually, the nonlinear term dominates and the proper nonlinear relaxation is displayed.) In that regime and in the absence of an external field the temporal relaxation from an initial state with a homogeneous order parameter is exponential. The range of validity of the linear approximation shrinks upon approaching the critical point.[60–63] At $T_{c,b}$ it is no longer possible to neglect the nonlinear contribution which causes m to relax as a function of time according to a power law. This general scenario can be modified by the presence of confining walls, which change the spectrum of the operator $-\Delta$ in Eq. (147). Thus, if this spectrum has a lower bound above zero (as it is the case for Dirichlet-Dirichlet boundary conditions in a film for which the zero mode is not allowed) the linear regime eventually dominates even at bulk criticality $\xi = \infty$. This is a consequence of the critical-point shift in the film geometry. On the other hand, for $T < T_{c,b}$, ξ^{-2} has to be replaced by $-\xi^{-2}/2$ (within MFT) and so, for $T = T_c(L) < T_{c,b}$, the spectrum of the operator $-\Delta - \xi^{-2}/2$ includes 0 and the nonlinear contribution is no longer negligible. Therefore at $T_c(L)$, m relaxes according to a power law as a function of time. Beyond MFT this power law is characterized by the critical exponents of a $d-1$-dimensional bulk system.

Before discussing the nonlinear relaxation in the confined geometry, we summarize briefly the results of the corresponding analysis of the semi-infinite geometry, i.e., the effects of a single surface[64–66] In particular we consider the typical relaxation process, realized by applying an external field $h(x_\perp, t) = h(x_\perp)\theta(-t)$ where $x_\perp$ is the normal distance from the single wall. In this case the subsequent evolution depends on the resulting initial order parameter profile $m_0(x_\perp) = m(x_\perp, t = 0)$. Within the field-theoretical approach it is possible to compute the scaling function for the evolving order parameter profile, as carried out in Refs. 64 and 66 for Model A:

$$m(x_\perp, t; \tau) = \mathfrak{m}_0 (t/T_0)^{-\beta/\nu z} \Psi((x_\perp/\xi_0)(t/T_0)^{-1/z}, t/T_R, \{(m_0(x'_\perp)/\mathfrak{m}_0)(t/T_0)^{\beta/\nu z}\}) \tag{148}$$

where the temperature enters via the relaxation time T_R (see Eq. (3)). For $(m_0(x'_\perp)/\mathfrak{m}_0) \times (t/T_0)^{\beta/\nu z} \gg 1$ the behavior of the system becomes independent of the initial configuration and follows a universal scaling function $\Psi(v, w, \infty)$. From a short-distance expansion it is found that $\Psi(v \to 0, w, \infty) \sim v^{(\beta_1 - \beta)/\nu}$, so that at criticality the magnetization close to the surface decays as $t^{-\beta_1/\nu z}$ for $t \to \infty$. For fixed $x_\perp$ and at criticality, after some (non-universal) initial transient behavior due to the finite initial magnetization, the order parameter relaxes as $m \sim t^{-\beta/\nu z}$, i.e., according to the "bulk" behavior. (Of course one has $\Psi(\infty, w, \infty) = \Psi_{\text{bulk}}(w)$).

As time passes (i.e., $t/T_0 \gtrsim (x_\perp/\xi_0)^z$) the effect of the surface reaches the point $x_\perp$ and the relaxation crosses over towards the surface behavior, i.e., $m \sim t^{-\beta_1/\nu z}$. (Note that for the ordinary surface universality class $\beta_1 > \beta$.) This crossover is nicely displayed in Monte Carlo simulation data[65] Off criticality this picture is modified only by the fact that when m becomes sufficiently small, i.e., $t \gg T_R$, the system enters the linear regime where the decay of m is finally exponential. Moreover the influence of the surface penetrates into the bulk only for a finite distance $\sim \xi$ from the surface. Well inside the non-critical bulk no crossover is expected between surface and bulk relaxation.

In Ref. 28 the relaxation close to the *bulk* critical point has been studied in a finite hypercubic geometry L^d with periodic boundary conditions (no surfaces breaking translational invariance), both by field-theoretical methods and Monte Carlo simulations, paying particular attention to the effects of a finite value of the uniform initial magnetization m_0. At the *bulk* critical point and independently of the value of $m_0 \neq 0$ the relaxation becomes *exponential* for $t \gg T_0(L/\xi_0)^z$ (as one would expect because a finite system does not display critical behavior). For m_0 large enough this stage is preceded by a *nonlinear* relaxation decay $m \sim t^{-\beta/\nu z}$, corresponding to the "bulk" behavior.

Focusing now on the film geometry, the corresponding nonlinear evolution equation for $m(\mathbf{x}, t)$ is still given by Eq. (147) together with the boundary conditions in Eq. (13). In order to proceed we introduce dimensionless quantities via

$$\bar{m}(\bar{\mathbf{x}}, \bar{t}\,) \equiv \sqrt{\frac{g_0}{3!}} L m(\bar{\mathbf{x}} L, \bar{t} L^2/\Omega) = \frac{L}{\xi_0^+} \frac{m(\bar{\mathbf{x}} L, \bar{t}\, T_0 (L/\xi_0)^z)}{\mathfrak{m}_0} \tag{149}$$

(using Eq. (41)) with $\bar{\mathbf{x}} \in \mathbb{R}^{d-1} \times [0, 1]$. Thus in the absence of the external field Eq. (147) turns into

$$\partial_{\bar{t}} \bar{m}(\bar{\mathbf{x}}, \bar{t}\,) + [-\Delta_{\bar{\mathbf{x}}} + \bar{\tau} + \bar{m}^2(\bar{\mathbf{x}}, \bar{t}\,)] \bar{m}(\bar{\mathbf{x}}, \bar{t}\,) = 0 \qquad \text{with} \qquad \bar{m}(\bar{\mathbf{x}}_{\mathcal{B}}, \bar{t}\,) = 0, \tag{150}$$

where $\bar{\tau} \equiv (L/\xi)^2$ for $\tau > 0$ and $\bar{\tau} \equiv -1/2(L/\xi)^2$ for $\tau < 0$. (We recall that, within mean-field theory, $\xi(\tau \to 0^+) = r_0^{-1/2}$ whereas $\xi(\tau \to 0^-) = (-2r_0)^{-1/2}$.) Using the scaled variables $\bar{\mathbf{x}}$, $\bar{t}$, and $\bar{\tau}$ there is no explicit dependence of the profile $\bar{m}(\bar{\mathbf{x}}, \bar{t}; \bar{\tau})$ on the size L of the layer. Static solutions of Eq. (150) have been discussed in detail in the literature for various boundary conditions (see, e.g., Refs. 46, 67, 68 and references therein). For $\bar{\tau} \geq \bar{\tau}_c$ ($\tau_c < 0$ determines the critical-point shift) the asymptotic solution of Eq. (150), $\bar{m}_\infty(\bar{\mathbf{x}}) = \lim_{\bar{t}\to\infty} \bar{m}(\bar{\mathbf{x}}, \bar{t}\,)$, is $\bar{m}_\infty(\bar{\mathbf{x}}) = 0$, whereas in the low-temperature phase, i.e., $\bar{\tau} < \bar{\tau}_c < 0$, the order parameter profile is non-trivial and its analytic expression can be found in Appendix D. The nonlinear partial differential equation (150) can be solved numerically. Starting from an arbitrary order parameter profile $\bar{m}_0(\bar{\mathbf{x}}) \equiv \bar{m}(\bar{\mathbf{x}}, \bar{t} = 0)$, with

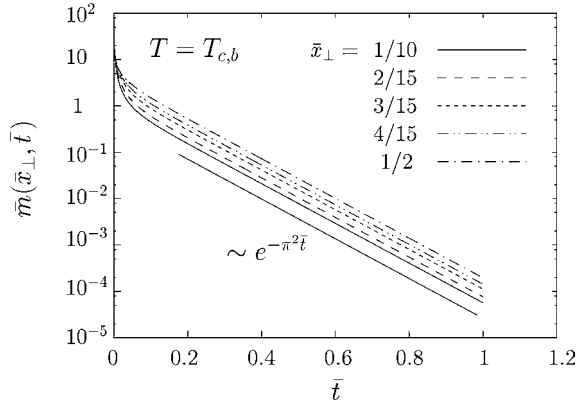

Fig. 16. Late relaxation of the order parameter $\bar{m}(\bar{x}_\perp, \bar{t}\,)$ at bulk criticality in a film of thickness L as a function of the reduced time variable $\bar{t} = (t/T_0)(\xi_0/L)^z$, for various values of the distance $\bar{x}_\perp = x_\perp/L$ from one wall. Already for $\bar{t} \gtrsim 0.2$, $\bar{m}(\bar{x}_\perp, \bar{t}\,)$ exhibits, independently of $\bar{x}_\perp$, its asymptotic long-time behavior, characterized by the exponential decay which is indicated as a straight line in the figure.

$\bar{m}_0(\bar{\mathbf{x}}_\mathcal{B}) = 0$, the profile evolves according to Eq. (150). In analogy with the results for the semi-infinite geometry,[64–66] we expect a non-universal behavior in the early stage of relaxation due to the fact that the order parameter profile we start with fulfills the Dirichlet boundary conditions and thus takes on *small* values near the confining walls, while universal properties are observed in the scaling limit of $\bar{m}_0(\bar{\mathbf{x}})$ being infinitely large. Note, however, that beyond MFT an additional initial stage of relaxation with *universal* features is expected to occur for finite $\bar{m}_0(\bar{\mathbf{x}})$, not only in the bulk[77] but also close to surfaces[7,78] and in finite volumes.[28,29,32] In the following we discuss the behavior of the system at bulk criticality $\bar{\tau} = 0$.

In Fig. 16 we show the results of the numerical solution of Eq. (150), evolving from an initial profile that is constant in the directions parallel to the confining walls and has a trapezoidal shape in the transverse direction, fulfilling the boundary conditions: $\bar{m}(\bar{x}_\perp, \bar{t} = 0) = K\bar{x}_\perp/D$ for $0 \le \bar{x}_\perp \le D$, $\bar{m}(\bar{x}_\perp, \bar{t} = 0) = K$ for $D < \bar{x}_\perp < 1 - D$, and $\bar{m}(\bar{x}_\perp, \bar{t} = 0) = K(1 - \bar{x}_\perp)/D$ for $1 - D \le \bar{x}_\perp < 1$. The parameters D and K have been suitably chosen to ensure the stability of the numerical solution of the equation (typical choices are $D \simeq 10^{-2}$ and $K \simeq 10^2$). Under this assumption the problem depends on a single space variable, given by the distance from a wall $0 \le \bar{x}_\perp \le 1/2$, and on the time variable $\bar{t}$. The solution for $1/2 < \bar{x}_\perp \le 1$ is obtained by taking into account the obvious symmetry of the problem, i.e., $\bar{m}(\bar{x}_\perp) = \bar{m}(1 - \bar{x}_\perp)$, provided the initial profile is chosen to share this symmetry. In Fig. 16 different curves refer to different distances from the wall. These data demonstrate clearly that asymptotically the relaxation is *exponential*

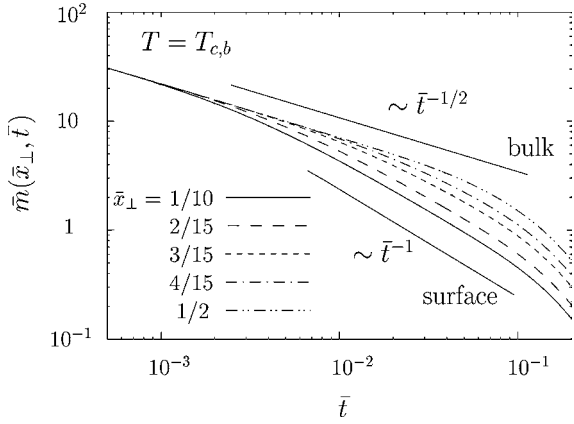

Fig. 17. Early relaxation of the order parameter $\bar{m}(\bar{x}_\perp, \bar{t})$ at bulk criticality in a film of thickness L as a function of the reduced time variable $\bar{t} = (t/T_0)(\xi_0/L)^z$, for various values of the distance $\bar{x}_\perp = x_\perp/L$ from one wall. This is a magnification, on a log-log scale, of the interval $\bar{t} < 0.2$ in Fig. 16. The two straight lines indicate the power-law behavior in the bulk (uppermost line) and close to surfaces, respectively. The crossover from bulk to surface and from surface to film behavior (i.e., exponential decay) is evident. For larger values of $\bar{x}_\perp$ the crossover occurs later.

in time, independently of $\bar{x}_\perp$, according to the behavior

$$m(\mathbf{x}, t \to \infty) \sim e^{-\pi^2 (t/T_0)(\xi_0/L)^z}. \tag{151}$$

This behavior can be explained by analyzing Eq. (150) for the special case we are discussing, i.e.,

$$\partial_{\bar{t}} \bar{m}(\bar{x}_\perp, \bar{t}) + \left[-\partial_{\bar{x}_\perp}^2 + \bar{m}^2(\bar{x}_\perp, \bar{t}) \right] \bar{m}(\bar{x}_\perp, \bar{t}) = 0 \tag{152}$$

with $\bar{m}(\bar{x}_\perp = 0, \bar{t}) = \bar{m}(\bar{x}_\perp = 1, \bar{t}) = 0$. In the linear regime (i.e., neglecting $\bar{m}^2$ in Eq. (152)) this equation can be solved straightforwardly, leading to

$$\bar{m}(\bar{x}_\perp, \bar{t}) = \sum_{n=1}^{\infty} \alpha_n e^{-\pi^2 n^2 \bar{t}} \sin(\pi n \bar{x}_\perp) \tag{153}$$

where the coefficients α_n are determined by the initial profile. Thus for generic values $\{\alpha_n\}$ the leading asymptotic decay is indeed exponential (see Eq. (151)) and its dependence on $\bar{x}_\perp$ is given by $\sin(\pi \bar{x}_\perp)$. As already stated at the beginning of this section, the exponential decay of the order parameter is intimately related to the fact that in Eq. (153) the sum contains no zero mode $n = 0$ and that we are considering the problem at the bulk critical point, located in the disordered phase of the confined system. This is analogous to what has been observed in the hypercubic geometry with periodic boundary conditions.[28] In the following we consider the behavior at early times as shown in the log-log plot in Fig. 17.

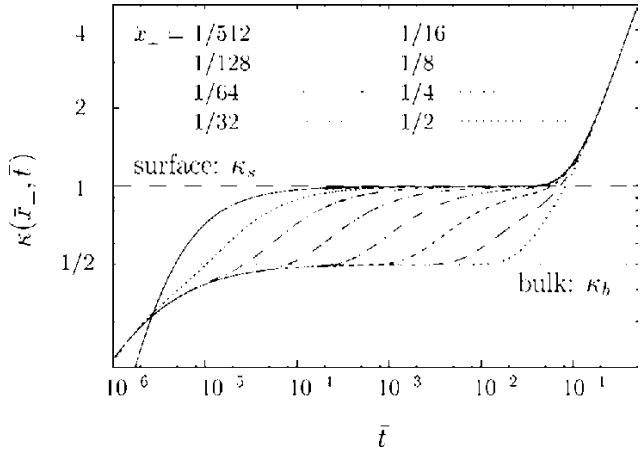

Fig. 18. Effective exponent $\kappa(\bar{x}_\perp, \bar{t}\,)$ for the order parameter relaxation at bulk criticality in a film of thickness L (see Eq. (154)) as a function of $\bar{t} = (t/T_0)(\xi_0/L)^z$ and for various values of $\bar{x}_\perp = x_\perp/L$. The two horizontal dashed lines represent the values of the exponent in the bulk ($\kappa = 1/2$) and close to a surface ($\kappa = 1$), respectively. For $\bar{t} < 10^{-4}$ the non-universal features of initial relaxation are evident. The linear increase of $\kappa(\bar{x}_\perp, \bar{t} \gtrsim 10^{-1}) = \rho\bar{t}$ indicates an exponential relaxation $\sim e^{-\rho\bar{t}}$ with $\rho = \pi^2$.

For small values of $\bar{x}_\perp$ (lower curves in Fig. 17) we note that the order parameter relaxes according to a power law $\sim t^{-\kappa_s}$ until the crossover towards exponential decay takes place. On the other hand, for $\bar{x}_\perp = 1/2$ (uppermost curve), the power law is different and relaxation follows the law $\sim t^{-\kappa_b}$ with $\kappa_b < \kappa_s$. For intermediate values of $\bar{x}_\perp$ there is a crossover between the two power laws. In order to elucidate this crossover, we compute the effective exponent of the relaxation as the logarithmic derivative of the magnetization profile, i.e.,

$$\kappa(\bar{x}_\perp, \bar{t}\,) \equiv -\frac{\partial \log \bar{m}(\bar{x}_\perp, \bar{t}\,)}{\partial \log \bar{t}}. \tag{154}$$

A power-law behavior corresponds to a value of κ independent of $\bar{t}$, while an exponential decay $\sim e^{-\rho\bar{t}}$ leads to $\kappa = \rho\bar{t}$. The behavior of $\kappa(\bar{x}_\perp, \bar{t}\,)$ is shown in Fig. 18

In accordance with the relaxation behavior in the semi-infinite geometry we expect the following qualitative picture of the order parameter evolution in a film. At the beginning of the relaxation process the effect of both boundaries on the relaxation behavior starts to propagate into the bulk. At a fixed distance from the wall the relaxation process is characterized by the bulk exponent κ_b until the influence of the closest surface reaches this point and changes the exponent into the surface one $\kappa_s > \kappa_b$. We expect that the final crossover towards the exponential decay (due to the presence of *two* confining walls with Dirichlet boundary

conditions) will take place via the intermediate stage of surface relaxation only if the spatial point under consideration can be reached sufficiently in time by the effect of one wall before the effect of the second wall arrives. This picture is confirmed by Fig. 18, which provides a quantitative analysis. The two exponents κ are readily determined as $\kappa_s = 1$ and $\kappa_b = 1/2$, corresponding to $\beta_1/\nu z$ and $\beta/\nu z$, respectively, as in the case of the semi-infinite geometry. There is a large degree of freedom in the definition of times at which crossovers take place. We define the following typical times:

$$\bar{t}_{c,b}(\bar{x}_\perp): \quad \kappa(\bar{t}_{c,b}, \bar{x}_\perp) = 0.4, \tag{155}$$

$$\bar{t}_{c,bs}(\bar{x}_\perp): \quad \kappa(\bar{t}_{c,bs}, \bar{x}_\perp) = 0.75, \tag{156}$$

$$\bar{t}_{c,e}(\bar{x}_\perp): \quad \kappa(\bar{t}_{c,e}, \bar{x}_\perp) = 1.1. \tag{157}$$

The first one, $\bar{t}_{c,b}$, is a measure of the time required to relax from the initial condition. Its dependence on $x_\perp$ carries non-universal information about the specific initial profile. In the scaling limit of infinite initial magnetization (in the bulk) $\bar{t}_{c,b} = 0$. The time $\bar{t}_{c,bs}$ is a measure of the time required to cross over from the *b*ulk to the *s*urface behavior. The value chosen in its definition is simply half way between κ_b and κ_s. The corresponding plot is given in Fig. 19 (a). It is useful to remark that $\bar{t}_{c,bs}(\bar{x}_\perp)$ is expected to be finite (given that it is still related to "surface" behavior) also in the limit $L \to \infty$ at fixed $x_\perp$, i.e., in the semi-infinite geometry. As a consequence, based only on scaling arguments, we can deduce the behavior of $\bar{t}_{c,bs}(\bar{x}_\perp)$ for small $\bar{x}_\perp$. Since κ is dimensionless one expects the scaling behavior $\kappa(x_\perp, t, L) = F_\kappa^{(3)}(x_\perp/L, (t/T_0)(\xi_0/L)^z)$ (compare Eq. (5)). Thus, according to the definition Eq. (156), it follows

$$\frac{t_{c,bs}}{T_0}\left(\frac{\xi_0}{L}\right)^z = F_{c,bs}(x_\perp/L). \tag{158}$$

A finite non-trivial limit for $L \to \infty$ for fixed $x_\perp$ exists provided

$$F_{c,bs}(y \to 0) = C_{bs} y^z \tag{159}$$

with a constant C_{bs} which implies

$$\frac{t_{c,bs}}{T_0}\left(\frac{\xi_0}{L}\right)^z = C_{bs}\left(\frac{x_\perp}{L}\right)^z, \quad \text{for} \quad x_\perp/L \ll 1, \tag{160}$$

so that

$$\bar{t}_{c,bs}(\bar{x}_\perp) = C_{bs}\bar{x}_\perp^z, \tag{161}$$

with $z = 2$ within MFT. This is in agreement with Fig. 19 (b) (apart from very small values of $\bar{x}_\perp$ which are numerically still influenced by the initial relaxation) yielding $C_{bs} \simeq 0.5$.

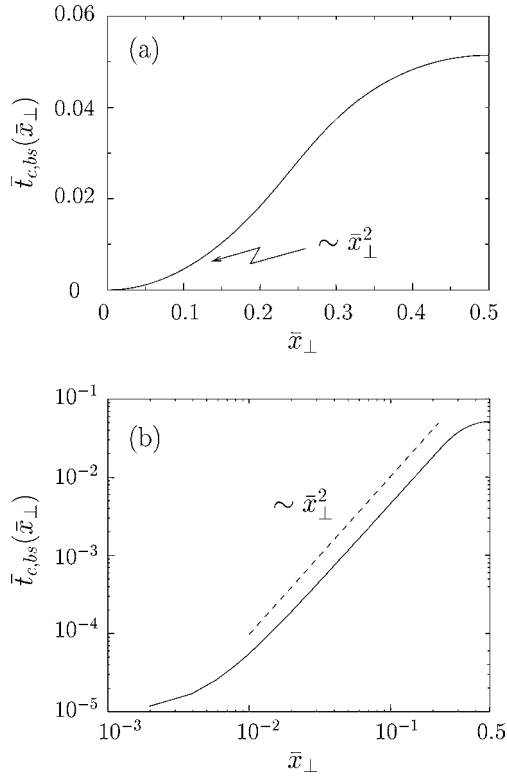

Fig. 19. (a) Crossover time $\bar{t}_{c,bs}$ (see Eqs. (156) and (161)) between bulk-like and surface-like behavior of relaxation. (b) Log-log plot of the crossover time $\bar{t}_{c,bs}$. The straight line indicates the quadratic law expected to hold for small $\bar{x}_\perp$ within mean-field theory according to scaling arguments (see Eq. (161)). For $\bar{t} \lesssim 10^{-2}$ there are deviations due to the non-universal initial relaxation. Beyond mean-field theory $\bar{t}_{c,bs}(\bar{x}_\perp \to 0) \sim \bar{x}_\perp^z$.

The time $\bar{t}_{c,e}$ measures the time required to enter the linear relaxation regime. As can be seen from Fig. 20, $\bar{t}_{c,e}(\bar{x}_\perp)$ attains a nonzero value for $\bar{x}_\perp \to 0$. This means that in the limit $L \to \infty$ at fixed $x_\perp$ one has

$$t_{c,e}(x_\perp, L \gg x_\perp)/T_0 = D_e(L/\xi_0)^z, \tag{162}$$

with $D_e \simeq 0.076$. This divergence of the crossover time as function of L is expected because in the semi-infinite geometry, i.e., for $L \to \infty$, the crossover towards an exponential decay never takes place.

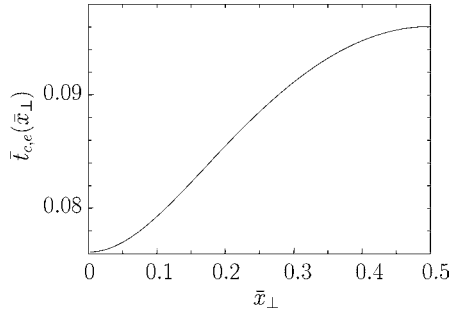

Fig. 20. Crossover time $\bar{t}_{c,e}$ (see Eq. (157)) towards the linear relaxation behavior characterized by an exponential decay of $\bar{m}(\bar{x}_\perp, \bar{t}\,)$.

6. SUMMARY

Within the field-theoretical approach, we have investigated various universal aspects of the relaxational critical dynamics [Model A, Eqs. (6)–(8)] in film geometry with Dirichlet boundary conditions, corresponding to the so-called ordinary surface universality class. We have obtained the1 following main results.

(1) (i) We have provided general scaling properties (see Section 2 and Subsec. 4.1) for the two-point response R and correlation functions C in the film geometry (Fig. 1). In particular, their Fourier transforms in the directions parallel to the confining walls (with conjugate momentum $\mathbf{p}$) scale as $R(\mathbf{p}, x_{1\perp}, x_{2\perp}, t) = (\hat{\mathfrak{o}}_R^{\pm}/T_0^{\pm})(L/\xi_0^{\pm})^{1-\eta-z}\bar{\mathscr{R}}_{\pm}(\bar{\mathbf{p}} = \mathbf{p}L, \bar{x}_{1\perp} = x_{1\perp}/L, \bar{x}_{2\perp} = x_{2\perp}/L, \bar{t} = (t/T_0^{\pm})(\xi_0^{\pm}/L)^z, \bar{L} = L/\xi)$ and $C(\mathbf{p}, x_{1\perp}, x_{2\perp}, t) = (\hat{\mathfrak{o}}_C^{\pm}/T_0^{\pm})\ \ (L/\xi_0^{\pm})^{1-\eta}\bar{\mathscr{C}}_{\pm}(\bar{\mathbf{p}}, \bar{x}_{1\perp}, \bar{x}_{2\perp}, \bar{t}, \bar{L})$, respectively, in terms of the film thickness L, the bulk correlation length $\xi(\tau = (T - T_{c,b})/T_{c,b} \to 0^{\pm}) = \xi_0^{\pm}|\tau|^{-\nu}$, and the relaxation time $T_R(\tau \to 0^{\pm}) = T_0^{\pm}|\tau|^{-\nu z}$ above and below the *bulk* critical temperature $T_{c,b}$, with the universal ratio $T_0^{+}/T_0^{-} = 3.3(4)$ in spatial dimension $d = 3$ (Appendix A). The semi-infinite limit of $\bar{\mathscr{R}}_{+}$ is discussed in Eqs. (59)–(62) and (91). The explicit forms of the associated universal scaling functions $\bar{\mathscr{R}}_{+}$ and $\bar{\mathscr{C}}_{+}$ have been computed within Gaussian approximation (denoted by $^{(0)}$).

(ii) The time evolution of the mean-field scaling function $\bar{\mathscr{R}}_{+}^{(0)}$ [see Eqs. (85) and (186)] for $\bar{\mathbf{p}} = 0$ and $T = T_{c,b}$ is shown in Fig. 2 for different values of the scaling variables $\bar{x}_{i\perp}$ and $\bar{t}$. The curves in Fig. 2 provide (apart from an amplitude) the time evolution of the order parameter profile across the film at $T = T_{c,b}$ after a laterally homogeneous perturbation confined to

the plane $x_\perp = x_{1\perp}$ and $\sim \delta(t)$ has been applied. A qualitative feature of interest is the time $\bar{t}_l(\bar{x}_{1\perp})$ at which the inflection points of these profiles reach the boundary $\bar{x}_{2\perp} = 0$, leading to a change in the shape of the profiles (see Fig. 3 and Appendix E).

(2) (i) We have discussed the *dy*namical effects of an external field $h(\mathbf{x} = (\mathbf{x}_\parallel, x_\perp), t)$ (conjugate to the order parameter) on the fluctuation-induced Casimir force $F_{l(r)}(\mathbf{x}_\parallel, \tau, L, t, \{h(\mathbf{x}, t)\})$ acting at the point $\mathbf{x}_\parallel$ on the *l*eft and *r*ight confining walls. Its scaling behavior is given by $F_{l(r)}(\mathbf{x}_\parallel, \tau > 0, L, t, \{h(\mathbf{x}, t)\}) = L^{-d}\, \mathscr{F}^{(\mathrm{dy})}_{l(r)}(\bar{\mathbf{x}}_\parallel = \mathbf{x}_\parallel/L, \bar{L}, \bar{t}, \{(L/\xi_0)^{\beta\delta/\nu}[h(\bar{\mathbf{x}}, \bar{t})/\mathfrak{h}_0]\})$ (see also Eq. (100)). Within Gaussian approximation we have provided the expressions for the scaling function $\mathscr{F}^{(\mathrm{dy})}_l$ for two specific instances of external field: (W) $h(\mathbf{x}, t) = h_W \delta(x_\perp - x_{1\perp})\delta(t - t_1)$ and (P) $h(\mathbf{x}, t) = h_P \delta(\mathbf{x}_\parallel - \mathbf{x}_{1\parallel})\delta(x_\perp - x_{1\perp})\delta(t - t_1)$. In both cases $\mathscr{F}^{(\mathrm{dy})}_l$ is the sum [Eqs. (107) and (113)] of the *st*atic Casimir force $\mathscr{F}^{(\mathrm{st})}$ corresponding to the ordinary-ordinary surface universality class considered here, and a dynamic term which is quadratic in the scaling variables $\hat{h}_{W,P}$ [see Eqs. (108) and (114)] proportional to the amplitudes $h_{W,P}$ of the external field. In particular we focused on the force at $T_{c,b}$ where $\mathscr{F}^{(\mathrm{st})} = (d-1)\Delta < 0$ [Eq. (101)]. For both cases W and P we have studied as function of time the maximum $A^{W,P}_\Delta$ of the field-induced contribution $[\mathscr{F}^{(\mathrm{dy})}_l - \mathscr{F}^{(\mathrm{st})}]/\hat{h}^2_{W,P}$.

(ii) It turns out that A^W_Δ is attained at $\bar{t} = \bar{t}_l(\bar{x}_{1\perp})$ discussed in the previous point (i). Figure 4 shows the dependence of A^W_Δ on the normal distance $\bar{x}_{1\perp}$ at which the perturbation has been applied (see Appendix F2). Figure 5 illustrates the time dependence of the normalized part of the field-induced Casimir force $\mathscr{F}^W_\Delta(\bar{x}_{1\perp}, \bar{t}) = [\mathscr{F}^{(\mathrm{dy})}_l - \mathscr{F}^{(\mathrm{st})}]/[\hat{h}^2_W A^W_\Delta(\bar{x}_{1\perp})]$ which decays $\sim e^{-2\pi^2\bar{t}}$.

(iii) A^P_Δ is attained at $\bar{t} = \bar{t}_M(\delta\mathbf{x}_\parallel, \bar{x}_{1\perp})$ (Fig. 6) which depends additionally on the scaled lateral distance $\delta\bar{\mathbf{x}}_\parallel \equiv (\mathbf{x}_\parallel - \mathbf{x}_{1\parallel})/L$ between the action of the force and the epicenter of the perturbation. The maximum of the force on the walls spreads with an asymptotically constant radial velocity which decreases with the film thickness (Eq. (117)). The force decreases monotonically for increasing lateral distances $|\delta\bar{\mathbf{x}}_\parallel|$. Figures 7 and 8 show the dependence of the corresponding maximum $A^P_\Delta(\delta\mathbf{x}_\parallel, \bar{x}_{1\perp})$ (attained at $\bar{t} = \bar{t}_M(\delta\mathbf{x}_\parallel, \bar{x}_{1\perp})$) on $|\delta\bar{\mathbf{x}}_\parallel|$ and $\bar{x}_{1\perp}$. The time dependence of the normalized part of the Casimir force $\mathscr{F}^P_\Delta(\delta\bar{\mathbf{x}}_\parallel, \bar{x}_{1\perp}, \bar{t}) = [\mathscr{F}^{(\mathrm{dy})}_l - \mathscr{F}^{(\mathrm{st})}]/[\hat{h}^2_P A^P_\Delta(\delta\bar{\mathbf{x}}_\parallel, \bar{x}_{1\perp})]$ is reported in Fig. 9; it decays $\sim \bar{t}^{-(d-1)} e^{-2\pi^2\bar{t}}$.

(3) We have computed the universal scaling function $\bar{\mathscr{C}}^{(0)}_+$ of the dynamical two-point correlation function [see the previous point (1)] within Gaussian

approximation. In Fig. 10 the time evolution of $\bar{\mathscr{C}}_{+}^{(0)}$ [see Eq. (122)] for $\bar{\mathbf{p}} = 0$ and $T = T_{c,b}$ is shown for different values of the scaling variables $\bar{x}_{i\perp}$ and $\bar{t}$. Figure 11 refers, instead, to the cases in which $\bar{t}_0 = 1/(\bar{\mathbf{p}}^2 + \bar{L}^2)$ is finite, i.e., if $T > T_{c,b}$ or $\mathbf{p} \neq 0$.

(4) (i) In view of the possibility to probe the spatial structure of correlations by means of neutron or X-rays scattering under grazing incidence, we have investigated the behavior of the frequency- and momentum-dependent correlation function in planes parallel to the surface of the film, i.e., of $C(\mathbf{p}, x_{1\perp} = x_\perp, x_{2\perp} = x_\perp, \omega) = \hat{\mathfrak{o}}_C^{\pm}(L/\xi_0^{\pm})^{1-\eta+z}\, \mathscr{C}_{\pm}(\bar{\mathbf{p}}, \bar{x}_\perp, \bar{x}_\perp, \bar{\omega} = \omega T_0^{\pm}(L/\xi_0^{\pm})^z, \bar{L})$ [see Eq. (44)].

(ii) Near the walls the surface behavior $\mathscr{C}_{+}(\bar{\mathbf{p}}, \bar{x}_\perp \to 0, \bar{x}_\perp \to 0, \bar{\omega}, \bar{L}) = \bar{x}_\perp^{2(\beta_1-\beta)/\nu}\, \mathscr{C}_W(\bar{\mathbf{p}}, \bar{\omega}, \bar{L})$ [see Eq. (63)] is recovered. The various asymptotic behaviors of $\mathscr{C}_W$ have been discussed in Subsection 4.1 [see Eqs. (64)–(71) and (132)–(134),(137)]. Within Gaussian approximation the scaling function $\mathscr{C}_W^{(0)}$ is shown and discussed Figs. 12 and 13. In contrast to the semi-infinite geometry, in films $\mathscr{C}_W^{(0)}$ attains a finite value at the origin of the $(\xi^{-1}, \mathbf{p}, \omega)$-space which diverges for $L \to \infty$.

(iii) The correlation function in the middle of the film is characterized by the scaling function $\mathscr{C}_I(\bar{\mathbf{p}}, \bar{\omega}, \bar{L}) \equiv \mathscr{C}_{+}(\bar{\mathbf{p}}, 1/2, 1/2, \bar{\omega}, \bar{L})$. Its asymptotic behaviors are discussed in Subsection 4.1 [see Eqs. (73)–(80) and (141)–(143),(145)]. Figures 14 and 15 show the shape of the scaling function $\mathscr{C}_I^{(0)}$ along the axes of the $(\xi^{-1}, \mathbf{p}, \omega)$-space.

(iv) Comparing the scaling functions $\mathscr{C}_W^{(0)}$ and $\mathscr{C}_I^{(0)}$ it turns out that, although their shapes are similar, the latter exhibits more rapid algebraic decays for $\bar{L}, \bar{\mathbf{p}}, \bar{\omega} \to \infty$.

(5) (i) We have considered the nonlinear relaxation from an initially ordered state by solving numerically the evolution equation for the scaled order parameter profile $\bar{m}(\bar{\mathbf{x}}, \bar{t})$ [see Eqs. (149) and (150)], which is proportional to the time-dependent mean value of the order parameter $\langle \varphi(\mathbf{x}, t) \rangle$ across the film. In particular we have analyzed the relaxation at the *bulk* critical point $T = T_{c,b}$ from an initial profile that is laterally constant and has a symmetric shape in the transverse direction which fulfills the Dirichlet boundary conditions. The universal aspects of the relaxation process are independent of the actual shape of the initial profile. In view of this symmetry the scaled order parameter profile $\bar{m}(\bar{\mathbf{x}}, \bar{t})$ depends only on $\bar{x}_\perp$ and $\bar{t}$.

(ii) In Fig. 16 the late stage of the relaxation of the order parameter is shown as a function of $\bar{t}$ for various values of $\bar{x}_\perp$. For all $\bar{x}_\perp$, $\bar{m}(\bar{x}_\perp, \bar{t} \to \infty)$ displays an *exponential* decay due to the critical point shift in the film geometry. On the other hand, during the early stage of relaxation, i.e., for $\bar{t} \lesssim 0.1$, a crossover between an algebraic surface- and bulk-like behavior clearly emerges (see Fig. 17). Close to the surface

one observes $\bar{m}(\bar{x}_\perp, \bar{t}) \sim \bar{t}^{-\beta_1/(\nu z)}$ ($\beta_1/(\nu z) = 1$ within mean-field theory), whereas upon moving inside the film $\bar{m}(\bar{x}_\perp, \bar{t}) \sim \bar{t}^{-\beta/(\nu z)}$ ($\beta/(\nu z) = 1/2$ within mean-field theory). This crossover is clearly detected by the time dependence of the effective exponent $\kappa(\bar{x}_\perp, \bar{t}) \equiv -\partial \log \bar{m}(\bar{x}_\perp, \bar{t})/\partial \bar{t}$ shown in Fig. 18. We have also defined (Eq. (156)) and studied (Fig. 19) the typical time $\bar{t}_{c,bs}(\bar{x}_\perp)$ at which the crossover from the *b*ulk to the *s*urface behavior takes place for a given distance $\bar{x}_\perp$ from the near wall, and that one for the crossover to the ultimate *e*xponential decay $\bar{t}_{c,e}(\bar{x}_\perp)$ (Eq. (157) and Fig. 20).

(iii) Thus the nonlinear relaxation of the order parameter in film geometry is characterized by a cascade of four clearly identifyable, successive decay modes: nonuniversal initial relaxation dominated by the initial profile, bulk-like power-law decay $\sim t^{-\beta/\nu z}$, surface-like power-law decay $\sim t^{-\beta_1/\nu z}$, and exponential decay $\sim \exp(-\pi^2 \bar{t})$. The initial relaxation lasts, in the present case, up to $\bar{t} \lesssim 10^{-5}$ and the exponential decay prevails for $\bar{t} \gtrsim 10^{-1}$. The crossover time between the two power laws depends on the distance of the point of observation from the near wall. Beyond MFT the scenario is even richer if the relaxation process starts with a (genericly) *finite* value of the order parameter $\bar{m}_0(\bar{\mathbf{x}})$. In fact $\bar{m}_0(\bar{\mathbf{x}})$ introduces an additional time scale $t_0 \sim T_0(m_0/\mathfrak{m}_0)^{-1/(\theta' + \beta/\nu z)}$,[77] where θ' is the so-called *initial-slip* exponent such that, for $t \leq t_0$ (but t sufficiently large to avoid the non-universal initial behavior), one observes an initial *increase* of the order parameter $m(\bar{\mathbf{x}}, \bar{t}) \sim m_0(\bar{\mathbf{x}})(t/t_0)^{\theta'}$. For $t \gg t_0$ a crossover towards the previously mentioned cascade of decay modes takes place. On the other hand, θ' at the surface (θ'_s) differs from θ' in the bulk (θ'_b) such that $\theta'_s = \theta'_b - (\beta_1 - \beta)/\nu z$.[78] Accordingly one expects, upon increasing the distance from the confining walls, the following possible sequences of relaxation processes: (1) m increases $\sim t^{\theta'_s}$, reaching a maximum after which it decreases first algebraically $\sim t^{-\beta_1/\nu z}$ and then exponentially. In this case the displayed behavior is always surface-like. (2) m first increases $\sim t^{\theta'_b}$ and then $\sim t^{\theta'_s}$, reaching a maximum after which it first decreases algebraically $\sim t^{-\beta_1/\nu z}$ and then exponentially. The crossover between bulk-like and surface-like behavior takes place during the initial increase of the order parameter. (3) m first increases $\sim t^{\theta'_b}$, reaching a maximum after which it decreases algebraically first $\sim t^{-\beta/\nu z}$, then $\sim t^{-\beta_1/\nu z}$, and finally exponentially. In this case the crossover takes place during the later stage of relaxation, characterized by an algebraically decreasing order parameter. (4) m first increases $\sim t^{\theta'_b}$, reaching a maximum after which it decreases algebraically $\sim t^{-\beta/\nu z}$ and then exponentially. Monte Carlo simulations and analytical computations should be able to disclose this rich scenario of phenomena.

APPENDIX A: UNIVERSAL DYNAMIC AMPLITUDE RATIOS

In this appendix we determine the universal amplitude ratio T_0^+/T_0^- as introduced in Sec. 2. We consider the model described in Sec. 3 in the absence of any confining wall (bulk behavior) and for the specific case of a one-component field (i.e., Ising universality class, $N = 1$). The linear response of this model in the presence of a finite external field h, and thus of a non-vanishing magnetization m, has been studied in Refs. 60 and 61 within a loop expansion up to one loop. The results obtained there allow one to compute the relaxation time of the system (a) in the high-temperature phase ($\tau > 0$, with $h = 0$ and thus $m = 0$) and (b) in the low-temperature phase ($\tau < 0$ and thus $m = M_0 \neq 0$ also for $h = 0$). In particular the value of the spontaneous magnetization M_0 for $\tau < 0$ and $h = 0$ can be determined from the equation of state reported in Eq. (5.1) of Ref. 60:

$$M_0(\tau < 0) = \sqrt{\frac{3}{u^*}}\mu^{(d-2)/2}(-2\tau)^\beta \left[1 + \frac{\epsilon}{6} + O(\epsilon^2)\right] \tag{163}$$

where $\epsilon = 4 - d$, $\beta = (1 - \epsilon/3)/2 + O(\epsilon^2)$ is the critical exponent of the spontaneous magnetization M_0, $\tau = (T - T_{c,b})/T_{c,b}$, μ is a momentum scale (see below), and u^* is the fixed-point value of the renormalized coupling constant (whose actual value is irrelevant for the rest of the computation). The true correlation length in the high-temperature phase is given by

$$\xi(\tau \to 0^+) = \mu^{-1}\tau^{-\nu}\left[1 + \frac{\epsilon}{12} + O(\epsilon^2)\right] \tag{164}$$

with $\nu = (1 + \epsilon/6)/2 + O(\epsilon^2)$. Accordingly, μ can be expressed in terms of the nonuniversal amplitude ξ_0^+ as $\mu = (\xi_0^+)^{-1}[1 + \epsilon/12 + O(\epsilon^2)]$.

The linear response function can be computed from Eq. (5.2) in Ref. 60, taking into account the different values of M_0 in the cases (a) ($M_0 = 0$) and (b) (see Eq. (163)). This equation expresses the deviation $m_1(t)$ of the magnetization from the constant value M_0 in terms of the small magnetic field $h_1(t)$ that gives rise to it, and thus provides an expression for the linear susceptibility χ defined through

$$m_1(t) = \int_{-\infty}^{t} \mathrm{d}s\ \chi(t - s)h_1(s). \tag{165}$$

It is straightforward to express the Fourier transform $\hat{\chi}_\pm(\omega) = \int_0^{+\infty} \mathrm{d}t\ e^{i\omega t}\chi_\pm(t)$ of $\chi_\pm(t)$ for $\tau \lessgtr 0$ as

$$\hat{\chi}_+^{-1}(\omega) = \omega_0^+\left[-i\frac{\omega}{\omega_0^+} + 1 - \frac{\epsilon}{6}\right] + O(\epsilon^2) \tag{166}$$

and

$$\hat{\chi}_-^{-1}(\omega) = \omega_0^- \left[-i\frac{\omega}{\omega_0^-} + 1 + \frac{\epsilon}{3} + \frac{\epsilon}{2} F_R(i\omega/\omega_0^-) \right] + O(\epsilon^2), \tag{167}$$

where

$$\omega_0^+ \equiv \Omega \mu^2 \tau^{\nu z} \tag{168}$$

and

$$\omega_0^- \equiv \Omega \mu^2 (-2\tau)^{\nu z}, \tag{169}$$

with $z = 2 + O(\epsilon^2)$ and

$$F_R(x) = \int_0^\infty \mathrm{d}u \, \frac{1 + u - e^u}{u^2} e^{-2u/x} = -1 + \left(1 - \frac{2}{x}\right) \ln\left(1 - \frac{x}{2}\right) \tag{170}$$

which has a branch cut on the real axis for $x > 2$. The kinetic coefficient Ω in Eqs. (168) and (169) can be expressed in terms of the non-universal amplitudes $T_{0,\mathrm{ac}}^+$ or $T_{0,\mathrm{exp}}^+$, and ξ_0^+ through, c.f., Eq. (174) or (176). For instance, $\Omega = (\xi_{0,\mathrm{exp}}^+)^2 / T_{0,\mathrm{exp}}^+ [1 + O(\epsilon^2)]$.

As it is the case for the (bulk) correlation length, there are different possible definitions of the relaxation time T_R. For example it can be defined as the inverse characteristic frequency (see, e.g., Eq. (3.17) in Ref. 2), i.e.,

$$T_{R,\mathrm{ac}}(\tau) = \frac{i}{\hat{\chi}^{-1}(\omega = 0)} \left. \frac{\partial \hat{\chi}^{-1}(\omega)}{\partial \omega} \right|_{\omega=0} \tag{171}$$

where the subscript ac stands for "autocorrelation." Indeed using the FDT (see, e.g., Eq. (34)) one can show that $T_{R,\mathrm{ac}}$ coincides with the so-called integrated autocorrelation time of the magnetization:

$$T_{R,\mathrm{ac}} = \int_0^\infty \mathrm{d}t \, \frac{C_M(t)}{C_M(0)}, \tag{172}$$

where $C_M(t)$ is the two-time dynamic (auto)correlation function of thermal equilibrium fluctuations (around M_0) of the magnetization; it is given via the FDT (see, e.g., Eq. (32)) by $C_M(t) = \int_{|t|}^{+\infty} \mathrm{d}s \, \chi(s)$. Another possible definition of T_R introduces the "true" relaxation time determined by the position of the frequency pole in $\chi(\omega)$ closest to the real axis:

$$\hat{\chi}^{-1}(\omega = -i T_{R,\mathrm{exp}}^{-1}(\tau)) = 0. \tag{173}$$

From Eq. (173) it follows that $T_{R,\mathrm{exp}}$ governs the long-time exponential decay $\sim \exp(-t/T_{R,\mathrm{exp}})$ of the correlation and linear response function away from T_c.

Using the previous expressions one finds that

$$T_{R,\mathrm{ac}} = \begin{cases} (\omega_0^+)^{-1}\left(1+\frac{1}{6}\epsilon\right)+O(\epsilon^2), & \tau>0, \\ (\omega_0^-)^{-1}\left(1-\frac{5}{24}\epsilon\right)+O(\epsilon^2), & \tau<0, \end{cases} \tag{174}$$

which yields the universal amplitude ratio

$$\frac{T^+_{0,\mathrm{ac}}}{T^-_{0,\mathrm{ac}}} = 2^{\nu z}\left(1+\frac{3}{8}\epsilon\right)+O(\epsilon^2). \tag{175}$$

Instead, for $T_{R,\mathrm{exp}}$ one finds

$$T_{R,\mathrm{exp}} = \begin{cases} (\omega_0^+)^{-1}\left(1+\frac{1}{6}\epsilon\right)+O(\epsilon^2), & \tau>0, \\ (\omega_0^-)^{-1}\left[1+(\frac{1}{6}-\frac{\ln 2}{2})\epsilon\right]+O(\epsilon^2), & \tau<0, \end{cases} \tag{176}$$

so that the corresponding universal amplitude ratio is given by

$$\frac{T^+_{0,\mathrm{exp}}}{T^-_{0,\mathrm{exp}}} = 2^{\nu z}\left(1+\frac{\ln 2}{2}\epsilon\right)+O(\epsilon^2). \tag{177}$$

In Ref. 49 the purely relaxational dynamics of the Ising model has been studied both analytically and numerically (in three dimensions). In particular the generalizations of $T_{R,\mathrm{ac}}$ and $T_{R,\mathrm{exp}}$ to the case of a non-vanishing wavevector have been considered for a generic point in the $(\tau,\, M_0)$-plane, and their universal scaling functions have been computed (see Eqs. (15), (16), and (19) therein). These results provide predictions also for the universal ratios $T^+_{0,\mathrm{exp}}/T^+_{0,\mathrm{ac}}$ and $T^-_{0,\mathrm{exp}}/T^-_{0,\mathrm{ac}}$. Using the notations of Ref. 49, $T^+_{0,\mathrm{exp}}/T^+_{0,\mathrm{ac}} = \mathcal{T}_{\mathrm{exp}}(0;\infty) = 1+O(\epsilon^2)$ and $T^-_{0,\mathrm{exp}}/T^-_{0,\mathrm{ac}} = \mathcal{T}_{\mathrm{exp}}(0;-1) = 1+(3/8-\ln 2/2)\epsilon+O(\epsilon^2)$, respectively. It is straightforward to check that the results reported in Eqs. (174) and (176) are in accordance with these predictions.

APPENDIX B: STATIC CORRELATION FUNCTION

The static (i.e., equal-time) correlation function $C^{(0)}_{\mathrm{st}}$ can be obtained from Eq. (30) by integrating $C^{(0)}(\mathbf{q}_n,\omega)$ over ω (see Eqs. (24) and (29)):

$$C^{(0)}_{\mathrm{st}}(\mathbf{p},x_{1\perp},x_{2\perp}) = \sum_{n=1}^{\infty}\Phi_n(x_{1\perp};L)\Phi_n(x_{2\perp};L)\frac{1}{\mathbf{q}_n^2+r_0}. \tag{178}$$

Using the relations (see Eq. (18))

$$\Phi_n(x_1;L)\Phi_n(x_2;L) = \frac{1}{L}\left\{\cos\left[\frac{\pi n}{L}(x_1-x_2)\right]-\cos\left[\frac{\pi n}{L}(x_1+x_2)\right]\right\}, \tag{179}$$

$\mathbf{q}_n^2 = \mathbf{p}^2 + \pi^2 n^2/L^2$, and the identity (see, e.g., §5.4.5-1 in Ref. 69)

$$\sum_{n=1}^{\infty} \frac{\cos(\pi n z)}{\pi^2 n^2 + \alpha^2} = \left\{ \frac{1}{2\alpha} \frac{\cosh[\alpha(|z|-1)]}{\sinh\alpha} - \frac{1}{2\alpha^2} \right\}, \quad \text{for} \quad -2 < z \leq 2, \tag{180}$$

(outside the range $|z| \leq 2$ this expression has to be extended periodically in z with period 2), one finds

$$C_{\rm st}^{(0)}(\mathbf{p}, x_{1\perp}, x_{2\perp}) = \frac{1}{2a} \frac{\cosh[a(|x_{1\perp} - x_{2\perp}| - L)] - \cosh[a(x_{1\perp} + x_{2\perp} - L)]}{\sinh(aL)} \tag{181}$$

where $a^2 \equiv \mathbf{p}^2 + \xi^{-2}$ (see footnote 8). By applying addition formulae for hyperbolic functions, Eq. (181) can be expressed as

$$C_{\rm st}^{(0)}(\mathbf{p}, x_{1\perp}, x_{2\perp}) = L \frac{\sinh[aL(x_\perp^</L)] \sinh[aL(1 - x_\perp^>/L)]}{aL \sinh(aL)}, \tag{182}$$

where $x_\perp^> = \max\{x_{1\perp}, x_{2\perp}\} = (x_{1\perp} + x_{2\perp} + |x_{1\perp} - x_{2\perp}|)/2$ and $x_\perp^< = \min\{x_{1\perp}, x_{2\perp}\} = (x_{1\perp} + x_{2\perp} - |x_{1\perp} - x_{2\perp}|)/2$, in agreement with Eq. (B4) in Ref. (53) (and with Eq. (4.1) of Ref. 6 in the case $c_0 = +\infty$). This result can also be found directly from Eq. (95) by using the FDT (see Eq. (35)): $C_{\rm st}^{(0)}(\mathbf{p}, x_{1\perp}, x_{2\perp}) = C^{(0)}(\mathbf{p}, x_{1\perp}, x_{2\perp}, t = 0) = R^{(0)}(\mathbf{p}, x_{1\perp}, x_{2\perp}, \omega = 0)$.

APPENDIX C: RESPONSE FUNCTION AND ITS ASYMPTOTIC TIME DEPENDENCE

With a view of the scaling function Ψ for the response function $R^{(0)}$ (see Eqs. (82) and (83)) we consider the sum

$$\sum_{n=1}^{\infty} \Phi_n(x_1; L)\Phi_n(x_2; L) e^{-\Omega(\pi n/L)^2 t} \equiv \frac{1}{L} \Psi(x_1/L, x_2/L, \Omega t/L^2) \tag{183}$$

with the eigenfunctions $\Phi_n(x; L)$ defined in Eq. (18). Using Eq. (179), Eq. (183) reduces to the evaluation of expressions of the form

$$\sum_{n=1}^{\infty} \cos(\pi n \mu) e^{-\pi^2 n^2 \tau} = -\frac{1}{2} + \frac{1}{2} \sum_{n=-\infty}^{+\infty} e^{i\pi n\mu - \pi^2 n^2 \tau} \tag{184}$$

which can be expressed, according to standard definitions (see, e.g., §16.27.3 in Ref. 70), in terms of Jacobi's theta function

$$\vartheta_3(z, q) = \sum_{n=-\infty}^{+\infty} q^{n^2} e^{2niz} \tag{185}$$

so that with $\bar{t} = \Omega t/L^2$ (see Eq. (84)) and $\bar{x}_i = x_i/L$

$$\Psi(\bar{x}_1, \bar{x}_2, \bar{t}\,) = \frac{1}{2}\left[\vartheta_3(\pi\frac{\bar{x}_1 - \bar{x}_2}{2}, e^{-\pi^2\bar{t}}) - \vartheta_3(\pi\frac{\bar{x}_1 + \bar{x}_2}{2}, e^{-\pi^2\bar{t}})\right]. \tag{186}$$

By using Poisson's resummation formula [i.e., $\sum_{n=-\infty}^{\infty} e^{2\pi i n x} = \sum_{n=-\infty}^{\infty} \delta(x - n)$] we obtain

$$\vartheta_3(\pi\bar{x}, e^{-\pi^2\bar{t}}) = \frac{1}{\sqrt{\pi\bar{t}}}\sum_{n=-\infty}^{+\infty} e^{-(n-\bar{x})^2/\bar{t}} \tag{187}$$

so that

$$\begin{aligned}\Psi(\bar{x}_1, \bar{x}_2, \bar{t}\,) = \frac{1}{\sqrt{4\pi\bar{t}}}\Bigg\{ & e^{-(\bar{x}_1-\bar{x}_2)^2/(4\bar{t}\,)} - e^{-(\bar{x}_1+\bar{x}_2)^2/(4\bar{t}\,)} \\ & + \sum_{n=1}^{\infty}\Big[e^{-(\frac{\bar{x}_1-\bar{x}_2}{2}-n)^2/\bar{t}} + e^{-(\frac{\bar{x}_1-\bar{x}_2}{2}+n)^2/\bar{t}} \\ & - e^{-(\frac{\bar{x}_1+\bar{x}_2}{2}-n)^2/\bar{t}} - e^{-(\frac{\bar{x}_1+\bar{x}_2}{2}+n)^2/\bar{t}}\Big]\Bigg\}.\end{aligned} \tag{188}$$

This expression is useful for discussing the semi-infinite limit of the response function (see Eq. (86)).

The long-time limit $\bar{t} = \Omega t/L^2 \to \infty$ of Eq. (183) follows from

$$\vartheta_3(\pi\bar{x}, e^{-\pi^2\bar{t}}) = 1 + 2e^{-\pi^2\bar{t}}\cos(2\pi\bar{x}) + O(e^{-4\pi^2\bar{t}}) \tag{189}$$

so that

$$\Psi(\bar{x}_1, \bar{x}_2, \bar{t} \to \infty) = e^{-\pi^2\bar{t}}[\cos\pi(\bar{x}_1 - \bar{x}_2) - \cos\pi(\bar{x}_1 + \bar{x}_2)] + O(e^{-4\pi^2\bar{t}}) \tag{190}$$

as expected also from Eq. (183) because in that limit the sum in Eq. (183) is dominated by its first term so that

$$\Psi(\bar{x}_1, \bar{x}_2, \bar{t} \to \infty) = L\,\Phi_1(x_1; L)\Phi_1(x_2; L)e^{-\pi^2\bar{t}} + O(e^{-4\pi^2\bar{t}}). \tag{191}$$

APPENDIX D: ANALYTIC EXPRESSION FOR THE MEAN-FIELD ORDER PARAMETER PROFILE

The rescaled mean-field order parameter profile $\bar{m}_\infty(\bar{\mathbf{x}})$ is the stationary solution of Eq. (150):

$$[-\Delta_{\bar{\mathbf{x}}} + \bar{\tau} + \bar{m}_\infty^2(\bar{\mathbf{x}})]\bar{m}_\infty(\bar{\mathbf{x}}) = 0 \tag{192}$$

with the Dirichlet boundary conditions $\bar{m}_\infty(\bar{\mathbf{x}}_\mathcal{B}) = 0$. Thus $\bar{m}_\infty(\bar{\mathbf{x}})$ is an extremum of the functional (8), which can be rewritten as

$$\mathcal{H}[m] = L^{d-4}\mathfrak{m}_0^2\xi_0^2 \int_{\bar{V}} \mathrm{d}^d\bar{x} \left[\frac{1}{2}(\nabla_{\bar{\mathbf{x}}}\bar{m}(\bar{\mathbf{x}}))^2 + \frac{1}{2}\bar{\tau}\bar{m}(\bar{\mathbf{x}})^2 + \frac{1}{4}\bar{m}(\bar{\mathbf{x}})^4\right] \tag{193}$$

by taking into account Eqs. (84) and (149), the definitions $\bar{\mathbf{x}} = \mathbf{x}/L$, $\bar{\tau} = (L/\xi)^2 = \bar{L}^2$ for $\tau > 0$, $\bar{\tau} = -1/2(L/\xi)^2 = -\bar{L}^2/2$ for $\tau < 0$, and $\bar{V} = \mathbb{R}^{d-1} \times [0, 1]$ as well as $\bar{m}(\bar{\mathbf{x}}_\mathcal{B}) = 0$. We recall that, within mean-field theory, $\xi(\tau \to 0^+) = r_0^{-1/2}$ whereas $\xi(\tau \to 0^-) = (-2r_0)^{-1/2}$ (Eq. (8)); in the main text we use also the abbreviation $L/\xi = \bar{L}$. Here and in the following ξ means ξ_- for $\tau < 0$ and ξ_+ for $\tau > 0$. In view of the translational symmetry in all directions parallel to the confining walls, finding the equilibrium profile reduces to solving a one-dimensional differential equation for $\psi(\bar{x}_\perp) = \bar{m}(\bar{\mathbf{x}})$ where $\bar{\mathbf{x}} = (\bar{\mathbf{x}}_\parallel, \bar{\mathbf{x}}_\perp)$:

$$\begin{aligned} -\psi''(\bar{x}_\perp) + \bar{\tau}\psi(\bar{x}_\perp) + \psi^3(\bar{x}_\perp) &= 0, \\ \psi(0) = \psi(1) &= 0, \end{aligned} \tag{194}$$

with the symmetry $\psi(\bar{x}_\perp) = \psi(1 - \bar{x}_\perp)$ so that for regular solutions $\psi'(1/2) = 0$. Accordingly a set of equivalent boundary conditions for Eq. (194) is $\psi(0) = 0$ and $\psi'(1/2) = 0$. Equation (194) has always the trivial solution $\psi(\bar{x}_\perp) \equiv 0$. Note that Eq. (194) describes the one-dimensional closed motion of a particle with coordinate ψ in a potential $V(\psi) = -\bar{\tau}\psi^2/2 - \psi^4/4$ as a function of "time" $\bar{x}_\perp$. Using this analogy one can show that the non-trivial solution $\psi(\bar{x}_\perp)$ of Eq. (194) is bounded by the non-trivial solution $\bar{\psi}$ of Eq. (194) with free boundaries resembling the bulk solution,

$$\bar{\psi} = \begin{cases} 0 & \text{for } \bar{\tau} > 0, \\ \sqrt{-\bar{\tau}} & \text{for } \bar{\tau} \le 0, \end{cases} \tag{195}$$

in the sense that $|\psi(\bar{x}_\perp)| \le \bar{\psi}$.[9] In view of this, in the following we consider $\bar{\tau} < 0$. Equation (194) can be integrated once by using the boundary condition $\psi(0) = 0$:

$$\psi'^2(\bar{x}_\perp) = \psi'^2(0) + \bar{\tau}\psi^2(\bar{x}_\perp) + \frac{1}{2}\psi^4(\bar{x}_\perp). \tag{196}$$

The solution of Eq. (196) (together with the boundary condition $\psi(0) = 0$) depends on $\psi'(0)$ which has to be determined as a function of $\bar{\tau}$ in order to fulfill the second boundary condition $\psi'(1/2) = 0$. It is convenient to introduce the scale

[9] For $\bar{\tau} < 0$, $\bar{\psi}$ is the position of the maximum of $V(\psi)$ for $\psi > 0$. A particle starting from the point $\psi = 0$ at the "time" $\bar{x}_\perp = 0$ with $\psi'(\bar{x}_\perp) > 0$ cannot perform a closed motion (and then return to the starting point at the "time" $\bar{x}_\perp = 1$) if its initial kinetic energy is large enough to overcome the potential barrier $V(\bar{\psi})$, which allows for $\psi > \bar{\psi}$. As a consequence, for a closed motion one has $|\psi| \le \bar{\psi}$.

transformation $\psi(\bar{x}_\perp) = \sqrt{2}k\zeta\,\sigma(\zeta\bar{x}_\perp)$, with $\sigma(0) = 0$ and $\sigma'(0) = 1$. In terms of $\sigma(w = \zeta\bar{x}_\perp)$ Eq. (196) turns into

$$\sigma'^2 = (1 - \sigma^2)(1 - k^2\sigma^2), \tag{197}$$

where

$$-\bar{\tau} = \zeta^2(k^2 + 1). \tag{198}$$

The two parameters $k > 0$ and $\zeta > 0$ just introduced have to be determined as a function of $\bar{\tau}$ in such a way that $\sigma'(\zeta/2) = 0$, corresponding to the condition $\psi'(1/2) = \sqrt{2}k\zeta^2\sigma'(\zeta/2) = 0$, and that Eq. (198) is satisfied. Equation (197) is solved by the Jacobian elliptic integral of the first kind with modulus k (assuming that $\psi'(\bar{x}_\perp) = \sqrt{2}k\zeta^2\sigma'(\zeta\bar{x}_\perp) > 0$ for $0 < \bar{x}_\perp < 1/2$),

$$\int_0^{\sigma(w)} \mathrm{d}s \frac{1}{\sqrt{(1 - s^2)(1 - k^2s^2)}} = w, \tag{199}$$

and thus (see, e.g., 8.144.1 in Ref. 71)

$$\sigma(w) = \mathrm{sn}(w; k). \tag{200}$$

The parameters k and ζ are related via Eq. (198). They are fixed by imposing the boundary condition $\sigma'(\zeta/2) = 0$. Thus Eq. (197) renders two possible values: $\sigma(\zeta/2) = 1$ and $\sigma(\zeta/2) = 1/k^2$. On the other hand, Eq. (195) implies that $\psi(1/2) = \sqrt{\bar{\tau}} = \sqrt{2}k\zeta\,\sigma(\zeta/2) \leq \bar{\psi} = \zeta\sqrt{k^2 + 1}$ (where we used Eq. (198)), so that $\sigma(\zeta/2) \leq \sqrt{(k^2 + 1)/(2k^2)}$, i.e., (a) $\sigma(\zeta/2) = 1$ for $0 < k < 1$ and (b) $\sigma(\zeta/2) = 1/k^2$ for $k > 1$. We first consider case (a). Using $\sigma(\zeta/2) = 1$ in Eq. (199) one finds the following relation between ζ and k (see, e.g., 8.111.2 and 8.112.1 in Ref. 71):

$$K(k) = \frac{\zeta}{2}, \tag{201}$$

where $K(k)$ is the complete elliptic integral of the first kind. This allows one to replace the variable ζ in Eq. (198):

$$-\bar{\tau} = [2K(k)]^2(k^2 + 1). \tag{202}$$

This is an implicit equation $k = k(\bar{\tau})$ for the modulus in terms of the physical variable $\bar{\tau} = -1/2(L/\xi)^2$ (as defined for $\bar{\tau} < 0$). Thus the solution of Eqs. (192) and (194) is given by

$$\psi(\bar{x}_\perp) = 2\sqrt{2}kK(k)\,\mathrm{sn}(2K(k)\bar{x}_\perp; k). \tag{203}$$

Since $K(k)$ is a monotonicly increasing function with $K(0) = \pi/2$, one has $[2K(k)]^2(k^2 + 1)\pi^2$ and therefore there is a non-trivial solution $\psi(\bar{x}_\perp) \neq 0$ only for

$$\bar{\tau} \leq -\pi^2. \tag{204}$$

This determines the well-known mean-field critical point shift in the film geometry with Dirichlet boundary conditions on both sides[46,67,72,73] ($\nu = 1/2$):

$$\tau_c = -\pi^2 \left(\frac{\xi_0^-}{L} \right)^{1/\nu}. \tag{205}$$

The discussion of case (b) proceeds accordingly. Using the property $\mathrm{sn}(ku; 1/k) = k\,\mathrm{sn}(u; k)$ (see, e.g., formula 106.01 in Ref. 74) one finds that the solution for case (b) is the same as for case (a) provided the modulus k is replaced by $1/k$.

These results can also be obtained from the findings in Ref. 68, in which the mean-field order parameter profile is analytically determined for the case of $(+,+)$ and $(+,-)$ boundary conditions (see Ref. 68 for details). Alternatively, Eq. (194) can be integrated so that

$$\psi'^2(\bar{x}_\perp) = \bar{\tau}\psi^2(\bar{x}_\perp) + \frac{1}{2}\psi^4(\bar{x}_\perp) - \bar{\tau}\psi^2(1/2) - \frac{1}{2}\psi^4(1/2), \tag{206}$$

using $\psi'(1/2) = 0$ which is valid both for Dirchlet-Dirichlet and $(+,+)$ boundary conditions. The function $u(\bar{x}_\perp)$ defined as

$$u(\bar{x}_\perp) = \frac{A}{\psi(\bar{x}_\perp)} \tag{207}$$

satisfies Eq. (206), provided that A is chosen according to

$$\frac{A^2}{2} = -\bar{\tau}\psi^2(1/2) - \frac{1}{2}\psi^4(1/2), \tag{208}$$

which is equivalent to $-\bar{\tau}u^2(1/2) - 1/2u^4(1/2) = A^2/2$. Therefore both $\psi(\bar{x}_\perp)$ and $u(\bar{x}_\perp)$ solve Eq. (206). If ψ satisfies $(+,+)$ boundary conditions, then u satisfies Dirichlet-Dirichlet boundary conditions and vice versa. Thus it is possible to take advantage of the result reported in Ref. 68 for the former case in order to solve the latter we are presently interested in. (Note that the normalizations used here are different from those used in Ref. 68, see Eq. (194) here and Eq. (A3) therein.) In Ref. 68 two different parameterizations are provided for the solution denoted as $m_{+,+}$: one for $\tau L^2 > -\pi^2$ in Eq. (A13) therein, and the other for $\tau L^2 \le -\pi^2$ in Eq. (A15) therein. One can see that in the former case the value of A^2 is negative, i.e., the corresponding solution for Dirichlet-Dirichlet boundary conditions is not real, and one is left only with the trivial solution which is identically zero. Instead, in the latter case, taking into account the different normalizations,

$$\psi_{+,+}(z) = 2\sqrt{2}K(k)\frac{1}{\mathrm{sn}(2K(k)z; k)}, \tag{209}$$

where k is determined according to Eq. (202). Thus $A^2 = 64k^2[K(k)]^4$ and the corresponding function $u_{D,D}(z) = A/\psi_{+,+}(z)$ is identical to the solution $\psi(z)$ given in Eq. (203).

From Eqs. (203) and (202) it is possible to recover the result for the mean-field profile in the semi-infinite geometry by considering the limit of large L for fixed ξ_- and $x_\perp$ which corresponds to $|\bar{\tau}| \gg 1$, $\bar{x}_\perp \ll 1$. For $|\bar{\tau}| \gg 1$ one has $k \to 1^-$ and thus one can use the approximation (see, e.g., formula 17.3.26 in Ref. 70)

$$K(k) = -\frac{1}{2} \ln\left(\frac{1-k^2}{16}\right)(1 + O(1-k)). \tag{210}$$

Given that $\mathrm{sn}(u, 1) = \tanh u$ (see, e.g., formula 127.02 in Ref. 74) one easily finds at leading order

$$\psi(\bar{x}_\perp) \simeq \bar{\psi} \tanh\left(\sqrt{\frac{-\bar{\tau}}{2}}\bar{x}_\perp\right) \quad \text{for} \quad \bar{x}_\perp \ll 1, |\bar{\tau}| \gg 1. \tag{211}$$

Using Eqs. (149) and (195) and the fact that within mean-field theory $\xi_0^+/\xi_0^- = \sqrt{2}$, one can express the profile as

$$m(\mathbf{x}, \tau) = \mathfrak{m}_0 \frac{\xi_0^-}{\xi} \tanh\left(\frac{1}{2}\frac{x_\perp}{\xi}\right) \underset{x_\perp \to \infty}{\longrightarrow} \mathfrak{m}_0 \tau^{1/2}(1 - 2e^{-x_\perp/\xi_-}), \tag{212}$$

where here $\xi \equiv \xi(\tau < 0) = \xi_-$. This expression agrees with the well-known result for the semi-infinite geometry.[75,76] In Fig. 21 the order parameter profile $\bar{\psi}(\bar{x}_\perp)/\bar{\psi}$ (normalized to the corresponding bulk value $\bar{\psi}$, see Eq. (195)) is shown for some values of $\bar{\tau}$. The comparison with the profile in the semi-infinite geometry (Eq. (211)) is also shown.

From Fig. 21 one can infer that for $\bar{\tau} \to -\infty$ the order parameter profile in the middle of the film $\bar{x}_\perp = 1/2$ approaches rapidly the bulk value. Indeed, defining $\delta\psi \equiv \psi(\bar{x}_\perp = 1/2) - \bar{\psi}$ one finds

$$-\frac{\delta\psi}{\bar{\psi}} = 1 - \frac{\sqrt{2}k}{\sqrt{1+k^2}}, \tag{213}$$

where k is determined by Eq. (202). Using Eq. (210) one finds that for $|\bar{\tau}| \gg 1$ (i.e., in the limit of large film thickness L at a fixed temperature)

$$-\frac{\delta\psi}{\bar{\psi}} = 4e^{-\sqrt{-\bar{\tau}/2}}(1 + O(e^{-\sqrt{-\bar{\tau}/2}})), \tag{214}$$

i.e., in the middle of the film the deviation of the order parameter profile from the bulk value due to the distant confining walls decays $\sim \exp[-L/(2\xi)]$.

APPENDIX E: RELAXATION OF THE RESPONSE FUNCTION

In the main text $\bar{t}_I = F_{t_i}(\bar{x}_{1\perp})$ has been defined as the reduced time at which the inflection point of the scaling function $\Psi(\bar{x}_{1\perp}, \bar{x}_{2\perp}, \bar{t})$ for the mean-field response function (as a function of $\bar{x}_{2\perp}$, see Fig. 2) close to $\bar{x}_\perp = 0$ disappears. The

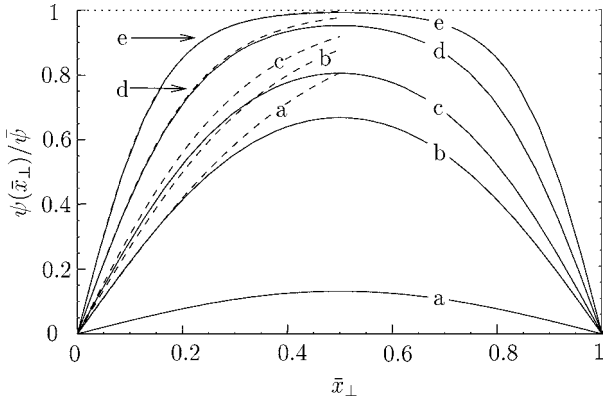

Fig. 21. Order parameter profile $\psi(\bar{x}_\perp)$ (normalized to the corresponding bulk value $\bar{\psi}$, see Eq. (195)) across the film, for some values of $\bar{\tau} = -1/2(L/\xi)^2$: -10 (a), -15 (b), -20 (c), -40 (d), -80 (e). The order parameter vanishes for $\bar{\tau} \geq -\pi^2 \simeq -9.87$ (Eq. (204)). The dashed lines for $\bar{x}_\perp \leq 1/2$ represent the corresponding profiles (normalized to the bulk value $\bar{\psi}$) in the semi-infinite geometry (given by Eq. (211)) in which the order parameter vanishes only for $\bar{\tau}0$. In the cases (d) and (e) these provide good approximations to the actual order parameter profile for $\bar{x}_\perp \leq 1/2$; for (e) the differences are barely visible.

position of this point $\bar{x}^I_{2\perp} = X_I(\bar{x}_{1\perp}, \bar{t}\,)$ is determined by the condition

$$\Psi^{(0,2)}(\bar{x}_{1\perp}, \bar{x}^I_{2\perp}, \bar{t}\,) = 0, \tag{215}$$

where, here and in the following, we use the notation $\Psi^{(n,m)}(\bar{x}_{1\perp}, \bar{x}_{2\perp}, \bar{t}\,) \equiv \partial^n_{\bar{x}_{1\perp}} \partial^m_{\bar{x}_{2\perp}} \Psi(\bar{x}_{1\perp}, \bar{x}_{2\perp}, \bar{t}\,)$. Accordingly, $\bar{t}_I$ is given by the time at which the inflection point reaches the surface at $\bar{x}_\perp = 0$, i.e., it is implicitly determined by the condition $X_I(\bar{x}_{1\perp}, \bar{t}_I) = 0$. This provides an equation for the function F_{t_I} (see Eq. (92)):

$$X_I(\bar{x}_{1\perp}, F_{t_I}(\bar{x}_{1\perp})) = 0. \tag{216}$$

The function shown in Fig. 3 has been determined by solving numerically Eqs. (215) and (216). Here we determine analytically the behavior of $F_{t_I}(\bar{x}_{1\perp})$ for $\bar{x}_{1\perp} \to 0$ and $\bar{x}_{1\perp} \to 1$. From Eq. (186) it follows that

$$\Psi(\bar{x}_{1\perp}, \bar{x}_{2\perp}, \bar{t}\,) = \Psi(\bar{x}_{2\perp}, \bar{x}_{1\perp}, \bar{t}\,), \quad \Psi(\bar{x}_{1\perp}, \bar{x}_{2\perp}, \bar{t}\,) = -\Psi(\bar{x}_{1\perp}, -\bar{x}_{2\perp}, \bar{t}\,), \tag{217}$$

and

$$\Psi(\bar{x}_{1\perp} = 0, \bar{x}_{2\perp}, \bar{t}\,) = \Psi(\bar{x}_{1\perp} = 1, \bar{x}_{2\perp}, \bar{t}\,) = 0. \tag{218}$$

Accordingly $\Psi^{(0,m)}(\bar{x}_{1\perp} = 0, \bar{x}_{2\perp}, \bar{t}\,) = \Psi^{(0,m)}(\bar{x}_{1\perp} = 1, \bar{x}_{2\perp}, \bar{t}\,) = 0$ and $\Psi^{(0,2m)}(\bar{x}_{1\perp}, \bar{x}_{2\perp} = 0, \bar{t}\,) = 0$. (Eq. (217) implies that Ψ is an odd function of $\bar{x}_{2\perp}$ if analytically continued to negative values of $\bar{x}_{2\perp}$ by using Eq. (186).) Therefore Eq. (215) is always trivially satisfied for $\bar{x}_{2\perp} = 0$, whatever the values

of $\bar{x}_{1\perp}$ and $\bar{t}$ are. The function F_{t_I} is given by the nontrivial solution of

$$\Psi^{(0,2)}(\bar{x}_{1\perp}, \bar{x}_{2\perp} \to 0, F_{t_I}(\bar{x}_{1\perp})) = 0. \tag{219}$$

This solution can be found by considering the series expansion of $\Psi^{(0,2)}$ for $\bar{x}_{2\perp} \to 0$, i.e.,

$$\Psi^{(0,2)}(\bar{x}_{1\perp}, \bar{x}_{2\perp} \to 0, F_{t_I}(\bar{x}_{1\perp})) = \Psi^{(0,3)}(\bar{x}_{1\perp}, 0, F_{t_I}(\bar{x}_{1\perp}))\, \bar{x}_{2\perp} + O(\bar{x}_{2\perp}^2). \tag{220}$$

Therefore $\bar{t}_I = F_{t_I}(\bar{x}_{1\perp})$ is determined by the condition

$$\Psi^{(0,3)}(\bar{x}_{1\perp}, 0, \bar{t}_I) = 0. \tag{221}$$

Let us consider the limiting case $\bar{x}_{1\perp} \to 0$, i.e., the behavior of $F_{t_I}(y \to 0)$. As discussed in Subsec. 4.2 (see Eq. (94)), in this limit one expects $t_I \to 0$. Using Eqs. (186) and (187), one realizes that in the limit $\bar{t}_I \to 0$ the terms of the sums with $n = 0$ are the leading contributions to $\Psi^{(0,3)}(\bar{x}_{1\perp}, 0, \bar{t}_I)$. (The terms with $n \neq 0$ give rise to exponentially small corrections.) Thus Eq. (221) reduces to

$$(\bar{x}_{1\perp}^2 - 6\bar{t}_I)\bar{x}_{1\perp} = 0, \tag{222}$$

that, apart from the expected trivial solution $\bar{x}_{1\perp} = 0$, is solved by

$$t_I = F_{t_I}(\bar{x}_{1\perp} \to 0) = \frac{\bar{x}_{1\perp}^2}{6}. \tag{223}$$

The full numerical solution shown in Fig. 3 is in accordance with this analytic result.

We now consider the case $\bar{x}_{1\perp} \to 1$, i.e., $F_{t_I}(1)$. Expressing Eq. (221) as before, one realizes that the leading contributions to $\Psi^{(0,3)}(\bar{x}_{1\perp} \to 1, 0, \bar{t}_I)$ stem from the terms in the sums with $n = 0, 1$ (Eqs. (186) and (187)). Indeed Fig. 3 shows that $\bar{t}_I$ is significantly smaller than 1 also for $\bar{x}_{1\perp} = 1$, allowing one to neglect terms that are suppressed by a factor $\sim \exp(-1/\bar{t}_I)$ compared to the leading one. This leads to

$$\bar{x}_{1\perp}\left(\bar{x}_{1\perp}^2 - 6\bar{t}_I\right) - (2 - \bar{x}_{1\perp})\left[(2 - \bar{x}_{1\perp})^2 - 6\bar{t}_I\right] \exp\left(\frac{\bar{x}_{1\perp} - 1}{\bar{t}_I}\right) = 0, \tag{224}$$

which has the expected trivial solution $\bar{x}_{1\perp} = 1$, whereas the nontrivial one for $\bar{x}_{1\perp} \to 1$ is given by

$$\bar{t}_I^2 - \bar{t}_I + \frac{1}{12} = 0, \tag{225}$$

yielding

$$\bar{t}_I = F_{t_I}(\bar{x}_{1\perp} = 1) \simeq \frac{1}{2} - \frac{1}{\sqrt{6}} \simeq 0.09176. \tag{226}$$

This provides a very accurate approximation of the actual value $F_{t_I}(1)$. Note that the second solution of the quadratic Eq. (225) can be discarded because it is

inconsistent with the assumption $\bar{t}_I \ll 1$, under which Eq. (225) has been derived. The actual value of $F_{t_I}(1)$ can be computed from Eq. (221) after having discarded the trivial solution $\bar{x}_{1\perp} = 1$. This can be done considering the expansion of $\Psi^{(0,3)}$ around $\bar{x}_{1\perp} = 1$, retaining only the leading term. This yields the implicit equation

$$\Psi^{(1,3)}(1, 0, \bar{t}_I) = 0. \tag{227}$$

Here we do not report the corresponding expression that can be easily worked out. The corresponding solution can be numerically determined and is given by

$$F_{t_I}(1) \simeq 0.0917918. \tag{228}$$

APPENDIX F: COMPUTATION OF THE CASIMIR FORCE

F.1. General Expression

According to Eq. (103) it is possible to compute the force exerted on the confining walls in terms of the stress-tensor $T_{\perp\perp}$. In order to determine the effect of a time-dependent external field on this force we first note that according to Eq. (12) within Gaussian approximation, due to $\langle\varphi\rangle_0 = 0$ and $\langle[\varphi]^n[\tilde{\varphi}]^m\rangle_0 = 0$ for $m > n$, one has

$$\begin{aligned}\langle\varphi(\mathbf{x}_1, t_1)\varphi(\mathbf{x}_2, t_2)\rangle_h = {} & \langle\varphi(\mathbf{x}_1, t_1)\varphi(\mathbf{x}_2, t_2)\rangle_0 \\ & + \int \mathrm{d}V'\mathrm{d}t'\mathrm{d}V''\mathrm{d}t''\, h(\mathbf{x}', t')h(\mathbf{x}'', t'') \\ & \times \Omega^2\langle\tilde{\varphi}(\mathbf{x}', t')\varphi(\mathbf{x}_1, t_1)\rangle_0\langle\tilde{\varphi}(\mathbf{x}'', t'')\varphi(\mathbf{x}_2, t_2)\rangle_0\end{aligned} \tag{229}$$

(higher order terms in h are zero because $n = 2$) where $\langle\cdot\rangle_h$ has been introduced after Eq. (11). Using Eq. (229) one finds

$$\begin{aligned}\langle T_{\perp\perp}(\mathbf{x}, t)\rangle_h|_{\mathbf{x}\in\partial V} = {} & \frac{1}{2}\,\partial_{x_{1\perp}}\partial_{x_{2\perp}}\langle\varphi(\mathbf{x}_1, t)\varphi(\mathbf{x}_2, t)\rangle_h\big|_{\mathbf{x}_1=\mathbf{x}_2=\mathbf{x}\in\partial V} = \langle T_{\perp\perp}\rangle_0|_{\partial V} \\ & + \frac{1}{2}\left[\int \mathrm{d}V'\mathrm{d}t'\; h(\mathbf{x}', t')\,\partial_{x_\perp}R^{(0)}(\mathbf{x}', t'; \mathbf{x}, t)|_{\mathbf{x}\in\partial V}\right]^2\end{aligned} \tag{230}$$

where the response function R is defined in Eq. (12). The previous equation provides the expression for the force density $F_{l(r)}(\mathbf{x}_\parallel)$ acting on the left (right) plate (depending on which part of the two boundaries ∂V is used in Eq. (230)) for a general external field. The previous expression can be expressed in terms of the corresponding dimensionless scaling variables (see Eqs. (43), (57), (85), (98), and (105)):

$$\mathscr{F}_l^{(\mathrm{dy})(0)}(\bar{L}, \bar{t}, \{\hat{h}\}) = \mathscr{F}^{(\mathrm{st})(0)}(0, \bar{L})$$

$$+\frac{1}{8}\Big[\int \frac{\mathrm{d}^{d-1}\bar{\mathbf{p}}}{(2\pi)^{d-1}}\mathrm{d}\bar{x}_{1\perp}\mathrm{d}\bar{t}_1\ \hat{h}(\bar{\mathbf{p}},\bar{x}_{1\perp},\bar{t}_1)$$

$$\times e^{-i\bar{\mathbf{p}}\bar{x}_{2\parallel}}\partial_{\bar{x}_{2\perp}}\bar{\mathscr{R}}^{(0)}(\bar{\mathbf{p}},\bar{x}_{1\perp},\bar{x}_{2\perp},\bar{t}-\bar{t}_1,\bar{L})|_{\bar{x}_{2\perp}=0}\Big]^2 \quad (231)$$

where the scaling variable $\hat{h}$ is defined by

$$\hat{h}(\bar{\mathbf{p}},\bar{x}_{1\perp},\bar{t}_1)\equiv\xi_0^{(d+2)/2}(L/\xi_0)^{\beta\delta/\nu}L^{-(d-1)}h(\bar{\mathbf{p}}/L,\bar{x}_{1\perp}L,\bar{t}_1T_0(\xi_0/L)^{-z}) \quad (232)$$

with

$$h(\mathbf{p},x_\perp,t)=\int \mathrm{d}^{d-1}x_\parallel\ h(\mathbf{x}_\parallel,x_\perp,t)\,\mathrm{e}^{i\mathbf{p}\cdot\mathbf{x}_\parallel}. \quad (233)$$

$\hat{h}$ is the analogue of $\bar{h}$ introduced after Eq. (105). Note that the former carries, compared to the latter, an extra factor $L^{-(d-1)}$, stemming from the Fourier transform in the $d-1$ parallel spatial directions. Moreover, within the Gaussian model ($g_0=0$) it is *not* possible to define, in accordance with Eq. (99), the scale factor $\mathfrak{h}_0$ for the external field h, whose engineering dimension $\xi_0^{-(d+2)/2}$ follows from the Gaussian action.

Note that, according to Eq. (230), the dependence of the Casimir force on the applied field is quadratic and therefore the effect of a sum of fields h_1+h_2 is *not* equal to the sum of the separate effects of each field.

F. 2. Specific Cases

In Subsection 4.3 we consider two different instances of externally applied fields: a perturbation $h(\mathbf{x},t)=h_W\delta(x_\perp-x_{1\perp})\delta(t-t_1)$ which is spatially constant in the plane $x_\perp=x_{1\perp}$ parallel to the confining walls and a perturbation $h(\mathbf{x},t)=h_P\delta(\mathbf{x}_\parallel-\mathbf{x}_{1\parallel})\delta(x_\perp-x_{1\perp})\delta(t-t_1)$ that is localized at a point $\mathbf{x}=(\mathbf{x}_{1\parallel},x_{1\perp})$ within the film. In the following we present the details of the computation of some relevant quantities determining the response to these external fields.

F. 2. 1. Planar Perturbation

Here we discuss the asymptotic behaviors of the amplitude $A_\Delta^W(\bar{x}_{1\perp})$ defined in Section 4.3 (see Eq. (111)), which determines the Casimir force maximum $(d-1)\Delta+\hat{h}_W^2A_\Delta^W(\bar{x}_{1\perp})$. In terms of the notation introduced after Eq. (215), A_Δ^W is given by

$$A_\Delta^W(\bar{x}_{1\perp})=\frac{1}{2}\left[\Psi^{(0,1)}(\bar{x}_{1\perp},0,\bar{t}_I(\bar{x}_{1\perp}))\right]^2. \quad (234)$$

Using Eqs. (186) and (187) one finds an expression of $\Psi^{(0,1)}$ which is suited to discuss some asymptotic behaviors at short times:

$$\Psi^{(0,1)}(\bar{x}_{1\perp}, 0, \bar{t}\,) = -\frac{1}{\sqrt{\pi}\bar{t}^{3/2}} \sum_{n=-\infty}^{+\infty} \left(n - \frac{\bar{x}_{1\perp}}{2}\right) \exp\left[-\frac{1}{\bar{t}}\left(n - \frac{\bar{x}_{1\perp}}{2}\right)^2\right]. \tag{235}$$

Accordingly,

$$\Psi^{(0,1)}(\bar{x}_{1\perp} \to 1, 0, \bar{t}\,) = \frac{(1-\bar{x}_{1\perp})}{\sqrt{\pi}\bar{t}^{3/2}} \times \sum_{n=-\infty}^{+\infty} \left[-\frac{1}{2} + \frac{(n-1/2)^2}{\bar{t}}\right] \times \exp\left[-\frac{(n-1/2)^2}{\bar{t}}\right] + O((1-\bar{x}_{1\perp})^2) \tag{236}$$

and

$$\Psi^{(0,1)}(\bar{x}_{1\perp} \to 0, 0, \bar{t}\,) = \frac{\bar{x}_{1\perp}}{2\sqrt{\pi}\bar{t}^{3/2}} \left\{\exp\left[-\bar{x}_{1\perp}^2/(4\bar{t}\,)\right] + O(e^{-1/\bar{t}})\right\}. \tag{237}$$

(Note that the approximation provided by this expression deteriorates upon increasing $\bar{t}$.) In Appendix E we found that, at leading orders, $\bar{t}_I(\bar{x}_{1\perp} \to 1) = F_{t_I}(1) \simeq 0.0918$ and $\bar{t}_I(\bar{x}_{1\perp} \to 0) = \bar{x}_{1\perp}^2/6$. From Eqs. (234) and (236) one has

$$A_\Delta^W(\bar{x}_{1\perp} \to 1) = a_1(1-\bar{x}_{1\perp})^2 \tag{238}$$

with

$$a_1 = \mathcal{L}_1(\bar{t}_I(1)) \simeq 17.535 \tag{239}$$

and where

$$\mathcal{L}_d(\bar{t}\,) = \frac{1}{(4\pi\bar{t}\,)^{d-1}} \frac{1}{2\pi\bar{t}^3} \left\{\sum_{n=-\infty}^{+\infty} \left[-\frac{1}{2} + \frac{(n-1/2)^2}{\bar{t}}\right] \exp\left[-\frac{(n-1/2)^2}{\bar{t}}\right]\right\}^2; \tag{240}$$

this function will be useful also for the discussion of the localized perturbation below. In the opposite limit $\bar{x}_{1\perp} \to 0$ Eqs. (234) and (237) yield

$$A_\Delta^W(\bar{x}_{1\perp} \to 0) = \mathcal{K}_1/\bar{x}_{1\perp}^4 \tag{241}$$

with

$$\mathcal{K}_1 \simeq 0.427888, \tag{242}$$

where we have introduced the constant

$$\mathcal{K}_d = \frac{1}{2}\frac{[2(d+2)]^{d+2}}{(4\pi)^d} e^{-(d+2)}. \tag{243}$$

Moreover, the asymptotic expressions for $\Psi^{(0,1)}$ in Eqs. (236) and (237) provide the corresponding ones for the function $\mathscr{F}_\Delta^W$ (see Eq. (112)) because

$$\mathscr{F}_\Delta^W(\bar{x}_{1\perp}, \bar{t}\,) = \left[\frac{\Psi^{(0,1)}(\bar{x}_{1\perp}, 0, \bar{t}\,)}{\Psi^{(0,1)}(\bar{x}_{1\perp}, 0, \bar{t}_I(\bar{x}_{1\perp}))}\right]^2. \tag{244}$$

For $\bar{x}_{1\perp} \to 1$, Eq. (236) gives

$$\mathscr{F}_\Delta^W(\bar{x}_{1\perp} \to 1, \bar{t}\,) = \frac{\mathcal{L}_1(\bar{t}\,)}{\mathcal{L}_1(\bar{t}_I(1))}, \tag{245}$$

whereas, for $\bar{x}_{1\perp} \to 0$, Eq. (237) and $\bar{t}_I(\bar{x}_{1\perp} \to 0) = \bar{x}_{1\perp}^2/6$ render

$$\mathscr{F}_\Delta^W(\bar{x}_{1\perp} \to 0, \bar{t}\,) = \left(\frac{e}{s}\right)^3 e^{-3/s}, \quad s = \bar{t}/\bar{t}_I(\bar{x}_{1\perp} \to 0). \tag{246}$$

These asymptotic behaviors are indicated in Fig. 5. Equation (115) allows one to determine the long-time behavior of $\mathscr{F}_\Delta^W(\bar{x}_{1\perp}, \bar{t}\,)$ for fixed $\bar{x}_{1\perp}$:

$$\mathscr{F}_\Delta^W(\bar{x}_{1\perp}, \bar{t} \to \infty) \sim e^{-2\pi^2\bar{t}}[1 + O(e^{-3\pi^2\bar{t}})], \tag{247}$$

which clearly displays the expected exponential decay for $\bar{t} \gg 1/(3\pi^2)$.

F. 2. 2. Localized Perturbation

In Subsec. 4.3 we have introduced the amplitude $A_\Delta^P(\delta\bar{\mathbf{x}}_\parallel = \mathbf{x}_\parallel - \mathbf{x}_{1\parallel}, \bar{x}_{1\perp})$ associated with the response to a point-like field (see Eq. (120)):

$$A_\Delta^P(\delta\bar{\mathbf{x}}_\parallel, \bar{x}_{1\perp}) = \frac{1}{2}\frac{e^{-(\delta\bar{\mathbf{x}}_\parallel)^2/[2\bar{t}_M(\delta\bar{\mathbf{x}}_\parallel, \bar{x}_{1\perp})]}}{[4\pi\,\bar{t}_M(\delta\bar{\mathbf{x}}_\parallel, \bar{x}_{1\perp})]^{d-1}}\left[\Psi^{(0,1)}(\bar{x}_{1\perp}, \bar{t}_M(\delta\bar{\mathbf{x}}_\parallel, \bar{x}_{1\perp}))|_{\bar{x}_{2\perp}=0}\right]^2. \tag{248}$$

Here we discuss its asymptotic behavior for $|\delta\bar{\mathbf{x}}_\parallel| \to 0$. The typical time $\bar{t}_M(\delta\bar{\mathbf{x}}_\parallel, \bar{x}_{1\perp})$ when the effect of the perturbation attains its maximum at a point with $|\delta\bar{\mathbf{x}}_\parallel| \ll 1$ is expected to be of the same order as that in the case of a planar perturbation at the same $\bar{x}_{1\perp}$, which is given by the function $\bar{t}_I(\bar{x}_{1\perp})$ shown in Fig. 3. Accordingly, $\bar{t}_M(\delta\bar{\mathbf{x}}_\parallel \to 0, \bar{x}_{1\perp}) \lesssim 0.1$ and therefore, in Eq. (248) we can use the expressions given in Eqs. (236) and (237) for $\Psi^{(0,1)}$ in order to obtain the asymptotic behaviors for $\bar{x}_{1\perp} \to 1$ and $\bar{x}_{1\perp} \to 0$, respectively. We expect that, as it is the case for A_Δ^W in Fig. 4, they provide good approximations of the actual dependence. Taking into account that $\bar{t}_M(\delta\bar{\mathbf{x}}_\parallel \to 0, \bar{x}_{1\perp} \to 0) = [\bar{x}_{1\perp}^2 + (\delta\bar{\mathbf{x}}_\parallel)^2]/[2(d+2)]$ (Eq. (119)) and using Eq. (237) one finds

$$A_\Delta^P(\delta\bar{\mathbf{x}}_\parallel \to 0, \bar{x}_{1\perp} \to 0) = \mathcal{K}_d\frac{\bar{x}_{1\perp}^2}{[\bar{x}_{1\perp}^2 + (\delta\bar{\mathbf{x}}_\parallel)^2]^{d+2}}, \tag{249}$$

and in particular

$$A_\Delta^P(\delta\bar{\mathbf{x}}_\parallel = 0, \bar{x}_{1\perp} \to 0) = \mathcal{K}_d/\bar{x}_{1\perp}^{2(d+1)}. \tag{250}$$

For $d = 3$ one has $\mathcal{K}_3 \simeq 0.169773$ whereas $\mathcal{K}_4 \simeq 0.148406$. For $\bar{x}_{1\perp} \to 1$ we consider only the case $\delta\bar{\mathbf{x}}_\parallel = 0$. From Eq. (236), one finds

$$A_\Delta^P(\delta\bar{\mathbf{x}}_\parallel = 0, \bar{x}_{1\perp} \to 1) = a_d(1 - \bar{x}_{1\perp})^2, \tag{251}$$

where (see Eq. (240))

$$a_d \equiv \mathcal{L}_d(\bar{t}_M(\delta\bar{\mathbf{x}}_\parallel = 0, \bar{x}_{1\perp} \to 1)). \tag{252}$$

Taking into account that [see the discussion after Eq. (118)] $\bar{t}_M(\delta\bar{\mathbf{x}}_\parallel = 0, \bar{x}_{1\perp} \to 1) = (4 - \sqrt{11})/10 \simeq 0.0683375$ for $d = 3$ and $\bar{t}_M(\delta\bar{\mathbf{x}}_\parallel = 0, \bar{x}_{1\perp} \to 1) = (9 - \sqrt{57})/20 \simeq 0.0604236$ for $d = 4$, one has $a_3 = \mathcal{L}_3(\bar{t}_M(\delta\bar{\mathbf{x}}_\parallel = 0, \bar{x}_{1\perp} \to 1)) \simeq 17.927$ and $a_4 = \mathcal{L}_4(\bar{t}_M(\delta\bar{\mathbf{x}}_\parallel = 0, \bar{x}_{1\perp} \to 1)) \simeq 19.416$.

Let us discuss the behavior of $A_\Delta^P(\delta\bar{\mathbf{x}}_\parallel, \bar{x}_{1\perp})$ for large $|\delta\bar{\mathbf{x}}_\parallel|$ and $0 < \bar{x}_{1\perp} < 1$ fixed. According to Eq. (116) one has, in leading order, $\bar{t}_M(\delta\bar{\mathbf{x}}_\parallel \to \infty, \bar{x}_{1\perp}) = |\delta\bar{\mathbf{x}}_\parallel|/(2\pi) - (d-1)/(4\pi^2) + O(1/|\delta\bar{\mathbf{x}}_\parallel|)$ and therefore one can use in Eq. (248) the asymptotic behavior of $\Psi^{(0,1)}$ reported in Eq. (115), finding

$$A_\Delta^P(\delta\bar{\mathbf{x}}_\parallel \to \infty, \bar{x}_{1\perp}) = 2\pi^2 \frac{e^{-2\pi|\delta\bar{\mathbf{x}}_\parallel|}}{(2|\delta\bar{\mathbf{x}}_\parallel|)^{d-1}} \sin^2(\pi\bar{x}_{1\perp}). \tag{253}$$

For $|\delta\bar{\mathbf{x}}_\parallel|, \bar{x}_{1\perp} \to 0$ one obtains from Eq. (249)

$$\frac{A_\Delta^P(\delta\bar{\mathbf{x}}_\parallel, \bar{x}_{1\perp})}{A_\Delta^P(\delta\bar{\mathbf{x}}_\parallel = 0, \bar{x}_{1\perp})} = \frac{1}{\left[1 + (\delta\bar{\mathbf{x}}_\parallel)^2/\bar{x}_{1\perp}^2\right]^{d+2}}, \tag{254}$$

which indeed provides a very good approximation of the actual curves already for $|\delta\bar{\mathbf{x}}_\parallel|, \bar{x}_{1\perp} \lesssim 0.5$ (see Fig. 8).

APPENDIX G: EXPANSION OF THE IN-PLANE CORRELATION FUNCTION

In Subsec. 4.4 we discuss the mean-field expression for the correlation function for points located within a plane parallel to the confining walls, i.e., $C^{(0)}(\mathbf{p}, x_\perp, x_\perp, \omega)$, with the corresponding scaling function given in Eq. (127). This expression depends actually on two variables: $\bar{a} \equiv aL$ and $\bar{x}_\perp \equiv x_\perp/L$ ($0 \le \bar{x}_\perp \le 1$). In order to discuss the behavior of Eq. (127) for $|\bar{a}| \ll 1$ (so that $|\bar{a}(1 - 2\bar{x}_\perp)| \ll 1$), we write

$$\frac{\cosh\bar{a} - \cosh\bar{a}(1 - 2\bar{x}_\perp)}{\bar{a}\sinh\bar{a}} = \sum_{n=0}^{\infty} \mathcal{P}_n(\bar{x}_\perp)\bar{a}^{2n} \tag{255}$$

where $\mathcal{P}_n$ is a polynomial of degree $2n+2$, has the symmetry $\mathcal{P}_n(\bar{x}_\perp) = \mathcal{P}_n(1-\bar{x}_\perp)$, and $\mathcal{P}_n(0) = 0$. From the series expansion of the l.h.s. of Eq. (255) one easily finds that

$$\mathcal{P}_0(x) = 2x(1-x), \tag{256}$$

$$\mathcal{P}_1(x) = -\frac{2}{3}x^2(1-x)^2, \tag{257}$$

$$\mathcal{P}_2(x) = \frac{2}{45}x^2(1-x)^2(1+2x-2x^2) \tag{258}$$

$$\mathcal{P}_3(x) = -\frac{4}{945}x^2(1-x)^2\left(1+2x-\frac{x^2}{2}-3x^3+\frac{3}{2}x^4\right). \tag{259}$$

Taking into account that $\bar{a}^2 \equiv \bar{\mathbf{p}}^2 + \bar{L}^2 - i\bar{\omega}$ (see Eq. (97)), one finds that

$$\begin{aligned}&\mathrm{Im}\frac{\cosh\bar{a} - \cosh\bar{a}(1-2\bar{x}_\perp)}{\bar{a}\sinh\bar{a}} \\ &\quad= \sum_{n=1}^{\infty}\mathcal{P}_n(\bar{x}_\perp)\sum_{k=0}^{2k+1\le n}(-1)^{k+1}\binom{n}{2k+1}\left(\bar{\mathbf{p}}^2+\bar{L}^2\right)^{n-(2k+1)}\bar{\omega}^{2k+1},\end{aligned} \tag{260}$$

and thus

$$\begin{aligned}&\mathscr{E}^{(0)}(\bar{\mathbf{p}}, \bar{x}_\perp, \bar{x}_\perp, \bar{\omega}, \bar{L}) \\ &\quad= 2\sum_{n=1}^{\infty}\mathcal{P}_n(x_\perp/L)\sum_{k=0}^{2k+1\le n}(-1)^{k+1}\binom{n}{2k+1}\left(\bar{\mathbf{p}}^2+\bar{L}^2\right)^{n-(2k+1)}\bar{\omega}^{2k}.\end{aligned} \tag{261}$$

ACKNOWLEDGMENTS

A. G. is indebted to Frank Schlesener for many helpful discussions. We also thank H. W. Diehl for a careful reading of the manuscript and for valuable comments and remarks.

REFERENCES

1. J. Zinn-Justin, *Quantum Field Theory and Critical Phenomena*, 3rd ed. (Clarendon, Oxford, 1996).
2. P. C. Hohenberg and B. I. Halperin, Theory of dynamic critical phenomena. *Rev. Mod. Phys.* **49**:435 (1977).
3. A. Pelissetto and E. Vicari, Critical phenomena and renormalization-group theory. *Phys. Rep.* **368**:549 (2002).
4. R. Folk and G. Moser, Critical dynamics in two loop order. *Acta Phys. Slov.* **52**:285 (2002).

5. K. Binder, *Critical Behaviour at Surfaces*, in *Phase Transition and Critical Phenomena*. Edited by C. Domb and J. L. Lebowitz (Academic, London, 1983), Vol. 8, p. 2.
6. H. W. Diehl, *Field-theoretical approach to critical behaviour at surfaces*, in *Phase Transition and Critical Phenomena*. Edited by C. Domb and J. L. Lebowitz (Academic, London, 1986), Vol. 10, p. 75.
7. M. Pleimling, Critical phenomena at perfect and non-perfect surfaces. *J. Phys. A: Math. Gen.* **37**:R79 (2004).
8. S. Dietrich and H. W. Diehl, The effects of surfaces on dynamic critical behavior. *Z. Phys. B* **51**:343 (1983).
9. H. W. Diehl and H. K. Janssen, Boundary conditions for the field theory of dynamic critical behavior in semi-infinite systems with conserved order parameter. *Phys. Rev. A* **45**:7145 (1992); H. W. Diehl, Universality classes for the dynamic surface critical behavior of systems with relaxational dynamics. *Phys. Rev. B* **49**:2846 (1994); F. Wichmann and H. W. Diehl, Dynamic surface critical behavior of systems with conserved bulk order parameter: detailed RG analysis of the semi-infinite extensions of model B with and without nonconservative surface terms. *Z. Phys. B* **97**:251 (1995).
10. M. N. Barber, *Finite-size Scaling*, in *Phase Transition and Critical Phenomena*. Edited by C. Domb and J. L. Lebowitz (Academic, London, 1983), Vol. 8, p. 145.
11. *Finite-size Scaling*, edited by J. L. Cardy (North-Holland, Amsterdam, 1988).
12. J. G. Brankov, D. M. Dantchev and N. S. Tonchev, *The Theory of Critical Phenomena in Finite-Size Systems—Scaling and Quantum Effects* (World Scientific, Singapore, 2000).
13. M. Krech and S. Dietrich, Free energy and specific heat of critical films and surfaces. *Phys. Rev. A* **46**:1886 (1992).
14. M. Krech and S. Dietrich, The specific heat of critical films, the Casimir force, and wetting films near critical end points. *Phys. Rev. A* **46**:1922 (1992).
15. M. Krech, *The Casimir Effect in Critical Systems* (World Scientific, Singapore, 1994).
16. F. Schlesener, A. Hanke and S. Dietrich, Critical Casimir forces in colloidal suspensions. *J. Stat. Phys.* **110**:981 (2003).
17. R. Klimpel and S. Dietrich, Structure factor of thin films near continous phase transitions *Phys. Rev. B* **60**:16977 (1999).
18. V. Dohm, The superfluid transition in confined ^{4}He: Renormalization-group theory. *Phys. Scripta T* **49**:46 (1993).
19. A. Onuki, *Phase transition dynamics* (Cambridge University Press, Cambridge, 2002).
20. S. Puri, Surface-directed spinodal decomposition. *J. Phys.: Condens. Matter* **17**:R101 (2005).
21. S. K. Das, S. Puri, J. Horbach and K. Binder, *Kinetics of phase separation in thin films: Simulations for the diffusive case*. e-print Phys. Rev. E 72, 061603 (2005).
22. Y. Y. Goldschmidt, Finite size scaling effects in dynamics, *Nucl. Phys. B* **280** [FS18], 340 (1987); reprinted in Ref.11.
23. J. C. Niel and J. Zinn-Justin, Finite size effects in critical dynamics. *Nucl. Phys. B* **280** [FS18], 355 (1987).
24. J. C. Niel, Critical dynamics, finite-size effects and supersymmetry. *Phys. Rev. B* **37**:2156 (1988).
25. H. W. Diehl, Finite size effects in critical dynamics and the renormalization group. *Z. Phys. B* **66**:211 (1987).
26. W. Koch, V. Dohm and D. Stauffer, Order-parameter relaxation times of finite three-dimensional Ising-like systems. *Phys. Rev. Lett.* **77**:1789 (1996).
27. K. Oerding, Relaxation times in a finite Ising system with random impurities. *J. Stat. Phys.* **78**:893 (1995).
28. U. Ritschel and H. W. Diehl, Long-time traces of the initial condition in relaxation phenomena near criticality. *Phys. Rev. E* **51**:5392 (1995); Dynamic relaxation and universal short-time behavior in finite systems: The renormalization-group approach. *Nucl. Phys. B* **464**:512 (1996).

29. H. W. Diehl and U. Ritschel, Dynamical relaxation and universal short-time behavior of finite systems, *J. Stat. Phys.* **73**:1 (1993).
30. W. Koch and V. Dohm, Finite-size effects on critical diffusion and relaxation towards metastable equilibrium. *Phys. Rev. E* **58**:R1179 (1998).
31. M. Krech and D. P. Landau, Spin-dynamics simulations of the three-dimensional XY model: structure factor and transport properties. *Phys. Rev. B* **60**:3375 (1999).
32. Z. -B. Li, U. Ritschel and B. Zheng, Monte Carlo simulation of universal short-time behavior in critical relaxation. *J. Phys. A: Math. Gen.* **27**:L837 (1994).
33. K. Nho and E. Manousakis, Scaling of thermal conductivity of helium confined in pores. *Phys. Rev. B* **64**:144513 (2001).
34. A. M. Kahn and G. Ahlers, Thermal conductivity of ^{4}He near the superfluid transition in a restricted geometry. *Phys. Rev. Lett.* **74**:944 (1995); D. Murphy, E. Genio, G. Ahlers, F. Liu and Y. Liu, Finite-size scaling and universality of the thermal resistivity of liquid ^{4}He near T_λ, *Phys. Rev. Lett.* **90**:025301 (2003).
35. V. Dohm, Renormalization-group flow equations of model F. *Phys. Rev. B* **44**:2697 (1991).
36. M. Töpler and V. Dohm, Finite-size effects on the thermal conductivity of ^{4}He near T_λ. *Physica B* **329-333**:200 (2003).
37. D. Frank and V. Dohm, Critical thermal boundary resistance of ^{4}He near T_λ. *Phys. Rev. Lett.* **62**:1864 (1989); Critical thermal resistance of confined ^{4}He above T_λ. *Physica B* **165&166**:543 (1990); Critical thermal boundary resistance of ^{4}He above and below T_λ: renormalization-group theory. *Z. Phys. B* **84**:443 (1991); V. Dohm and R. Haussmann, The superfluid transition of ^{4}He in the presence of a heat current: renormalization-group theory. *Physica B* **197**:215 (1994).
38. K. Kuehn, S. Mehta, H. Fu, E. Genio, D. Murphy, F. Liu, Y. Liu and G. Ahlers, Singularity in the thermal boundary resistance between superfluid ^{4}He and a solid surface. *Phys. Rev. Lett.* **88**:095702 (2002).
39. J. K. Bhattacharjee, Critical diffusivity in restricted geometry: Decoupled mode approximation. *Phys. Rev. Lett.* **77**:1524 (1996).
40. R. A. Ferrell, Decoupled-mode dynamical scaling theory of the binary-liquid phase transition. *Phys. Rev. Lett.* **24**:1169 (1970).
41. M. Calvo and R. A. Ferrell, Critical diffusion in a bounded fluid. I, *Phys. Rev. A* **31**:2570 (1985); M. Calvo, Critical diffusion in a bounded fluid. II. Temperature-dependent effects. *Phys. Rev. A* **31**:2588 (1985).
42. S. Battacharyya and J. K. Bhattacharjee, Critical ultrasonics near the superfluid transition: finite-size effects. *J. Phys. A: Math. Gen.* **31**:L575 (1998); Superfluid transition in a finite geometry: Critical ultrasonics. *Phys. Rev. B* **58**:15146 (1998).
43. D. Bartolo, A. Ajdari and J.-B. Fournier, Effective interactions between inclusions in complex fluids driven out of equilibrium. *Phys. Rev. E* **67**:061112 (2003).
44. A. Najafi and R. Golestanian, *Forces induced by non-equilibrium fluctuations: The Soret-Casimir effect*. e-print cond-mat/0308373v1 (2003). Part of this work has been published in Europhys. Lett. **68**:776 (2004).
45. E. Frey and F. Schwabl, Critical dynamics of magnets. *Adv. Phys.* **43**:577 (1994).
46. H. Nakanishi and M. E. Fisher, Critical point shifts in films. *J. Chem. Phys.* **78**:3279 (1983).
47. Y. Rouault, J. Baschnagel and K. Binder, Phase separation of symmetrical polymer mixtures in thin-film geometry. *J. Stat. Phys.* **80**:1009 (1995).
48. D. O'Connor and C. R. Stephens, Renormalization group theory of crossovers. *Phys. Rep.* **363**:425 (2002).
49. P. Calabrese, V. Martin-Mayor, A. Pelissetto and E. Vicari, Dynamic structure factor of the three-dimensional Ising model with purely relaxational dynamics. *Phys. Rev. E* **68**:016110 (2003).

50. V. Privman, P. C. Hohenberg and A. Aharony, *Universal critical-point amplitude ratios*, in *Phase Transition and Critical Phenomena*. Edited by C. Domb and J. L. Lebowitz (Academic, New York, 1991), Vol. 14, p. 1.
51. H. K. Janssen, Lagrangean for classic field dynamics and renormalization group calculations of dynamical critical properties. *Z. Phys. B* **23**:377 (1976); R. Bausch, H. K. Janssen and H. Wagner, Renormalized field-theory of critical dynamics. *Z. Phys. B* **24**:113 (1976).
52. F. Langouche, D. Roekaerts and E. Tirapegui, Functional integral methods for stochastic fields. *Physica A* **95**:252 (1979).
53. M. Krech, E. Eisenriegler and S. Dietrich, Energy density profiles in critical films. *Phys. Rev. E* **52**:1345 (1995).
54. G. Gompper and H. Wagner, Conformal invariance in semi-infinite systems: application to critical surface scattering. *Z. Phys. B* **59**:193 (1985).
55. S. Dietrich, Static and dynamic critical phenomena at surfaces, in *Magnetic Properties of Low-Dimensional Systems II*, Edited by L. M. Falicov, F. Mejía-Lira, and J. L. Morán-López (Springer, Berlin, 1990), p. 150.
56. D. Dantchev and M. Krech, Critical Casimir force and its fluctuations in lattice spin models: Exact and Monte Carlo results. *Phys. Rev. E* **69**:046119 (2004).
57. D. Bartolo, A. Ajdari, J.-B. Fournier and R. Golestanian, Fluctuations of fluctuation-induced Casimir-like forces. *Phys. Rev. Lett.* **89**:230601 (2002).
58. M. J. Dunlavy and D. Venus, Critical slowing down in the two-dimensional Ising model measured using ferromagnetic ultrathin films. *Phys. Rev. B* **71**:144406 (2005).
59. S. Dietrich and A. Haase, Scattering of X-rays and neutrons at interfaces. *Phys. Rep.* **260**:1 (1995).
60. R. Bausch and H. K. Janssen, Equation of motion and nonlinear response near the critical point. *Z. Phys. B* **25**:275 (1976).
61. R. Bausch, E. Eisenriegler and H. K. Janssen, Nonlinear critical slowing down of the one-component Ginzburg-Landau field. *Z. Phys. B* **36**:179 (1979).
62. Z. Rácz, Nonlinear relaxation near the critical point: molecular-field and scaling theory. *Phys. Rev. B* **13**:263 (1976).
63. M. E. Fisher and Z. Rácz, Scaling theory of nonlinear critical relaxation. *Phys. Rev. B* **13**:5039 (1976).
64. H. Riecke, *Nichtlineare Relaxation in halbunendlichen Systemen*, diploma thesis, Ludwig-Maximilians-Universität, München (1982).
65. M. Kikuchi and Y. Okabe, Monte Carlo Study of Critical Relaxation near a Surface. *Phys. Rev. Lett.* **55**:1220 (1985).
66. H. Riecke, S. Dietrich and H. Wagner, Field theory for nonlinear critical relaxation near a surface. *Phys. Rev. Lett.* **55**:3010 (1985).
67. M. E. Fisher and H. Nakanishi, Scaling theory for the criticality of fluids between plates. *J. Chem. Phys.* **75**:5857 (1981).
68. M. Krech, Casimir forces in binary liquid mixtures. *Phys. Rev. E* **56**:1642 (1997).
69. A. P. Prudnikov, Yu. A. Brychkov and O. I. Marichev, *Integrals and Series, Vol. 1: Elementary Functions* (Gordon and Breach, New York, 1986).
70. *Handbook of Mathematical Functions*, edited by M. Abramowitz and I. A. Stegun (Dover, New York, 1970).
71. I. S. Gradshteyn and I. M. Ryzhik, *Table of Integrals, Series, and Products* (Academic, London, 1965).
72. M. I. Kaganov and A. N. Omel'yanchuk, Phenomenological theory of phase transition in a thin ferromagnetic plate. *Sov. Phys. JETP* **34**:895 (1972); *Zh. Eksp. Teor. Fiz.* **61**, 1679 (1971).
73. M. I. Kaganov, Surface magnetism. *Sov. Phys. JETP* **35**:631 (1972); *Zh. Eksp. Teor. Fiz.* **62**, 1196 (1972).

74. P. F. Byrd and M. D. Friedman. *Handbook of Elliptic Integrals for Engineers and Scientist* (Springer, Berlin, 1971).
75. P. Kumar, Magnetic phase transition at a surface: mean-field theory. *Phys. Rev. B* **10**:2928 (1974).
76. T. C. Lubensky and M. H. Rubin, Critical phenomena in semi-infinite systems II: mean-field theory. *Phys. Rev. B* **12**:3885 (1975).
77. H. K. Janssen, B. Schaub and B. Schmittmann, New universal short-time scaling behaviour of critical relaxation processes. *Z. Phys B* **73**:539 (1989); H. K. Janssen, On the renormalized field theory of nonlinear critical relaxation, in *From Phase Transitions to Chaos– Topics in Modern Statistical Physics*. Edited by G. Györgyi, I. Kondor, L. Sasvári and T. Tel (World Scientific, Singapore, 1992).
78. U. Ritschel and P. Czerner, Universal short-time behavior in critical dynamics near surfaces, *Phys. Rev. Lett.* **75**:3882 (1995); S. N. Majumdar and A. M. Sengupta, Nonequilibrium dynamics following a quench to the critical point in a semi-infinite system. *Phys. Rev. Lett.* **76**:2394 (1996); M. Pleimling and F. Iglói, Nonequilibrium critical dynamics at surfaces: cluster dissolution and nonalgebraic correlations. *Phys. Rev. Lett.* **92**:145701 (2004).